

UCSF

UC San Francisco Electronic Theses and Dissertations

Title

Regulation and function of MEF2C in the neural crest and anterior heart field

Permalink

<https://escholarship.org/uc/item/07h874qp>

Author

Verzi, Michael

Publication Date

2006

Peer reviewed|Thesis/dissertation

Regulation and function of MEF2C in the neural crest and anterior heart field

by

Michael Verzi

DISSERTATION

Submitted in partial satisfaction of the requirements for the degree of

DOCTOR OF PHILOSOPHY

in

Biochemistry and Biophysics

in the

GRADUATE DIVISION

of the

UNIVERSITY OF CALIFORNIA, SAN FRANCISCO



This work is dedicated to teachers, particularly all of my teachers, both in school and in laboratories. They give up time (and frequently money) to give the gift of knowledge and ask for nothing in return.

UCSF LIBRARY

Acknowledgements

I must begin by thanking my wife Megan for sacrificing her choices to come to San Francisco so I could do this work. She has been incredibly supportive and understanding of a scientist's life.

Brian has been an outstanding mentor. With the exception of his innate intelligence and enthusiasm, two characteristics that cannot be learned, Brian tried to teach me everything else there is to succeeding in science. His approaches towards identifying and solving problems are now part of my scientific toolbox, and I am grateful for these invaluable tools. Brian has been patient in imparting knowledge to his students, which speaks volumes to those who know of his patience. Outside of direct scientific mentorship, Brian has created an outstanding work environment and has been sympathetic to a student's needs. I can't thank him enough.

Didier Stainier and Matthias Hebrok served exceptionally as my thesis committee and have made important contributions to my graduate work at all stages of its development. I am most appreciative of the time and energy they have devoted to my education.

Don Lovett, R. Paul Malchow, and Grigori Enikolopov all welcomed me into their labs as an undergraduate student (with no obvious benefits to themselves) and taught me volumes about research that I could never understand from a text. Their mentorship helped me find my way down this career path. I especially thank Don and Paul for their continued advice over the ensuing years.

It's been a pleasure to share lab space with an amazing group of people over the last 5 years. Rather than name them all, I'll just say that each has made the experience

exciting and fun, provided much help (both emotional and technical), and has become a very good friend. Additionally, on a technical note, Dave McCulley, Brian Gilliss, Sarah DeVal, Josh Anderson, and Evie Dodou have all contributed to work in this thesis and figure 7A was carried out by Pooja Agarwal. I thank Eric “The Horse” Ho for his technical assistance as well as his help in preparing this document.

Finally, I have been blessed with an incredible family, each of whom has been unwavering in their support of my career and who have always stressed the importance of education. Megan, Carol (mom), Paul (dad), Lisa and Mary (ahhh, sisters) Verzi have all been great to me.

The majority of the 4th chapter of this work and its accompanying figures were reprinted from *Developmental Biology*, volume 287(1), by Michael P. Verzi, David J. McCulley, Sarah DeVal, Evdokia Dodou, and Brian L. Black, entitled: **The right ventricle, outflow tract, and ventricular septum comprise a restricted expression domain within the secondary/anterior heart field**, Pages No. 134-145, Copyright (2005), with permission from Elsevier.

1100211000ADN

Abstract

Regulation and function of MEF2C in the neural crest and anterior heart field

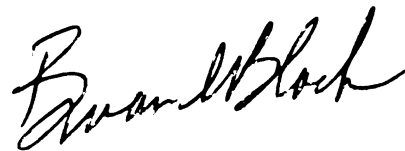
Michael Verzi

Mef2c is a transcription factor expressed in multiple embryonic tissues. In skeletal and cardiac muscle development, *mef2c* sits at a critical point of the transcriptional network downstream of specification factors and upstream of differentiation genes. In this role, *mef2c* is crucial for cellular differentiation of skeletal and cardiac muscle, yet its function in other developing tissues is unknown. Here, we explore *mef2c*'s transcriptional regulation and function in the developing embryo and reveal a novel and essential function for *mef2c* in the neural crest.

Mef2c's transcriptional regulation was explored by examining conserved, non-coding regions of the *mef2c* locus for enhancer function in transgenic embryos. Of the multiple modular enhancers identified, one enhancer, active in developing neural crest and in ventricular myocardium, was selected to understand how *mef2c* participates in the transcriptional regulatory networks of these tissues. In the neural crest, *mef2c* is found to be under direct transcriptional control of the transcription factor SOX10, a neural crest specification gene, while in the heart, the *mef2c* enhancer's activity is dependent upon TEF factors. In both the developing heart and neural crest, the enhancer's activity is maintained in an autoregulatory fashion by a critical MEF2 element. Because little is known about *mef2c* function in the neural crest, its function in these tissues was explored

further and a neural crest-specific knockout of *mef2c* was generated. MEF2C is shown to function as an interaction partner and transcriptional co-regulator of SOX10, while sharing a *sox10* haploinsufficient pigmentation phenotype. Additionally, mice lacking *mef2c* in the neural crest exhibit severe craniofacial defects and defects in pigmentation. We propose a model where *mef2c* functions as a transcriptional target and partner of SOX10 in neural crest differentiation.

Finally we characterize a genetic fate map of the anterior heart field cells expressing *mef2c* under control of its anterior heart field (AHF) enhancer. This fate map shows that the entire right ventricle, the ventricular septum, and portions of the left ventricle are descendants of the *mef2c*-AHF expressing cells.



11007 11000000

Table of Contents

Dedication.....	iii
Acknowledgements.....	iv
Abstract.....	vi
Table of Contents.....	viii
List of Tables.....	ix
List of Figures.....	x
General Introduction.....	1
Chapters:	
I. Transcriptional regulation of <i>mef2c</i> in the neural crest and its function in the Sox10/Waardenburg pathway.....	5
II. MEF2C function in the Neural Crest is essential for proper Craniofacial Development.....	46
III. Transcriptional regulation of <i>mef2c</i> in the heart.....	67
IV. The right ventricle, outflow tract, and ventricular septum are derived from the anterior heart field.....	90
Final Conclusions.....	122

11007 / 100000

List of tables

Table 1. Genotypes from $wnt-1\ cre^{tg/0}; mef2c^{-/-}$ X $mef2c^{flox/flox}$ crosses	pg. 33
--	--------

UNCE LIBRARY

List Figs or Illustrations

- Figure 1. The *mef2c* locus contains multiple, modular transcriptional enhancers.....pg. 34
- Figure 2. The *mef2c* neural crest enhancer is active in multiple neural crest derived cell lineages.....pg. 35
- Figure 3. The *mef2c* enhancer is active in the developing enteric nervous system.....pg. 36
- Figure 4. Identification of a minimal neural crest enhancer region.....pg. 37
- Figure 5. The *mef2c* neural crest enhancer contains multiple, conserved candidate transcription factor-binding sites.....pg. 38
- Figure 6. Sox10 binds to three predicted SOX-binding sites and activates the *mef2c* neural crest enhancer.....pg. 39
- Figure 7. MEF2C can bind to and induce transcriptional activation through the *mef2c* neural crest enhancer.....pg. 40
- Figure 8. The *mef2c* neural crest enhancer is a direct target of Sox10 in the developing neural crest.....pg. 41
- Figure 9. Mice deficient in *mef2c* have pigmentation defects.....pg. 42
- Figure 10. *Mef2c* in the neural crest is required for normal melanocyte development.....pg. 43
- Figure 11. MEF2C and SOX10 interact and cooperatively induce transcription.....pg. 44
- Figure 12. Model for *mef2c* function in the neural crest.....pg. 45
- Figure 13. *Mef2c* is required in the neural crest for postnatal viability.....pg. 60
- Figure 14. Mice lacking *mef2c* in the neural crest fail to breathe.....pg. 61
- Figure 15. Mice lacking *mef2c* in the neural crest exhibit craniofacial defects.....pg. 62
- Figure 16. A number of craniofacial defects are observed in *mef2c* neural crest knockout mice.....pg. 63
- Figure 17. Craniofacial defects are manifested early in the development of *mef2c* neural crest knockout embryos.....pg. 64

Figure 18. The *mef2c*-F1 enhancer is active in craniofacial precursor cells.....pg. 65

Figure 19. The *mef2c*-F1 enhancer activity is dependent upon endothelin signaling..pg. 66

Figure 20. The *mef2c*-F1 enhancer is active in the developing ventricular myocardium.....pg.67

Figure 21. The *mef2c*-F1 enhancer is active in the developing ventricular myocardium.....pg. 68

Figure 22. TEAD and GATA family members both bind to the *mef2c*-F1 enhancer.....pg. 69

Figure 23. The *mef2c*-F1 enhancer is dependent upon TEF proteins for activation and MEF2 proteins to maintain this activity.....pg. 70

Figure 24. The anterior heart field contributes to the common ventricular chamber in *mef2c* null embryos.....pg. 116

Figure 25. Generation of an anterior heart field specific-Cre transgenic mouse line.....pg. 117

Figure 26. The *mef2c*-AHF-Cre fate map overlaps with the expression of anterior heart field markers during early cardiac development.....pg. 118

Figure 27. The right ventricle, outflow tract, and ventricular septum are derived from the anterior heart field.....pg. 119

Figure 28. The right ventricular endocardium and the endothelium and myocardium of the outflow tract are derived from the anterior heart field.....pg. 120

Figure 29. The epicardium and coronary vessels are not derivatives of the anterior heart field.....pg. 121

UCSF LIBRARY

GENERAL INTRODUCTION

The most fundamental problem in developmental biology is transforming a single fertilized egg into an entire organism. This process is dependent upon cellular differentiation, the process by which a parent cell can give rise to many different and diverse cellular fates. The fertilized egg has the potential to differentiate into cells as diverse as muscle cells, neurons, osteoblasts, or any other cell in the organism. This process of differentiation relies upon the differential activation of genes unique to a particular cell type and is under highly regulated transcriptional control.

One transcription factor strongly implicated in driving the cellular differentiation program is *mef2c*. *Mef2c* is a member of the MADS domain family of transcription factors, named for the first four members of the family to be identified MCM-1, *Agamous*, *Deficiens*, and Serum Response Factor (Shore and Sharrocks, 1995). MADS domain transcription factors are found in organisms as diverse as bacteria, yeast, plants, flies and mammals. Mice and humans have four MEF2 family members: MEF2A, MEF2B, MEF2C, and MEF2D. MEF2 transcription factors form homo-dimers or hetero-dimers with other MEF2 family members and bind to a consensus DNA-binding element known as a MEF2 (5'-YTAWWWWTAR-3') (Black and Olson, 1998). MEF2 proteins are known to interact with a large number of transcriptional regulatory proteins and can function as both positive and negative regulators of gene transcription (Black and Olson, 1998; McKinsey et al., 2001).

11/07/2011

MEF2 transcription factors are essential for driving the differentiation program in multiple different cell types. This has been demonstrated most clearly in mutant flies lacking functional MEF2. These animals express known progenitor markers of somatic, visceral, and cardiac muscle cells, but fail to show any evidence of cellular differentiation in these tissues (Lilly et al., 1995). MEF2 function is also critical for development in the developing mammalian embryo. Mice lacking *mef2c* fail to form functional hearts and die as a result at mid-gestation (Lin et al., 1997). These mice also fail to form a proper vasculature system, potentially implicating *mef2c* in endothelial cell development (Bi et al., 1999; Lin et al., 1998). In the cardiac and skeletal muscle lineages, the transcriptional regulation of *mef2c* is under the direct control of specifying transcription factors, which are a category of transcription factors that confer cell fate and promote the onset of cellular differentiation. In the heart, *mef2c* is under control of the GATA family of specification factors, while in skeletal muscle, MyoD factors activate *mef2c* transcription (Dodou et al., 2004; Dodou et al., 2003).

Mef2c is expressed in other developing tissues, including B and T lymphocytes, neurons in the brain, neural crest cells, skeletal, and smooth muscle, but due to the early embryonic lethality of *mef2c* knockout mice, the function of *mef2c* in these tissues has not been addressed (Leifer et al., 1997; Lyons et al., 1995; Swanson et al., 1998).

Because previous work has shown *mef2c* is a direct target of specifying transcription factors in the skeletal and cardiac muscle lineages, we hypothesized that *mef2c* could function downstream of specification factors in other developing lineages. We therefore

proposed to study transcriptional regulation of *mef2c* to identify regulatory networks involving *mef2c* and its upstream specification factors.

The following work identified upstream regulatory pathways directing *mef2c* expression in developing cardiac and neural crest derived tissues. In chapter 1, a transcriptional enhancer of *mef2c* was identified and shown to be active in neural crest lineages. This enhancer is under the direct transcriptional control of Sox10, a neural crest specification factor [REF!!!]. Further work on this pathway demonstrated that MEF2C functions as a transcriptional partner of Sox10 to activate genes in the developing neural crest, and that *mef2c* function is critical for proper development of neural crest tissues. Chapter 2 investigates the function of *mef2c* in craniofacial development by examining mice lacking *mef2c* in developing neural crest lineages. This work identified another critical role for *mef2c* in development, as mutant mice exhibit multiple craniofacial abnormalities, including hypoplasia or loss of craniofacial skeletal structures. Chapter 3 investigates the transcription of *mef2c* in the developing heart. In studies presented in that chapter, we examined the regulation of a *mef2c* cardiac enhancer, which is dependent upon both an autoregulatory MEF2 element and the function of TEA-domain transcription factors.

Knowledge gained from investigating *mef2c*'s transcriptional regulatory pathways was then applied to further study a population of cardiac progenitor cells in chapter 4. A transcriptional enhancer from *mef2c* was identified to mark a population of cells known as the anterior heart field. This progenitor population was only recently appreciated and

11007 11007

its contributions to the adult heart are not yet well known (Kelly et al., 2001; Mjaatvedt et al., 2001; Waldo et al., 2001). We used the *mef2c* anterior heart field enhancer to direct expression of Cre recombinase and generate a fate map of *mef2c*-expressing anterior heart field cells.

Together, the work presented in these chapters describes an emerging paradigm for *mef2c* function in embryonic development: *Mef2c* is under direct transcriptional control of lineage-restricted specification factors in multiple developing cell types and functions in cooperation with these specification factors to drive cellular differentiation programs.

UNIVERSITY OF MICHIGAN

Chapter 1: Transcriptional regulation of *mef2c* in the neural crest and its function in the Sox10/Waardenburg pathway

I. Introduction

The neural crest lineage is composed of cells that delaminate from the embryonic neural tube, migrate throughout the developing embryo, and give rise to a wide array of tissues, including melanocytes, the craniofacial skeleton, the adrenal medulla, and the glial cells of the peripheral and enteric nervous systems (Le Douarin and Kalchheim, 1999).

Numerous congenital anomalies are due to improper development of the neural crest and its derivatives, and a common cause for neural crest disorders is the mutation of one of the many transcription factors that direct neural crest development (Tassabehji et al., 2005; Noden and Trainor, 2005). Waardenburg syndromes are examples in which disruption of normal transcription factor function results in a number of different symptoms, including hypopigmentation, deafness, and aganglionic colon (Baxter et al., 2004; Spritz et al., 2003). For example, Pax3, MITF, Slug, and Sox10 are each transcription factors known to be important for neural crest development, and all have been implicated in Waardenburg disorders (Epstein et al., 1991; Epstein et al., 1993; Tassabehji et al., 1994; Wollnik et al., 2003; Britsch et al., 2001; Herbarth et al., 1998; Hodgkinson et al., 1993; Hughes et al., 1993; Perez-Losada et al., 2002; Pingault et al., 1998; Sanchez-Martin et al., 2003; Sanchez-Martin et al., 2002; Southard-Smith et al., 1998; Tachibana et al., 2003). Identification of additional transcriptional regulators of neural crest development and determination of how all of these factors interact for proper

UCSF LIBRARY
MARTIN

neural crest development will be important for understanding the etiologies of Waardenburg syndromes and other neural crest disorders.

Among the transcription factors implicated in neural crest development, Sox10 is a key early regulator of neural crest specification and is known to play a role in human congenital anomalies (Pingault et al., 1998; Inoue et al., 2004). As a result, Sox10 function has been intensely studied. Sox10 is an HMG domain transcription factor of the SRY-box family that is essential for neural crest development. Mice lacking *Sox10* fail to develop a functional peripheral nervous system and lack pigmentation (Britsch et al., 2001; Potterf et al., 2001; Southard-Smith et al., 1998; Herbarth et al., 1998). Neural crest cells in these animals fail to migrate and do not survive as efficiently as wild-type cells, and subsequent differentiation to glial cells of the peripheral nervous system and pigment cells in the dermis fails to occur in *Sox10* null embryos (Britsch et al., 2001; Potterf et al., 2001; Southard-Smith et al., 1998; Herbarth et al., 1998). Animals haploinsufficient for *Sox10* exhibit pigmentation deficits on the distal regions of the appendages and on the ventral surface, and frequently develop megacolon as a result of a distal aganglionic or hypoganglionic bowel (Lane and Liu, 1984; Southard-Smith et al., 1998; Herbarth et al., 1998). A mutation in Sox10 in mice was originally identified due to the pigmentation and megacolon phenotypes caused by haploinsufficiency and is referred to as *Dominant Megacolon (Dom)* (Lane and Liu, 1984; Herbarth et al., 1998; Southard-Smith et al., 1998). The phenotypes exhibited by *Sox10* and *Dom* mutant mice serve as an excellent animal model for Waardenburg syndrome in humans (Southard-Smith et al., 1999). Patients haploinsufficient for *SOX10* exhibit symptoms of

11007 11000000

Waardenburg syndrome type IV, or Hirschsprung disease, which include areas of hypopigmentation, auditory pigment disorders, and aganglionic colon (Spritz et al., 2003). In both the mouse and human, the frequency and the severity of Waardenburg symptoms are highly variable (Southard-Smith et al., 1999; Tachibana et al., 2003). This implies that other genes are likely to have modifying effects on the severity of a phenotype in a *SOX10* haploinsufficient individual.

Several genetic modifiers of *Sox10* have been identified in mice. Mutations in *Endothelin receptor B* (*EdnrB* or ET_B) and *Sox8* have been shown to increase both the severity and frequency of the observed *Sox10* phenotype (Cantrell et al., 2004; Maka et al., 2005). *Sox8* functions as a modifier of *Sox10*, as animals haploinsufficient for both *Sox8* and *Sox10* were less than one-third as likely to survive to weaning as animals haploinsufficient for only *Sox10* (Maka et al., 2005). In this case, increased cell death in the vagal neural crest before gut colonization is responsible for the more severe phenotype (Maka et al., 2005). Similarly, ET_B functions as a genetic modifier of *Sox10* by affecting both the severity and frequency of megacolon in *Sox10*^{+/-} animals (Cantrell et al., 2004; Zhu et al., 2004). It is likely that additional genetic causes and modifiers of Waardenburg syndrome are yet to be identified. One way to identify additional genes involved in the Waardenburg syndrome and other neural crest disorders is to identify the transcriptional regulatory networks directed by *Sox10* in the developing neural crest. Indeed, modifier roles for *Sox8* and ET_B in the mouse model of Hirschsprung disease were identified by a candidate approach based upon their common function and expression in *Sox10* regulated tissues (Cantrell et al., 2004; Maka et al., 2005).

Here we show that *mef2c*, a MADS domain containing transcription factor, is a direct target of Sox10 in developing neural crest lineages. *Mef2c* has previously been shown to be essential for proper cardiac development, as embryos lacking *mef2c* die at midgestation due to defects in cardiovascular development (Lin et al., 1997). In other lineages, transcriptional regulation of *mef2c* is under the direct control of specification factors, which are the earliest transcription factors to confer cell fate and promote the onset of cellular differentiation. In skeletal muscle, for example, *mef2c* is activated directly by MyoD, which is critical for myoblast specification during development (Dodou et al., 2003; Wang et al., 2001). Interestingly, MEF2C has also been shown to function as a transcriptional co-regulator of MyoD by cooperatively activating genes required for muscle differentiation (Black et al., 1998). The essential role for MEF2 activity in differentiation is exemplified in *Drosophila* (Lilly et al., 1995). Mutation of the single *mef2* gene in flies results in disruption of development in all three muscle lineages, yet each lineage expresses normal specification markers. In mice, *mef2c* expression has been documented in the developing neural crest, but its regulation and function in that lineage has not been investigated (Edmondson et al., 1994). Based upon *mef2c* function in other developing tissues, we hypothesized that it would function downstream of specification factors and act as a critical transcription factor driving the differentiation of neural crest-derived tissues.

In this work, we identified an enhancer element from *mef2c* that directs transcription to the developing neural crest and its derivatives. These neural crest derived lineages

include melanocytes and the glia of the peripheral and enteric nervous systems. We show that *mef2c* enhancer function in the neural crest is dependent upon SOX DNA-binding elements, which are efficiently bound by Sox10 protein and are essential for Sox10 dependent *trans*-activation in cell culture-based reporter assays. We also investigated the function of *mef2c* in the neural crest through conditional inactivation in mice, which demonstrates that *mef2c* is required for proper melanocyte development. Finally, we show that MEF2C physically interacts with Sox10, and together, these proteins cooperatively activate transcription. Thus, we propose a model for MEF2C function in the neural crest as a direct transcriptional target and partner of Sox10.

I. Results

*Identification of a *mef2c* enhancer that directs expression to developing neural crest lineages*

Several transcription factors are known to be required for proper development of the neural crest, and deficiencies of these factors can lead to human disease. *Mef2c* has been implicated in the development of a number of tissues including, but not limited to, skeletal muscle, vascular endothelium, myocardium, and neuronal tissues of the CNS, and it is believed to play critical roles in the development and function of these systems. It also has been reported that *mef2c* is expressed in neural crest cells (Edmondson et al., 1994), though the regulation and function of *mef2c* in the neural crest has not been examined.

UCSF LIBRARY

To understand how *mef2c* expression is controlled in such a diverse number of developmental lineages and to identify the transcriptional regulatory networks in these lineages, previous work sought to define transcriptional enhancers in the *mef2c* locus. These studies showed that the transcriptional regulation of the *mef2c* locus is controlled by multiple distinct, evolutionary conserved, modular enhancers (De Val et al., 2004; Dodou et al., 2004; Dodou et al., 2003). For example, enhancer modules that drive expression in skeletal muscle, anterior heart field, and vascular endothelium have all been recently identified (Fig. 1A and De Val et al., 2004; Dodou et al., 2004; Dodou et al., 2003; Wang et al., 2001). Using a similar approach, we sought to identify enhancers that direct *mef2c* expression to the neural crest. Regions of non-coding DNA in the *mef2c* locus with strong evolutionary conservation were systematically tested for enhancer activity *in vivo*. These non-coding sequences were cloned upstream of the Hsp68 promoter and *lacZ*, and the resulting constructs were used to generate transgenic mouse embryos and assayed for enhancer activity via β -galactosidase activity. Using this approach, a 7 kb region of the *mef2c* locus, residing between 7 and 14 kb upstream of the first coding exon, exhibited enhancer activity in developing cardiac, bone, and neural crest tissues (Fig. 1B and C). This 7 kb enhancer region was named *mef2c*-F1. The activity of this enhancer in the developing cardiac and osteoblast lineages will be discussed later in this work (chapter 4 and general conclusions), while enhancer activity in neural crest lineages will be described in this chapter.

Transgenic embryos bearing the *mef2c*-F1 enhancer construct were studied in detail to understand the spatial and temporal expression directed by this *mef2c* enhancer in the

neural crest. Enhancer activity in the neural crest was detected as early as 8.25 dpc in the neural fold mesenchyme (Fig. 2A, B). By 9.5 dpc, β -gal activity was detected in cranial ganglia as well as in the rostral most dorsal root and sympathetic ganglia (Fig. 23A). At 10.5 dpc, enhancer activity was less robust in the craniofacial mesenchyme, particularly in the first and second branchial arches, while expression associated with the developing cranial nerves became more pronounced (Fig. 1B and Fig. 18A). In addition, expression in the developing melanocyte lineages became apparent at this stage. By 11.5 dpc, expression in the craniofacial mesenchyme was no longer detected, however enhancer activity associated with the cranial nerves, dorsal root ganglia, sympathetic chain ganglia, and enteric ganglia was evident (Fig. 2C). Enhancer activity in melanocyte precursors remained robust, with expression detected more readily in rostral melanocytes than in caudal melanocytes (Fig. 2C, G).

The expression pattern directed by the *mef2c* neural crest enhancer at 11.5 dpc was almost identical to the expression pattern of *Sox10*, with overlap in the ganglia of the peripheral nervous system, in the cranial nerves, and in the enteric ganglia (Fig. 2, compare panels C & D). The major difference in expression pattern driven by the *mef2c* enhancer with that of *Sox10* was that while the *mef2c* enhancer was active in the developing myocardium, *Sox10* was not expressed in the heart. However, the similar expression pattern of *Sox10* and the activity of the *mef2c* neural crest enhancer suggested the possibility that *Sox10* and MEF2C might function in the same transcriptional regulatory network.

By 13.5 dpc, *mef2c* enhancer activity continued throughout the peripheral nervous system, as well as in melanocytes, cranial nerves, and in the developing enteric nervous system (Fig. 2E). Sagittal sections of *mef2c*-F1-*lacZ* embryos exhibited β -gal activity within a number of neural crest derived tissues including the nerves projecting from the trigeminal ganglion (cranial nerve V), within the dorsal root ganglia, and in sympathetic chain ganglia (Fig. 2F).

Mef2c neural crest enhancer activity marks developing melanocyte and PNS glial cells

Expression directed by *mef2c* in the developing melanocyte lineage began at approximately 10.5 dpc and continued throughout development. β -gal activity was apparent in single cells of the peri-ocular region of the embryo at 11.5 dpc (Fig. 2G). Early activity of the *mef2c*-F1 enhancer appeared to be more robust in rostral melanocyte populations than in the more dorsal cells when compared to known melanocyte markers such as *pmel17* or *Dct* (Fig. 2C and data not shown). β -gal activity was observed in melanocytes into postnatal stages as revealed by sections through perinatal skin (Fig. 2H). Staining was apparent in follicular melanocytes as well as in the melanocytes that occupy the dermal-epidermal border at 18.5 dpc (Fig. 2H). While robust β -gal activity was observed throughout prenatal development in the melanocyte lineage, the *mef2c*-F1 enhancer reached maximal activity in the developing peripheral and enteric nervous systems earlier in development.

Expression directed by the *mef2c* neural crest enhancer in PNS glial cells was examined more closely in the developing phrenic nerve and within the enteric nervous system (Fig. 2I, J and Fig. 3). The phrenic nerve projects from the third to fifth cervical nerves and stimulates contraction of the diaphragm, which is required for breathing. Neural crest-derived Schwann cells associate with the phrenic nerve as it develops. At 13.5 dpc, *mef2c*-F1-*lacZ* expression was detected in a robust pattern in the diaphragm, consistent with the neural crest-derived Schwann cells associated with the phrenic nerve (Fig. 2I). Enhancer activity associated with the phrenic nerve continued at 16.5 dpc, however the terminal branches were now the focus of enhancer activity rather than the nerve trunk (Fig. 2J). Expression associated with the phrenic nerve, as well as other nerves of the PNS, appeared to peak around 13.5 dpc and then diminish in late gestation. This pattern of expression suggests that *mef2c* may function early in the differentiation of the PNS glial cells. A similar wave of *mef2c*-F1 enhancer activity was observed in the developing enteric nervous system. At 11.5 dpc, β -gal activity was observed throughout the developing gut (Fig. 3A). Robust enhancer activity was also observed in the 13.5 dpc dissected gut, but by 16.5 dpc, expression of β -gal began to diminish (Fig. 3C, D). Sections through the developing gut revealed that β -gal expression directed by the *mef2c*-F1-*lacZ* enhancer was within the myenteric plexus (Fig. 3B). Again, the pattern of *mef2c* enhancer expression in the developing enteric nervous system suggests that *mef2c* is likely to function early in ENS development.

UCSF LIBRARY

The mef2c neural crest enhancer contains multiple, functional cis-regulatory elements

To identify the specific *cis*-regulatory elements responsible for directing expression in the neural crest lineage, we generated a series of deletions within the 7 kb enhancer that targeted areas of high mouse – opossum homology. These constructs were then assayed for enhancer function in transgenic mouse embryos. A summary of the results is depicted in Figure 4A. These deletional analyses identified a 300 bp region of the enhancer that is both sufficient for enhancer function (the 300 bp region alone is capable of driving *lacZ* expression in the same pattern driven by the full length enhancer, compare Fig. 4B and 4C) and required for enhancer function (when the 300 bp region is deleted, β -gal activity is no longer detected in transgenic embryos, Fig. 4D). When this 300 bp element was examined for potential *cis*-regulatory that might be involved in neural crest expression, we identified three putative SOX binding sites (5'-WWCAAWG-3'), which bind members of the SRY-box family of HMG-domain containing transcription factors, and a single MEF2 binding site (5'-YTAWWWWTAR-3')(Andres et al., 1995; Schlierf et al., 2002) (Fig. 5).

Sox10 was assayed for DNA binding to the putative SOX elements within the *mef2c*-F1 enhancer by electrophoretic mobility shift assay (EMSA) (Fig. 6). Rabbit reticulocyte lysate expressing Sox10 DNA binding domain bound to radiolabeled oligonucleotides containing a control Sox10 binding site from the *protein zero* promoter and retarded the mobility of the probe (Fig. 6A, lane 2) (Peirano and Wegner, 2000). This was efficiently competed with an excess of unlabeled oligonucleotide containing control SOX binding

UCSF LIBRARY

site, but not by excess oligonucleotide containing a mutant version of this control site (Fig. 6A, lanes 3, 4). Excess unlabeled oligonucleotides with sequence from any of the three putative SOX elements from the *mef2c* neural crest enhancer also competed for Sox10 interaction with the control probe. In each case, the competition was dependent upon the predicted SOX binding sequence, as mutant versions of these oligos no longer competed for the interaction between Sox10 and the control probe (Fig. 6A, lanes 5-10). Sox10 programmed lysate also induced a mobility shift with radiolabeled oligonucleotides containing the putative SOX elements from the *mef2c* neural crest enhancer (Fig. 6B). In each case, the mobility shift depended upon the SOX binding sequence, as excess unlabeled probe efficiently competed for Sox10 interaction with the radiolabeled probe, but mutant versions of these oligonucleotides failed to compete with the wild type probe (Fig. 6B). Thus, Sox10 appears to bind directly to each of the predicted Sox10-responsive elements in the *mef2c*-F1 enhancer region.

Sox10 has been shown to mediate strong transcriptional activation of several genes expressed in the developing glial and melanocyte lineages, including *Mitf*, *Dct*, *Protein zero*, *Connexin 32*, and *ET_B* (Bondurand et al., 2000; Lee et al., 2000; Verastegui et al., 2000; Potterf et al., 2000; Jiao et al., 2004; Potterf et al., 2001; Peirano et al., 2000; Bondurand et al., 2001; Zhu et al., 2004). We assayed whether Sox10 might activate *mef2c* expression through the 300 bp *mef2c* neural crest enhancer element. When Sox10 expression plasmid was co-transfected into C3H10T $\frac{1}{2}$ with a control reporter construct, very little reporter gene activity was detected (Fig. 6C, lane 2). Similarly, when the 300 bp *mef2c*-F1 enhancer was transfected in the absence of Sox10, little reporter gene

UCSF LIBRARY

activity could be detected (Fig. 6C, lane 3). However, when Sox10 expression plasmid was co-transfected with the 300 bp *mef2c* reporter, robust activation of the reporter gene occurred (Fig. 6C, lane 4). This activation was dependent upon the presence of the SOX binding sites, since mutation of these elements eliminated Sox10-dependent activation of this enhancer (Fig. 6C, lane 6). Taken together, the results of Fig. 6 strongly support the notion that the SOX binding sites in the *mef2c*-F1 enhancer represent *bona fide* Sox10 responsive elements and that *mef2c* is a direct transcriptional target of Sox10.

In a similar set of experiments, the MEF2 element within the 300 bp enhancer was tested for MEF2 protein binding and responsiveness to MEF2-dependent activation. MEF2C was shown to interact with the 300 bp MEF2 element in an EMSA assay (Fig. 7A, provided by Pooja Agarwal). When MEF2 was co-transfected with the reporter construct, reporter gene activity was detected at levels approximately 10-fold higher than in controls (Fig. 7B, lanes 2-4). This activity was dependent upon a functional MEF2 *cis*-regulatory element as mutation of the MEF2 binding site eliminated reporter gene activity (Fig. 7B, lanes 5-6). Taken together, the results of Fig. 7 support the notion that a *bona fide* MEF2 element resides within the *mef2c*-F1 enhancer.

Mef2c is a direct transcriptional target of Sox10 in developing neural crest lineages

To test further the notion that Sox10 and MEF2 interact with the *mef2c* enhancer, we tested the requirement for the *cis*-regulatory elements *in vivo* in transgenic embryos. To test the functionality of the SOX binding elements, each was mutated in the context of the

UCSF LIBRARY

7 kb *mef2c*-F1 enhancer. Using the wild type enhancer, β -gal expression was observed in developing neural crest derived lineages, including melanocytes, glial cells throughout the peripheral nervous system, and in the enteric nervous system at 11.5 dpc (Fig. 8A). β -gal expression was also observed in the developing hearts of embryos with the wild type enhancer transgene (Fig. 8A). In contrast, the enhancer with mutated SOX elements could no longer direct expression in neural crest-derived lineages and was only capable of directing cardiac expression *in vivo* (Fig. 8C). Loss of expression in neural crest-derived tissues further suggests that *mef2c* is a direct transcriptional target of SOX factors in the neural crest, and that these factors are required for activation of the *mef2c* neural crest enhancer. Because humans and mice haploinsufficient for *Sox10* display symptoms of Waardenburg-Hirschsprung disease, we wanted to examine the function of the *mef2c* neural crest enhancer in the *Sox10*^{Dom/+} mouse model of this disease (Lane and Liu, 1984). Mice containing the *mef2c*-F1-*lacZ* transgene were crossed with mice harboring the *Dom* allele. Indeed, enhancer activity was significantly reduced in all neural crest lineages in the *Dom*/+ background, while expression in the developing heart was unaffected (Fig. 8B). The decrease in *mef2c*-F1 enhancer activity in *Sox10*^{Dom/+} mice strongly supports the hypothesis that Sox10, rather than other Sox family members, is responsible for activating the *mef2c* enhancer in neural crest derivatives in the peripheral and enteric nervous systems and in melanocytes. In addition, the decrease in *mef2c* enhancer activity in the mouse model of Waardenburg-Hirschsprung disease suggests the possibility that *mef2c* may be involved in neural crest disorders such as Waardenburg syndromes in humans as well.

UCSF LIBRARY

Mice deficient in mef2c exhibit pigmentation defects

Humans and mice haploinsufficient for *Sox10* and other important neural crest transcription factors often exhibit symptoms of neurocristopathies such as Waardenburg syndrome, which can include hypopigmentation, nervous system disorders, and aganglionic colon (Lane and Liu, 1984; Herbarth et al., 1998; Pingault et al., 1998; Southard-Smith et al., 1998; Inoue et al., 2004). To determine whether *mef2c* is required for normal function of neural crest derived tissues, we examined pigmentation and nervous system function in mice heterozygous for *mef2c*. Indeed, approximately 7% of adult mice heterozygous for *mef2c* have a white belly spot, (Fig. 9A), which is a characteristic lack of pigmentation on the ventral side of the animal and is commonly found in other examples of transcription factor gene heterozygosity in the neural crest, including *Pax3* and *Sox10* (Epstein et al., 1991; Auerbach R, 1954; Lane and Liu, 1984). Belly spotting in the *mef2c*^{+/-} mice was typically less severe than belly spotting in *Sox10*^{Dom/+} mice (Fig. 9B). Because *mef2c* null animals die at 9.5 dpc with severe cardiovascular defects, the complete loss of *mef2c* function in the neural crest has not been examined previously. To circumvent this early neonatal lethality, we conditionally inactivated a floxed allele of *mef2c* in the neural crest using the *Wnt1-cre* transgene to drive Cre expression in the neural crest (Vong et al., 2005; Danielian et al., 1998). Animals lacking *mef2c* in the neural crest were born at the expected Mendelian ratios (see table 1), but die at birth due to an airway obstruction caused by severe craniofacial defects (to be discussed further in chapter 2).

UCSF LIBRARY

Because *mef2c* functions downstream of Sox10 in the neural crest, we examined *mef2c*^{flox/tm1;Wnt1-cre/0} animals for the defects typically observed in animals lacking *Sox10*. No phenotype was observed in the enteric or peripheral nervous system of *mef2c* conditional knockouts. Markers of neurofilament and associated glia all appeared normal (data not shown). While we did not observe any obvious Schwann cell defects, neural crest conditional knockout animals exhibited a decrease in the levels of pigment in the dermis (Fig. 10). Compared to wild type littermates, neonatal mice had fewer pigmented hair follicles in dermis (Fig. 10A, knockout skin on top, control on bottom). The number of melanocyte clusters in wild type and *mef2c* conditional knockout animals was quantified; revealing knockouts had roughly half the number of melanocyte clusters as wild type mice (Fig. 10C, D). In addition, within each cluster of melanocytes, there appeared to be substantially less pigment in *mef2c* neural crest knockout skin than in control skin (arrow in Fig. 10A). These data could result from less pigment being produced in each cell or from fewer melanocytes per cluster, although this is not known presently. While *mef2c* neural crest conditional knockouts clearly exhibited a significant reduction in pigment levels, it was not as severe as that exhibited in *Sox10*^{Dom/Dom} animals, which completely lack all pigment (Fig. 10B, and as reported by (Southard-Smith et al., 1998; Potterf et al., 2001). Taken together, these data indicate that *mef2c* function in the neural crest is important for melanocyte development. Additionally, the shared melanocyte phenotype between animals lacking *Sox10* and animals lacking *mef2c* further implicates *mef2c* in the Sox10 pathway.

UCSF LIBRARY

MEF2C and Sox10 physically interact and cooperatively activate transcription

We have shown that *mef2c* is a direct transcriptional target of Sox10. In addition, loss of *mef2c* function in the neural crest results in a similar phenotype to some aspects of the phenotypes observed in *Sox10* mutants. In other tissues, MEF2C functions as a transcriptional partner of its upstream activator. For example, MEF2C directly interacts with MyoD to synergistically activate transcription of skeletal muscle genes (Black et al., 1998; Molkenin et al., 1995). A similar interaction has been observed with MEF2C and GATA4 in the developing heart (Morin et al., 2000). Based on these examples, we hypothesized that MEF2C might function as a transcriptional partner of Sox10 in the neural crest. As a first step, we determined whether MEF2C and Sox10 physically interact. A GST-MEF2C fusion protein was constructed and used in pulldown assays with recombinant Sox10 (Fig. 11A). In control reactions, neither radiolabeled Sox10, nor the N-terminal portion of Sox10 alone, which includes the protein's HMG DNA-binding domain, interacted with GST alone (Fig. 11A, lanes 2, 4). However, full-length Sox10 and the HMG domain of Sox10 alone each interacted with the GST-MEF2C fusion protein (Fig. 11A, lanes 1, 3). Interaction of GST-MEF2C with the N-terminal portion of Sox10 was more robust than the interaction with the full-length protein (compare Fig. 11A lanes 1 and 3). A stronger interaction with the N-terminal portion of Sox10 is consistent with the interaction that has been observed previously between Sox18 and MEF2C in endothelial cells (Hosking et al., 2001).

UCSF LIBRARY
MORNING

The direct interaction between MEF2C and Sox10 suggests these factors may function as transcriptional partners. To test whether Sox10 and MEF2C cooperatively activate transcription, we examined the ability of these proteins to activate the neural crest enhancer of *mef2c*, which contains binding sites for Sox10 and MEF2C (Fig. 5). Interestingly, when Sox10 and MEF2C were co-transfected with the *mef2c*-F1-*lacZ* 300 bp reporter construct, they synergistically activated reporter gene expression (Fig. 11B). Reporter gene activation by either Sox10 or MEF2C alone was roughly 10-15 fold above background levels, whereas co-transfection of both Sox10 and MEF2C resulted in 75-fold activation of the reporter (Fig. 11B, lanes 5-7). Taken together, the results presented in figure 11 strongly support a model in which Sox10 and MEF2C are transcriptional partners, and suggest a potential mechanism for MEF2C function in the neural crest. In this model, MEF2C functions as a partner of Sox10 to activate neural crest differentiation (Fig. 12), which is consistent with MEF2C function in other developmental lineages (Black and Olson, 1998; McKinsey et al, 2001).

I. DISCUSSION

While the role of *mef2c* in development has been studied in several developmental contexts including the cardiac and skeletal muscle lineages, its expression and function in the developing neural crest lineages was not defined prior to the present studies. For the first time, work shown here identifies pathways involving *mef2c* in the developing neural crest lineages. We show that a *mef2c* neural crest enhancer is under the direct transcriptional control of Sox10 in the developing glial and melanocyte lineages, and that *mef2c* expression is compromised in a mouse model of neural crest disease. We have

UCSF LIBRARY

also shown that MEF2C and Sox10 function as transcriptional partners, and that deficiency of *mef2c* in the neural crest results in pigmentation defects reminiscent of Waardenburg syndrome. Finally, we propose that MEF2C plays a critical function in neural crest development as both a transcriptional target and partner of Sox10, which implicates *mef2c* as a potential cause or modifier of human disorders of the neural crest.

MEF2C as a transcriptional co-regulator

As we have shown here, Sox10 is required to activate the *mef2c*-F1 enhancer in the neural crest. MEF2 factors are also necessary to maintain this enhancer's activity, since deletion of a conserved MEF2 element within the enhancer ablates enhancer function at later developmental timepoints (Fig. 23, and discussed in Chapter 3). Further, we show that MEF2C and Sox10 can cooperate to activate the *mef2c* neural crest enhancer. Based upon MEF2C function in other developing lineages, one might predict that MEF2C and Sox10 will coordinately regulate the expression of multiple genes in developing neural crest lineages (Fig. 12). Indeed, a brief search of known Sox10-responsive enhancers showed several with putative MEF2 binding sites that could potentially be subject to cooperative regulation by the two factors (data not shown). Future studies will elaborate on the function of MEF2C in the neural crest and identify the genes under its transcriptional control in that lineage and its derivatives.

UCSF LIBRARY

Is mef2c implicated in neural crest disorders?

Of the patients exhibiting symptoms of Hirschsprung disease, only 50% harbor mutations in known disease loci (Parisi and Kapur, 2000). A genetic cause in the other 50% of these cases remains unknown. Further, in many of the cases with known genetic causes, the severity or the symptoms are highly variable (Black, 2006). This is likely due to genetic variability at modifier loci. *Sox8* and *EdnrB* were identified as candidate modifiers of the *Sox10* phenotype in mice due to their common phenotypes and expression patterns (Cantrell et al., 2004; Maka et al., 2005). Mice with one or two of these mutant modifier alleles have an increased susceptibility to and severity of the symptoms observed in the *Sox10*^{+/-} background (Cantrell et al., 2004; Maka et al., 2005). *Mef2c* neural crest conditional knockout mice do not exhibit a phenotype as severe as in mice lacking *Sox10*. Yet because *mef2c* lies downstream of *Sox10* and functions as a transcriptional partner of *Sox10*, we propose *mef2c* as a candidate modifier of *Sox10* or other genes in the Waardenburg/Hirschsprung pathway, including those of the endothelin signaling pathway, *EdnrB* and *ECE-1*. Indeed, a relationship between the *mef2c* neural crest enhancer and endothelin signaling will be investigated further in chapter 2.

Mice lacking *mef2c* in the neural crest do not exhibit megacolon, which is typical of Hirschsprung disease, and have no obvious defects in the PNS. Lack of these phenotypes could be due to functional redundancy by other MEF2 family members. Interestingly, a conserved region of the *mef2d* locus also contains multiple conserved SOX elements and

UCSF LIBRARY

a MEF2 element and could regulate transcription in a similar fashion to *mef2c* (Data not shown).

As Hirschsprung disease is usually manifested after birth, when the *mef2c* neural crest knockout mice die, it is also a possibility that these animals might exhibit symptoms if allowed to progress further in development. Use of alternate Cre drivers that will specifically ablate neural crest cells not affecting craniofacial development may circumvent the neonatal lethality observed in the *Wnt1-cre* generated knockouts and allow further investigation of *mef2c* function in the PNS and melanocyte populations past postnatal day zero.

UCSF LIBRARY

Chapter1 Figure legends

Fig. 1. The *mef2c* locus contains multiple, modular transcriptional enhancers. (A) Regions of the *mef2c* locus with high mouse-human sequence homology (indicated as yellow or green boxes) were systematically tested for enhancer function by cloning upstream of the HSP68-*lacZ*-SV40 polyA reporter construct and assaying for function in transgenic mice. Previously identified enhancers are depicted with red arrows. The neural crest/ventricular myocardium enhancer, known as *mef2c*-F1, is shown in green. Exons are delineated with vertical black lines. Exon 5 is the first translated exon. Examples of *mef2c*-F1 enhancer activity are shown in B and C. *mef2c*-F1-*lacZ* transgenic embryos were assayed for β -gal activity at 10.5 dpc (B) or 16.5 dpc (C). Note expression in the neural crest-derived tissues (B), in the developing heart (arrow in B), and in the developing osteoblasts (C).

Fig.2. The *mef2c* neural crest enhancer is active in multiple neural crest derived cell lineages. Embryos containing a transgene driving *lacZ* expression under control of the *mef2c* neural crest enhancer were analyzed for β -gal activity at multiple developmental timepoints. Neural crest expression is first detected at approximately 8.0 dpc in the ectomesenchyme of the neural folds (arrow in A). Expression at this time is also observed in the heart and in cells lateral to the somites. Transverse sections through 8.0 dpc neural folds show β -gal positive cells in the mesenchyme (arrows in B). In 11.5 dpc embryos, β -gal activity is observed throughout the developing peripheral nervous system, in both the dorsal root ganglia and sympathetic ganglia (arrow) and in the brachial nerve (BN) (C). Expression is also seen in the trigeminal ganglia and is robust in the maxillary

USF 10/21/01

component of the trigeminal nerve. At this stage, expression is also observed in the developing melanocytes, and in the developing heart (C). Sox10 mRNA was detected by *in situ* hybridization at 11.5 dpc (D). Sox10 message is detected in the majority of cells that contain active *mef2c* enhancer including the dorsal root and sympathetic ganglia, trigeminal ganglion and associated nerves, and in the brachial nerve (compare C and D). In 13.5 dpc embryos transgenic for the *mef2c* enhancer – *lacZ*, expression is detected throughout the peripheral nervous system, in melanoblasts, and in the developing enteric nervous system (arrowhead) (E). Section of a 12.5 dpc transgenic embryo reveal β -gal activity associated with dorsal root (arrowhead) and sympathetic ganglia (F). Staining is also associated with the branches of the trigeminal ganglion (T) (F). A higher magnification image of the 11.5 dpc embryo reveals staining in the melanocytes near the eye (G). Staining in this image is also prominent in the maxillary component of the trigeminal nerve. A section through the skin on the trunk of an 18.5 dpc mouse reveals β -gal positive melanocytes at the dermal-epidermal border as well as in the hair follicles (arrowhead) (H). Staining of diaphragm hemisegments at 13.5 dpc (I) and 16.5 dpc (J) reveals that the *mef2c* enhancer is more active in Schwann cell precursors, and becomes less active as development proceeds. Compare staining in the trunk of the phrenic nerve at the two timepoints.

Fig. 3 The *mef2c* enhancer is active in the developing enteric nervous system. Staining is observed throughout the enteric nervous system as early as 11.5 dpc, as exhibited in an embryo that has been partially cleared to reveal the developing gut (A). Sections through the 13.5 dpc gut show β -gal staining associated with the myenteric plexus (B). Whole

1/11/07 12:50 PM

mount staining of a dissected 13.5 dpc gut reveals robust enhancer activity throughout the developing gastrointestinal tract (C). This staining occurs in a net-like pattern consistent with the developing enteric nervous system. By 16.5 dpc, the enhancer activity in the gut lessens, with the more rostral gut becoming almost devoid of β -gal activity (D). Note that in the inset, a non-transgenic gut was stained for comparison of endogenous β -gal activity. Transgene specific staining is still observed in the caudal gut at this stage. st, stomach; arrowheads point to distal gut.

Fig. 4 Identification of a minimal neural crest enhancer region. The 7 kb *mef2c* intronic region was analyzed for regions of high sequence conservation between the mouse and the opossum (red boxes). This information was used to guide a series of deletions of the enhancer construct to isolate the sequence responsible for enhancer activity. On the right, a plus sign indicates the depicted fragment could replicate the full-length transgene activity while the minus sign indicates no enhancer activity for the given fragment (A). This analysis revealed a 300 bp element that is both sufficient to direct transgene expression (see construct 3.0-3.3kb) and necessary to direct transgene expression (see construct del3-3.3kb). Representative wild-type (B), 3.0-3.3kb (C), and del3-3.3kb (D) transgenic 11.5 dpc embryos are shown as an example of the data depicted in panel A.

Fig. 5 The *mef2c* neural crest enhancer contains multiple, conserved candidate transcription factor-binding sites. ClustalW analysis comparing the enhancer sequence of mouse, rat, human, and chick revealed multiple pockets of evolutionary conservation. Among the pockets of evolutionary conservation were three consensus Sox10 binding

UCSF LIBRARY
MAR 27 2007

sites (orange), an MCAT element (yellow), two consensus GATA elements (green), and a MEF2-binding element (purple). Note that GATA elements are only well-conserved among mammalian species. Asterisks indicate nucleotides conserved amongst all four species.

Fig. 6 Sox10 binds to three predicted SOX-binding sites and activates the *mef2c* neural crest enhancer. EMSA analysis was used to test the putative SOX-binding elements of the *mef2c* neural crest enhancer. (A) Oligos containing a protein zero promoter SOX-binding element were radiolabeled and assayed for an ability to bind to lysate programmed to express Sox10 protein. Unprogrammed lysate did not form a specific interaction with the radiolabeled oligonucleotides (A, lane 1), however, lysate programmed with Sox10 induced a gel mobility shift (A, lane 2). This shift could be competed by adding an excess of unlabeled oligos containing control SOX-elements (A, lane 3), but would not be competed with mutant versions of these oligos (A, lane 4). Oligos containing the putative SOX-binding sites from the *mef2c* neural crest enhancer (labeled S1-3) could all compete for binding to programmed lysate (lanes 5, 7, 9) while the mutant versions of these oligos could not (lanes 6, 8, 10). (B) In this experiment, oligos containing the putative SOX elements were each radiolabeled for EMSA. In lanes 1-6, the first SOX element is labeled, in lanes 7-12, the second SOX element is labeled, and in lanes 13-18, the third element is labeled. In each case, the mobility shift of the radiolabeled oligos was dependent upon lysate programmed for Sox10, and could not be induced by unprogrammed lysate (compare lanes 1 & 2, 7 & 8, and 13 & 14). Also in each case, binding of the radiolabeled oligos could be competed with an excess of cold

UCSF LIBRARY

oligos containing the protein zero SOX-binding site, but not by mutant versions of these oligos (lanes 3 & 4, 9 & 10, and 15 & 16). Also in each case, the binding could be competed with an excess of cold oligo containing the corresponding *mef2c* SOX-binding site, but not by an oligo containing the mutant version of these sites (lanes 5 & 6, 11 & 12, and 17 & 18). In panel C, 10T ½ fibroblast cells were transfected with a β -galactosidase reporter construct either containing the wild-type *mef2c* 300 bp enhancer or a mutant version of this enhancer with the SOX-binding elements disrupted. When the wild-type enhancer/reporter construct is co-transfected with a Sox10 expression plasmid, strong activation of the reporter gene is observed (C, lane 4). This activation is not observed when the wild-type enhancer is transfected without the Sox10 expression plasmid (lane 3) or when Sox10 plasmid is co-transfected with the mutant version of the enhancer/reporter (lane 6).

Fig. 7 MEF2C can bind to and induce transcriptional activation through the *mef2c* neural crest enhancer. (A) Oligos containing a *myogenin* MEF2-binding element were radiolabeled and assayed for an ability to bind to lysate programmed to express MEF2C protein. Unprogrammed lysate did not form a specific interaction with the radiolabeled oligonucleotides (A, lane 1), however, lysate programmed with MEF2C induced a gel mobility shift (A, lane 2). This shift could be competed by adding an excess of unlabeled oligos containing control *myogenin* MEF2-element (A, lane 3), but would not be competed with mutant versions of this oligo (A, lane 4). Oligos containing the putative MEF2-binding sites from the *mef2c* neural crest enhancer (labeled wtM) could compete for binding to programmed lysate (A, lane 5) while the mutant version of this oligo could

UCSF LIBRARY

not (A, lane 6). In lanes 7-12, the MEF2 site of the *mef2c* enhancer was radiolabeled and assayed for direct binding to unprogrammed lysate (A, lane 7) or lysate programmed to express MEF2C protein (A, lane 8-12). In panel B, 10T ½ fibroblast cells were transfected with a β -galactosidase reporter construct either containing the wild-type *mef2c* 300 bp enhancer or a mutant version of this enhancer with the MEF2-binding elements disrupted. This experiment shows that MEF2C can induce reporter gene activation through the *mef2c* enhancer (lane 4). This activation was dependent upon co-transfection of MEF2C expression plasmid (lane 3). The presence of a wild-type MEF2-binding element was also required as a mutant version of this construct was no longer responsive to MEF2C-dependent *trans*-activation (lane 6).

Fig. 8. The *mef2c* neural crest enhancer is a direct target of Sox10 in the developing neural crest. The 7 kb *mef2c* enhancer-*lacZ* reporter construct directs β -gal expression in the neural crest derivatives including throughout the peripheral nervous system, in melanoblasts, and in the enteric nervous system (A). Expression is also detected in the developing heart (A). In the *Sox10*^{+/-} embryo, the *mef2c* transgene activity is diminished in all neural crest derived tissues, but remains robust in the developing heart, indicating that Sox10 is required for normal activation of the *mef2c* enhancer in the neural crest (B). A mutant version of the 7 kb *mef2c* transgene reporter with disruptions in the SOX-binding sites is not active within neural crest derived tissues (C). Disruption of the SOX elements does not prevent activation in the developing heart (C).

MSK
1/25/07

Fig. 9 Mice deficient in *mef2c* have pigmentation defects. Some *Mef2c*^{+/-} mice exhibit hypopigmentation on their ventral side (A). This “belly spotting” phenotype is less severe and occurs less frequently than in *Sox10*^{+/-} mice (B).

Fig. 10 *Mef2c* in the neural crest is required for normal melanocyte development. In neonatal mice lacking *mef2c* in the neural crest, less pigment is frequently observed than in wild-type littermates. On panel A, the top half shows the dermal side of skin from the back of a *mef2c* neural crest conditional knockout animal, while the bottom half of the panel shows the skin from a wild-type littermate. Panel B contains equivalent skin preparations from a *Sox10*^{-/-} neonate on top, and a wild-type littermate on bottom. Note that animals lacking *Sox10* are completely deficient in pigmentation (B). Panels C and D compare the pigment levels in the dorsal skin of wild-type versus *mef2c* neural crest knockout neonates. Shown is the average pigment levels in these two populations (E) and a scatter plot of the data used to generate the averages (F). Red dots in F represent the average pigment levels for each population.

Fig. 11 MEF2C and SOX10 interact and cooperatively induce transcription. MEF2C and Sox10 interact in a GST-pulldown assay (A). GST-MEF2C or GST only conjugated beads were used as a bait to pulldown radiolabeled Sox10 (Sox10 FL) or the N-terminal portion of Sox10 including the DNA-binding domain (Dox10 DBD). After washing, the beads were eluted and resolved by SDS-PAGE. More Sox10 protein was bound to GST-MEF2C coupled beads than GST-only beads (compare lanes 1 & 2 and lanes 3 & 4). Note that MEF2C formed a stronger interaction with Sox10 DBD (lane 1) than with full

MEF2C
SOX10

length Sox10 (lane 3). Loading controls are shown in lanes 5 and 6. (B) Sox10 and MEF2C cooperatively activate transcription. Either Sox10 or MEF2C expression plasmids can each mediate *trans*-activation of a reporter gene through the *mef2c* neural crest enhancer (lanes 5 and 6). When MEF2C and Sox10 expression plasmids are co-transfected with the reporter construct, activation of the reporter exceeds the sum of activity observed by either plasmid alone (lane 7), suggesting these factors function to cooperatively activate transcription.

Fig. 12 Model for *mef2c* function in the neural crest.

RECEIVED
JUN 15 2000

	observed	expected
wnt-1 cre^{tg/0}; mef2c^{+flox}	69	64.25
wnt-1 cre^{tg/0}; mef2c^{-flox} **	63	64.25
mef2c^{+flox}	54	64.25
mef2c^{-flox}	71	64.25

Table 1. P0 genotypes from wnt-1 cre^{tg/0}; mef2c^{-/-} X mef2c^{flox/flox} crosses

** while wnt-1 cre^{tg/0}; mef2c^{-flox} animals are born at expected frequency, 100% die within one hour after birth

Table 1

10/20/07
 10/20/07

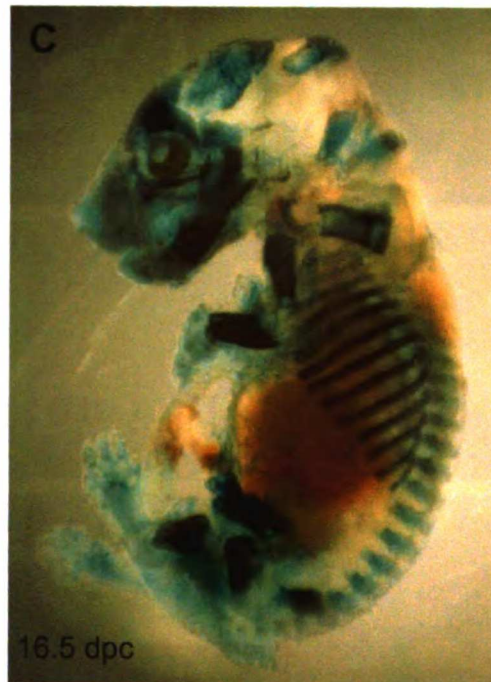
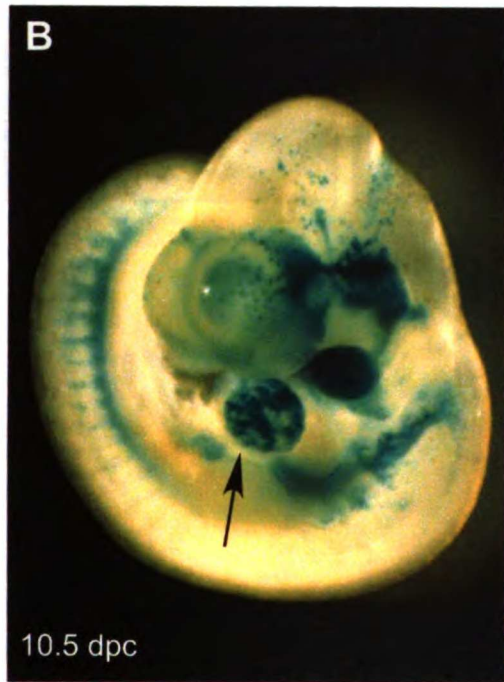
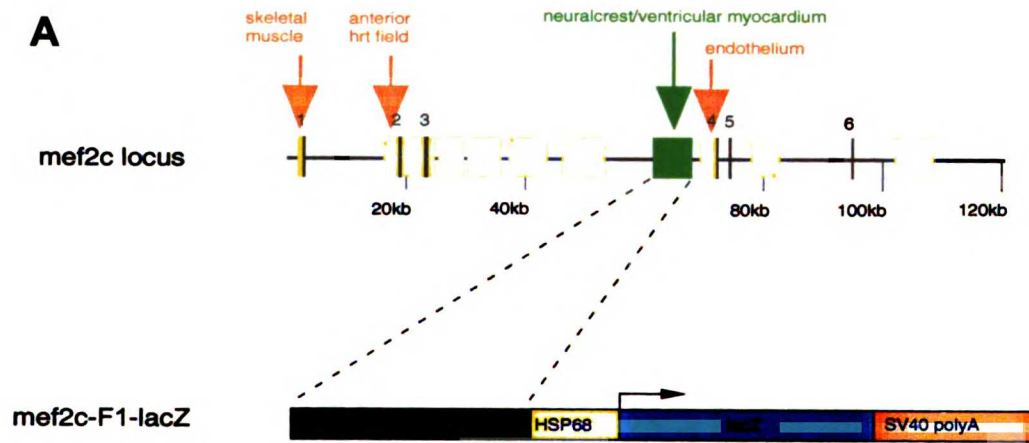


Figure 1

UCST LIBRARY

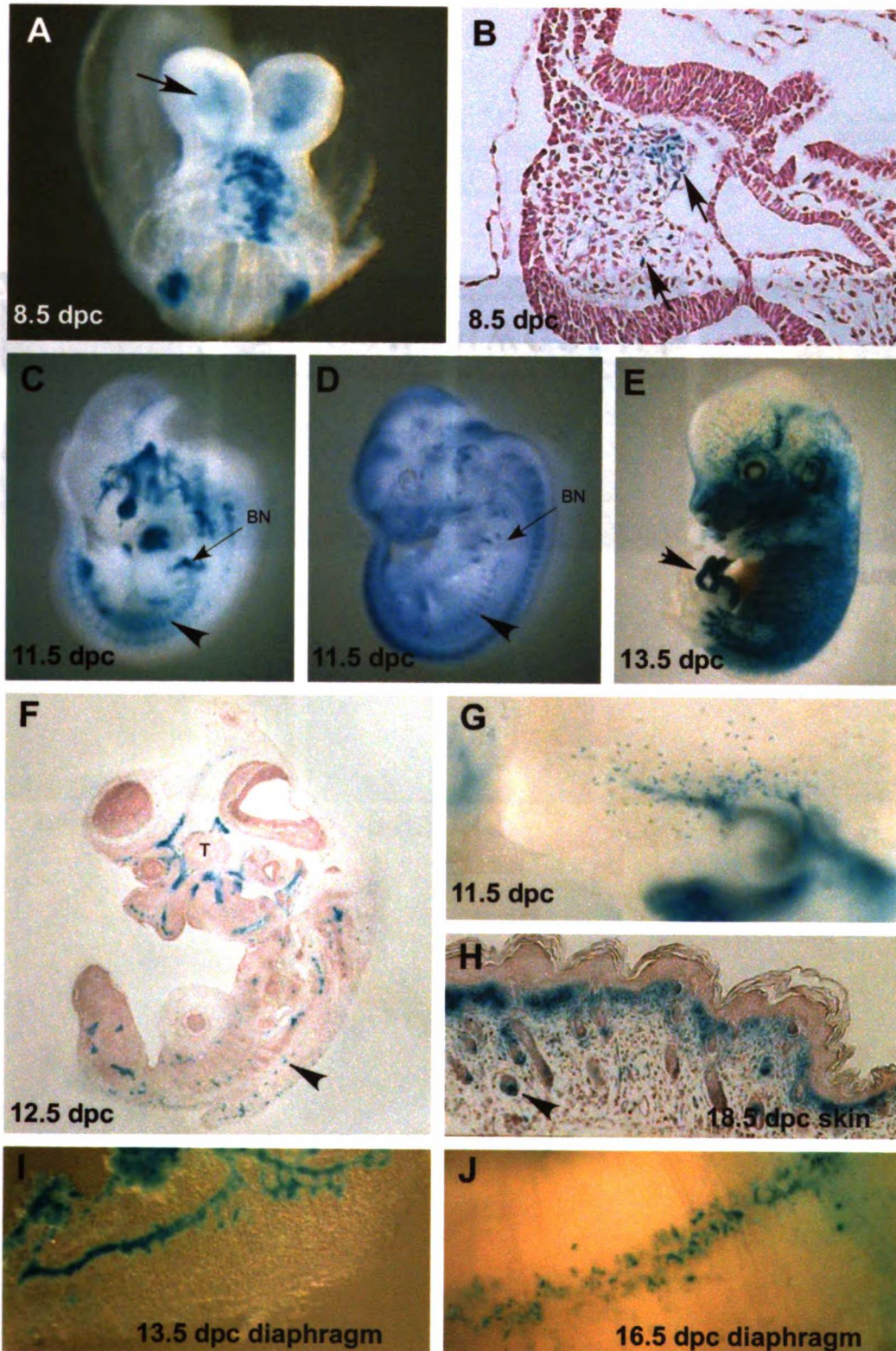


Figure 2

UCST LIBRARY

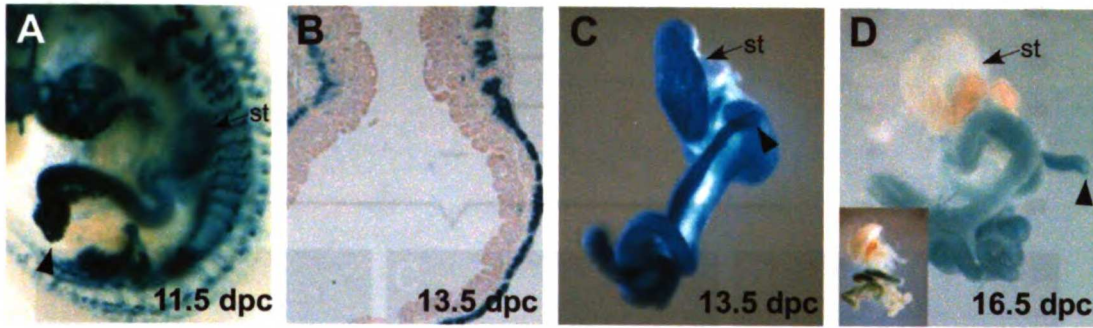
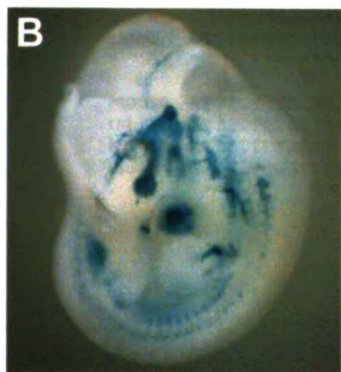
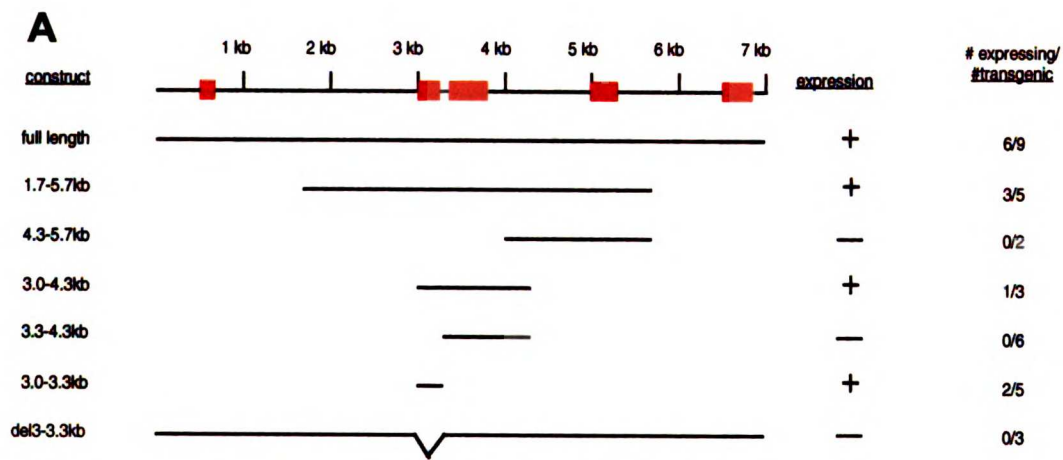
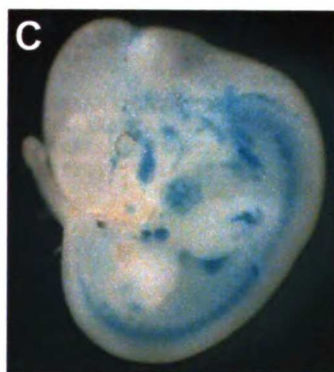


Figure 3

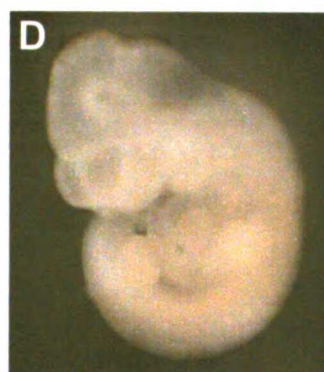
UCSF LIBRARY
HERBERT FSN



full length-*lacZ*



3-3.3-*lacZ*



del 3-3.3-*lacZ*

Figure 4

UCSF LIBRARY

	GATA(a)		TEF1/MCAT		SOX-1
mouse	CAC	AGGAAGGATACAGTTGGGAG	AGGAATGC	ACTGACT	TACAAAGTGCATCC-TG
rat	CGC	AGGAAGGATACAGTTCCG	AGGAATGC	ACTGACT	TACAAAGTGCATCC-TG
human	CAC	AGGGAGGATATAGTTT	TGAGGAATGC	TATAACT	TACAAAGTGCATCC-TG
chick	AGC	GGACATGCTGT-GTTTT	CAGGAATGT	CTTGAA	AACAAAGTGCATCAATG
	*	* * * *	*****	* *	***** **
		SOX-2		SOX-3	
mouse	AAGGCCATTTAGCT	CACAATGA	AAGGTCTGTGTTTT	AAAAATAGCTCTAT	AACAAAGTAACT
rat	AAGGCCGTTTAGCT	CACAATGA	AAGGTCTGTGTTTT	AAAAATAGCTCTAT	AACAAAGTAACT
human	AAGGCCATTTAGCT	CACAATGA	AAGGTCTGTGTTTT	AAAAATAGCACTAT	AACAAAGTAACT
chick	AAGGCCACCTCAGT	CACAATGA	AAGTTCTGTCTTCT	AAAAATAGCACT	AAACAAAATAACT
	*****	* * *****	*****	*****	***** **
		MEF2			
mouse	ACAGAGTGTGGCAAGGGCTCCA	CTATTATAG	AACTGAGTAAGGCGTGGT	AAATACCG	
rat	ACAGAGTGTGGCAAGGGCTCCA	CTATTATAG	AACTGAGTAAGGCGTGGT	AAATACCG	
human	ACAGAGTTTTGGCAAGGGCTCCA	CTATTATAG	AACTAAGTAAGGAATAGT	AAATAGTG	
chick	GTTGTGTTTTGGCAAGGGCTTAA	CTATTATAG	CGC-AAGTCAGA-ACAG	AAAAATAGTG	
	* * * *****	**	* * * * *	* * * * *	* * * * *
mouse	CCACGGTACCCA-GTTCTCCCT	TGCCACAACCCCAA	AACTTATAAGAAGCACT	GTAATTAT	
rat	CCACGGTACCCA-GTTCTCCCT	TGCCACAACCCCAA	AACTTATAAGAAGCACT	GTAATTAT	
human	CCACAGTACCCA-GTTCTCCCT	TGCCATAACCCCAA	AACTTATAAGAAGCACT	TATAATTAT	
chick	CTTTAGTATCCACATCCCCCA	AAGTTGTA	AACTCCAAACCTGGA	AGAAATACTATATTTAG	
	* * * * *	* * * * *	* * * * *	* * * * *	
		GATA(b)			
mouse	ATTTTCTACTTGGGAAAAAAAT	CATAGTAGC		CAGTTT	
rat	ATTTTCTACTTGG-AAAAAAAT	TATAGTAGC		CAGTTT	
human	ATTTTCTACTT---AAAAAAAT	CGTAGTAGC		CAGTTT	
chick	GTTGTGGGTTTTTTTTTTTTTT	TGTAGTTTT		TTTTCT	
	*** * **	* ****		* *	

Figure 5

HARVARD
 UST LIBRARY
 12/17/2007

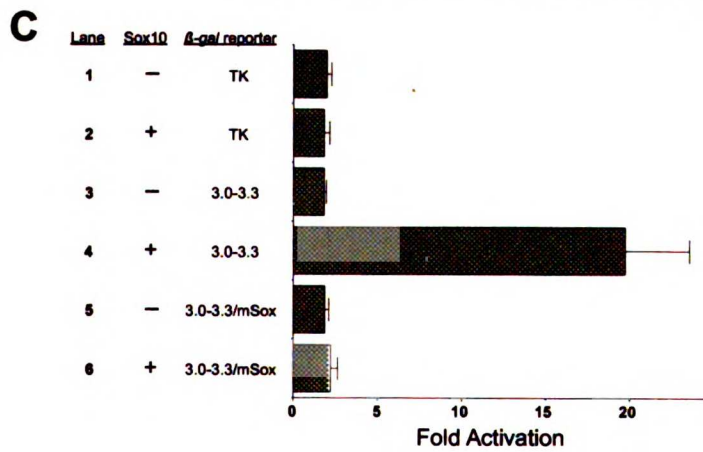
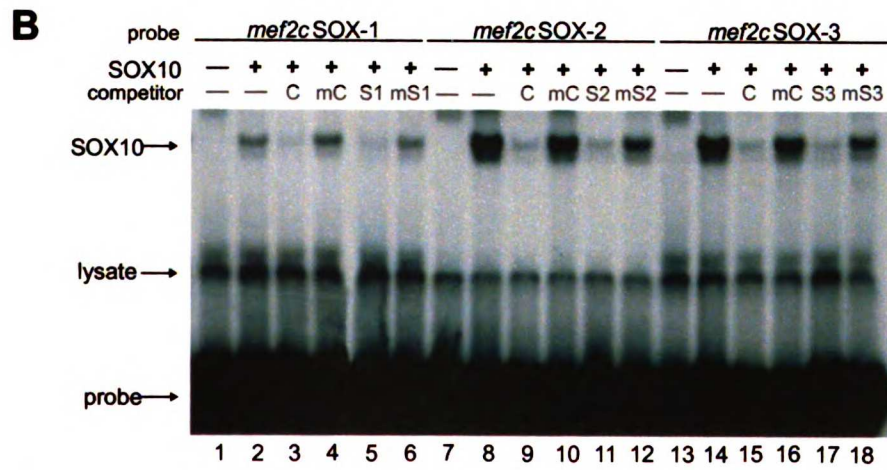
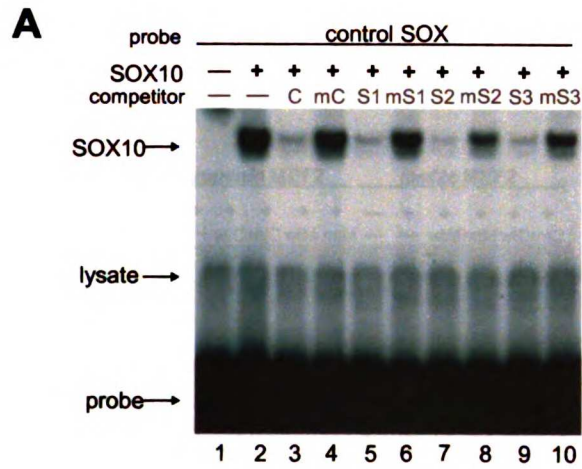


Figure 6

UCST LIBRARY

A

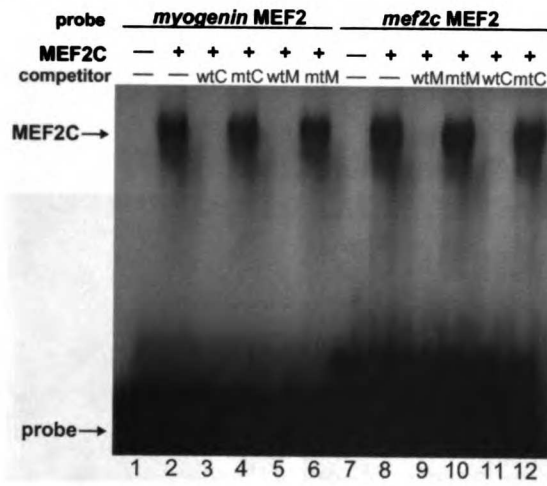


Fig. 7A data provided by Pooja Agarwal

B

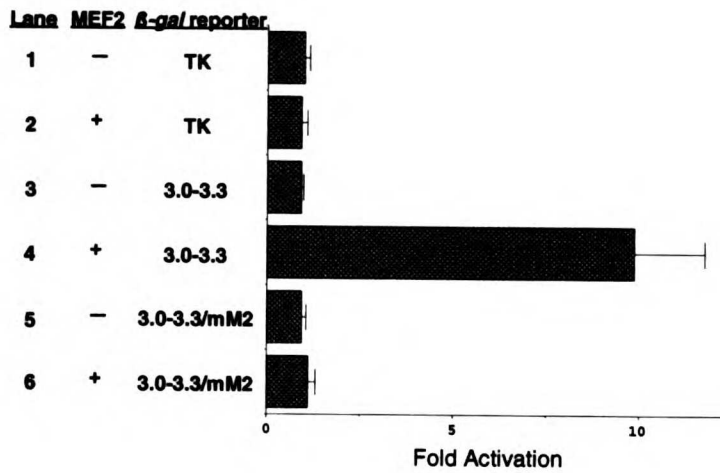


Figure 7

UST LIBRARY
 11/19/07 12:50 PM

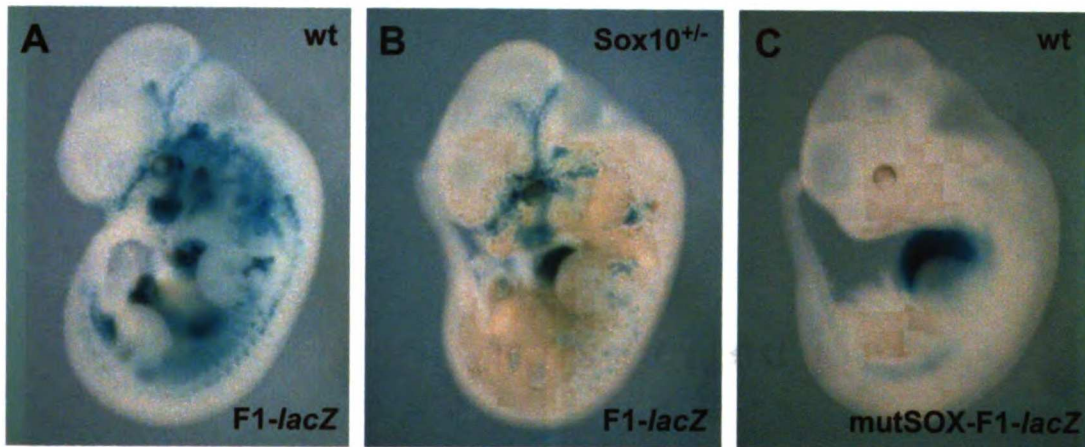


Figure 8

WUST LIBRARY
MAY 17 1997
12:30



Figure 9

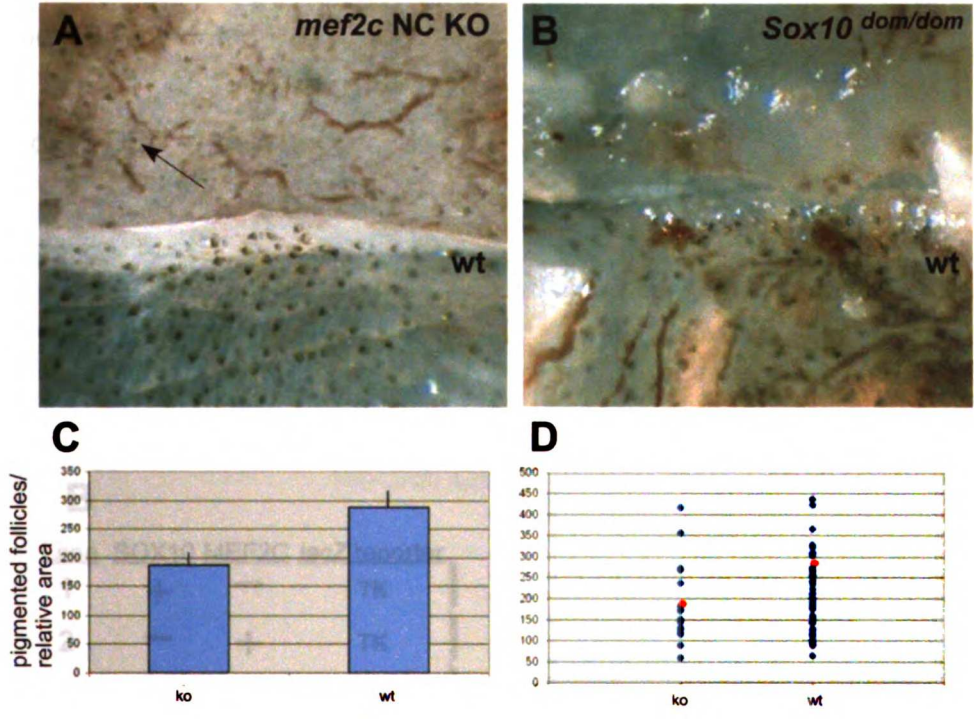


Figure 10

UCSF LIBRARY

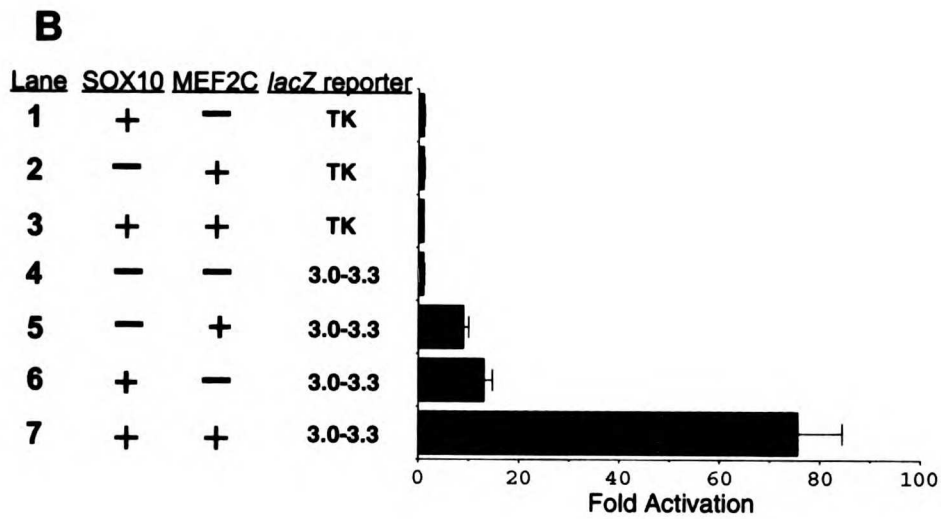
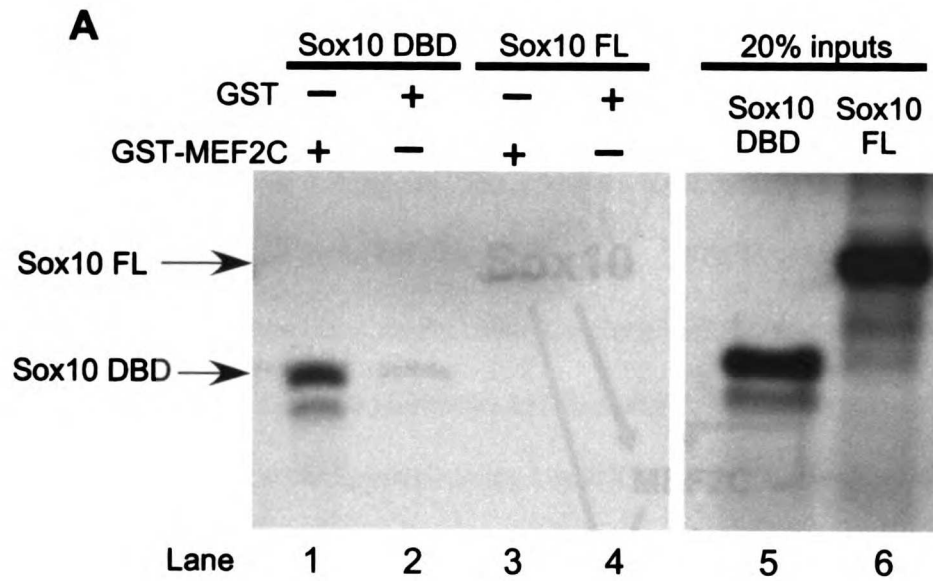


Figure 11

UCST LIBRARY

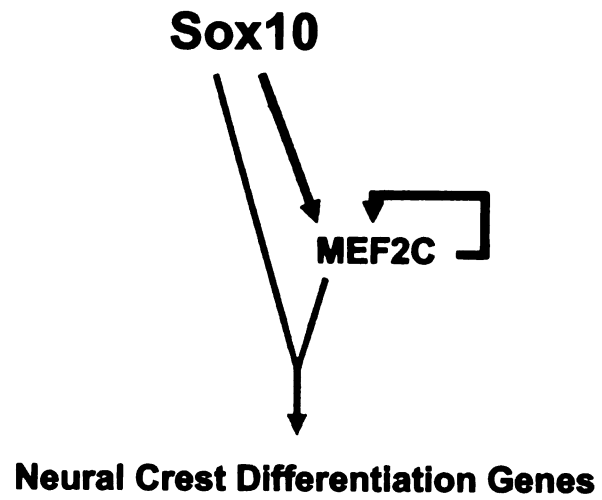


Figure 12

WU
LIBRARY

Chapter II. MEF2C function in the Neural Crest is essential for proper Craniofacial Development

II. Introduction

Craniofacial disorders are among the most common birth defects accounting for one third of all congenital neonatal disorders (Tassabehji et al., 2005; Noden and Trainor, 2005; Trainor, 2005). Common craniofacial defects include cleft lip and palate, which occur at a frequency as high as 1 in 750 (Johnston and Bronsky, 1995), and upper airway obstruction, which occurs in approximately 1 in 8000 births (Dinwiddie, 2004). Underlying causes for craniofacial disorders include improper development of the neural crest, which is a cell population whose descendants give rise to the cartilage, bones, and loose connective tissues of the craniofacial skeleton (Noden and Trainor, 2005; Le Douarin, and Kalchheim, 1999).

Neural crest cells originate from the dorsal neural tube at the border between the neural plate and the lateral epidermis (Baker and Bronner-Fraser, 1997; Knecht and Bronner-Fraser, 2002; Trainor, 2005). When induced by contact mediated signals, (Baker and Bronner-Fraser, 1997; Selleck and Bronner-Fraser, 1995), neural crest precursor cells undergo an epithelial to mesenchymal transition, migrate throughout the developing embryo, and give rise to various tissues including the dorsal root and sympathetic ganglia, pigment cells, adrenal medulla, and skeletal elements of the face (Le Douarin and Kalchheim, 1999). Cephalic neural crest cells comprise the most rostral population of neural crest cells and will give rise to the cranial ganglia and the connective tissues of

12/11/2005

underlying formation of craniofacial structures and the complications that result in congenital defects.

Earlier in this work, a role for the transcription factor MEF2C in developing neural crest lineages was revealed (see Chapter 1). We identified a transcriptional enhancer of *mef2c* that directs expression in Schwann cells, melanocytes, and the neural crest-derived craniofacial mesenchyme. We showed that *mef2c* function in the neural crest is required for postnatal survival. The work presented in chapter 2 elaborates on the cause of neonatal lethality in mice lacking *mef2c* in the neural crest. We show that mice lacking *mef2c* in the neural crest die due to an airway obstruction caused by severe craniofacial defects. In the absence of *mef2c* in the neural crest, mice exhibit hypoplastic mandible, zygoma, and frontal bones, are missing the tympanic ring, and exhibit cleft palate. These defects are observed early in craniofacial development, beginning at 13.5 dpc. Finally, we show that a transcriptional enhancer from *mef2c* is active in the precursor cells of the craniofacial skeleton and that enhancer activity in these cells is dependent upon endothelin signaling. We propose *mef2c* plays an essential function in craniofacial development downstream of endothelin signaling.

II. Results

Mice lacking mef2c in the neural crest die at birth due to upper airway obstruction

As described in the previous chapter, conditional knockout of *mef2c* in the neural crest results in mice that are born at normal Mendelian frequency (Table 1). Mice lacking

mef2c in the neural crest exhibit pigmentation defects (Fig. 10) and die shortly after birth. In the work presented in this chapter, I will discuss the cause of the neonatal lethality and the nature of the severe craniofacial defects observed in *mef2c* neural crest knockout mice.

Mice lacking *mef2c* in the neural crest were animated and responsive to touch, but quickly became cyanotic and died within an hour of birth (Fig. 13). Cyanosis is caused by lack of oxygen delivery to the tissues. We suspected that the cause of cyanosis in *mef2c* neural crest knockouts might be due to an airway blockage, improper diaphragm function, or poor blood circulation. The hearts and diaphragms of *mef2c* neural crest null mice were examined for gross morphology, histology, and expression of normal histological markers, revealing no apparent differences from wild type littermates (data not shown). In contrast, a comparison of lungs from knockout and wild type animals demonstrated that lungs from the knockout animals were never inflated, implying that the cyanosis was caused by a failure to breathe (Fig. 14A, B).

Lack of air in the lungs may be the result of improper function of the muscles that control breathing, improper breathing control, defects within the lungs themselves, or airway blockage. The shape of the heads in *mef2c* neural crest conditional knockouts appeared abnormal (Fig. 15) so we examined the airway of wild type and knockout animals (Fig. 15). Wild type animals showed a patent airway with normal development of the pleural and lung musculature and trachea (Fig. 15A). In contrast, *mef2c* neural crest conditional knockouts often exhibited a constricted airway with a hypoplastic trachea and pleural

WEST LINDSEY
UNIVERSITY
CANBERRA

palate, and irregular tongue musculature, which is a secondary defect of a hypoplastic mandible (Fig. 15B). Comparison of the underside of the palate by whole mount preparation of wild type and knockout skulls demonstrated a posterior cleft in the palate of conditional knockout animals (Fig. 15C) but not in control littermates (Fig. 15D). To verify that cyanosis was caused by the upper airway obstruction, animals were tracheostomized with a 30G needle to bypass the upper airway. This bypass allowed for normal breathing and temporary recovery from cyanosis prior to humane euthanasia (data not shown). These results demonstrate that mice lacking *mef2c* in the neural crest die at birth with asphyxiation caused by upper airway obstruction.

Mef2c function in the neural crest is required for craniofacial development

To examine the craniofacial defects in *mef2c* neural crest knockout animals in detail, skeleton preparations of the mutant animals were compared to those of wild type littermates (Fig. 16). A lateral view of the wild type neonatal skull showed normal development of the mandible and its processes joining with the temporal bone, a normal zygomatic arch, and a developed tympanic ring bone situated around the ear (Fig. 16A, G). In contrast, *mef2c* neural crest conditional mutant skulls showed several hypoplastic or missing structures, including a hypoplastic mandible, zygoma, and temporal bone. Additionally, the processes of the temporal and mandibular bone were either hypoplastic or missing, and the tympanic ring was absent (Fig. 16B, H). A coronal view of the skulls revealed additional differences between the control and knockout animals (Fig. 16C, D). The distance between the neural crest derived frontal bones was typically larger in

[Vertical text or stamp, possibly a signature or institutional mark]

knockout animals and likely the result of hypoplasia of the frontal bones (Fig. 16D). In contrast, the parietal bones, which are not of neural crest origin, appear normal in the *mef2c* knockout animals, illustrating that the defects observed in these animals are specific to the neural crest (Fig. 16C, D). An inferior view of the wild-type and knockout neonatal skulls showed that, in addition to hypoplasia of the knockout skeletal elements, there were also differences in the persistence of Meckel's cartilage, a fetal precursor to the mandible that normally diminishes in normal development (Fig. 16E, F). The mandibles of the conditional knockout animals also lacked the cartilage present at the symphysis of the wild type mandibles (Fig. 16E, F). From this view it was also evident that the hyoid bone, which anchors the tongue, was also hypoplastic (Fig. 16E, F arrows) and that the palate was incomplete (Fig. 16E, F). Closer examination of the temporal mandibular joints of wild type and knockout animals revealed that the coronoid, condular, and angular processes of the mutant mandibles were severely hypoplastic when compared to wild type littermate controls (Fig. 16G, H). These results show that MEF2C function in the neural crest is required for proper craniofacial development.

As a first step towards defining the underlying defect in the craniofacial mesenchyme in the absence of *mef2c*, we wanted to define the earliest evidence of defects in *mef2c* conditional knockouts. We began by examining the developing skeletons in 13.5 dpc and 16.5 dpc embryos. Compared to wild type littermates, the skeletons of the 16.5 dpc knockout embryos exhibited hypoplastic Meckel's cartilage and a decrease in the amounts of ossification in the developing mandible and maxilla as shown by alizarin red staining (compare Fig. 17A and Fig. 17B). The differences in skeletal development could

11
12
13
14
15
16
17
18
19
20
21
22
23
24
25
26
27
28
29
30
31
32
33
34
35
36
37
38
39
40
41
42
43
44
45
46
47
48
49
50
51
52
53
54
55
56
57
58
59
60
61
62
63
64
65
66
67
68
69
70
71
72
73
74
75
76
77
78
79
80
81
82
83
84
85
86
87
88
89
90
91
92
93
94
95
96
97
98
99
100

be observed as early as 13.5 dpc, a time prior to the onset of ossification, when the Meckel's cartilage was already hypoplastic in knockout animals (data not shown). Thus, it appears that the craniofacial defects observed in mice lacking *mef2c* in the neural crest are likely to have their origins relatively early in craniofacial differentiation.

Mef2c is expressed in the embryonic precursors of the craniofacial skeleton and is dependent on the endothelin signaling pathway

To define pathways upstream of *mef2c* early in craniofacial development, we examined the expression of the *mef2c-F1-lacZ* transgene described in chapter 1. β -gal expression directed by the *mef2c* neural crest enhancer in the craniofacial mesenchyme is particularly strong in the first branchial arch, and is also observed within the second branchial arch and in neural crest-derived craniofacial mesenchyme (Fig. 18A). The robust staining in the mandibular component of the first branchial arch is of significant interest, considering that the most severe phenotypes observed in the neonatal skulls of *mef2c* conditional knockout animals are in structures derived from the first arch (Figs. 16 and 17). *Mef2c* neural crest enhancer activity within the mandibular component of the first arch is restricted to the neural crest-derived mesenchyme and not within the overlying ectoderm or within the pharyngeal mesoderm (Fig. 18B).

The *mef2c* neural crest knockout phenotype in the craniofacial skeleton is consistent with the phenotype observed in mice lacking genes that encode components of the endothelin signaling pathway. Mice lacking *ECE-1*, *Endothelin-1*, or *Endothelin receptor A* exhibit

18A

hypoplastic mandibles, cleft palate, and missing or shortened tympanic bones, similar to the defects observed in mice lacking *mef2c* in the neural crest (Clouthier and Schilling, 2004). The strongest *mef2c*-F1 enhancer activity was observed within the branchial arch mesenchyme, which is a population of cells known to be responsive to endothelin signals (Clouthier et al., 1998; Yanagisawa et al., 1998a). To test whether *mef2c* is under the control of endothelin signaling, we examined *mef2c* enhancer activity in embryos cultured either in the presence or absence of Bosentan, an inhibitor of both endothelin receptors (gift of Actelion Pharmaceuticals Ltd). Embryos harvested at 9.0 dpc and cultured in the presence of bovine serum albumin (BSA) displayed robust levels of *mef2c*-F1 enhancer activity in the developing craniofacial mesenchyme (Fig. 19A). By contrast, embryos harvested and cultured under the same conditions but in the presence of Bosentan showed a dramatic decrease in β -gal activity (Fig. 19B). Inhibition of β -gal activity by Bosentan was specific to the *mef2c* neural crest enhancer, as the activity of a different enhancer, *smooth muscle alpha actin*, showed no change in activity when cultured in the presence or absence of Bosentan (compare Fig. 19C and 19D). These results demonstrate that *mef2c* expression mediated by the neural crest enhancer in the embryonic precursors of the craniofacial skeleton is dependent on the endothelin signaling pathway.

II. Discussion

MEF2C function in the neural crest is required for proper craniofacial development.

Mice lacking *mef2c* in the neural crest exhibited a number of craniofacial abnormalities, including cleft palate, missing tympanic ring, and hypoplastic mandible, zygoma, hyoid,

and frontal bones. These mice also lacked proper joint formation between the mandible and temporal bones. The craniofacial defects observed in *mef2c* neural crest knockout mice led to asphyxiation and death at birth. Craniofacial defects in *mef2c* neural crest knockout mice were observed as early as 13.5 dpc, suggesting that *mef2c* function is required early in craniofacial development. Finally, we identified an endothelin-dependent enhancer of *mef2c* that directs transcription within the neural crest-derived mesenchyme of the branchial arches and frontonasal region. Taken together, we have revealed a novel role for function of *mef2c* in craniofacial development.

This work implicates *mef2c* downstream of the endothelin signaling pathway. Mice lacking *mef2c* in the neural crest share a number of phenotypes with mice harboring mutations in endothelin signaling pathway components. These shared phenotypes include specific craniofacial defects as well as disruption of normal pigment formation (Baynash et al., 1994; Clouthier et al., 1998; Hosoda et al., 1994). Interestingly, both *mef2c* and endothelin are co-expressed in a number of other tissues during embryonic development. While not elaborated upon in this chapter, the *mef2c* enhancer studied here is also active in the developing heart, and it appears that cardiac enhancer activity is also sensitive to a loss in endothelin signaling (Fig. 19). It will be interesting to see if a relationship between MEF2 factors and endothelin signaling exists in other cell populations, such as in the developing vasculature or in the enteric nervous system.

Mef2c neural crest knockout mice exhibited craniofacial defects that are also similar to those found in *gooseoid*, *Mhox (Prx1)*, and *Hand2* knockout animals. These shared

defects include a hypoplastic mandible, missing tympanic bone, cleft palate, disruptions in the zygomatic bone, and disruptions to the developing Meckel's cartilage (Rivera-Perez et al., 1995; Yamada et al., 1995; Martin et al., 1995; Yanagisawa et al., 2003). Interestingly, *gooseoid* and *Hand2* have also been shown to lie downstream of endothelin signaling (Clouthier et al., 1998; Charite et al., 2001). We are currently examining expression of these genes in the *mef2c* neural crest knockout to determine if they function downstream of *mef2c*. Both Gooseoid and Prx1 are homeodomain containing proteins and will also be tested for the ability to bind to putative HOX sites in the *mef2c* neural crest enhancer to determine whether these proteins may function as transcriptional regulators of *mef2c* in the developing craniofacial mesenchyme (Fig. 5).

Craniofacial abnormalities account for a large proportion of congenital birth defects. Frequently, craniofacial defects coincide with other congenital abnormalities (Suri, 2005). While we have shown that *mef2c* neural crest knockout animals die at birth with severe craniofacial abnormalities, it would not be surprising to uncover additional defects in an individual with mutations at the *mef2c* locus. Indeed, we already know that *mef2c* is critical for proper heart formation and for normal levels of pigmentation (see chapter 1, chapter 3, and Lin et al., 1997). It would be interesting to assess the function of *mef2c* in the neural crest after postnatal day zero using different Cre drivers that are active in subsets of the neural crest, but silent in craniofacial precursors. One example, the Pax3 proximal promoter Cre driver, is active in much of the neural crest derived tissues, including Schwann cells and melanocytes, but is largely silent in the craniofacial mesenchyme and other developing tissues (Li et al., 2000). Use of such a Cre line would

Chapter 2 Figure legends

Fig. 13. *Mef2c* is required in the neural crest for postnatal viability. Animals lacking *mef2c* in the neural crest were generated by crossing *mef2c^{flox/flox}* animals with *mef2c^{+/-}*; *wnt1-Cre^{Tg0}* mice as described. Knockout animals (left) quickly become cyanotic after birth and die shortly thereafter. Additionally, the lower jaw in these animals was reduced in size compared to wild-type littermates (right). Also note the misshaped head in knockout animals (arrow).

Fig. 14. Mice lacking *mef2c* in the neural crest fail to breathe. Lungs of wild-type (A) and mutant (B) neonates were sectioned to show lack of air in the knockout animal's lungs, indicating a failure to breathe.

Fig. 15. Mice lacking *mef2c* in the neural crest exhibit craniofacial defects. Sagittal sections through the upper airway of wild-type (A) and knockout (B) littermates reveal an incomplete secondary palate (red asterisks), disorganized muscle in the tongue (black asterisk), and a constricted airway (black arrow) in the knockout animals. Images showing the roof of the oral cavity in wild-type (C) and *mef2c* knockout animals (D) reveal a cleft of the secondary palate in *mef2c* knockout animals (D). The jaw had been dissected away in these animals to allow inspection of the palate.

Fig. 16. A number of craniofacial defects are observed in *mef2c* neural crest knockout mice. Skeleton preparations were performed on wild-type (A, C, E, G) and *mef2c* neural crest knockout (B, D, F, H) neonates. Lateral images of wild-type (A) and mutant (B)

skulls reveal multiple defects in the knockout animals. These include a missing tympanic ring (arrow), and hypoplastic mandible (compare bars on wild-type and knockout skulls). Superior views of the skulls reveal an increased distance between the frontal bones in knockout animals (compare bars in panels C and D). Inferior views of the skulls reveal a hypoplastic hyoid bone in the knockout skulls (arrow) and exposed Meckel's cartilage (arrowhead). Higher magnification images of the temporal region show multiple defects in knockout animals, including disruptions of temporal processes (1), a hypoplastic zygomatic bone (2), severely hypoplastic coronoid, condular, and angular processes of the mandible (3), and missing tympanic rings (4).

Fig. 17. Craniofacial defects are manifested early in the development of *mef2c* neural crest knockout embryos. Skeleton preparations of wild-type (A) and *mef2c* neural crest knockout (B) 16.5 dpc embryos reveal that mutant animals have shorter Meckel's cartilage, and decreased levels of ossification when compared to wild-type littermates. Arrowheads point to differences in ossification in the mandibles.

Fig. 18. The *mef2c*-F1 enhancer is active in craniofacial precursor cells. Embryos containing the *mef2c*-F1-*lacZ* transgene show robust β -gal activity in the frontonasal, first and second branchial arch regions as observed in whole mount 10.5 dpc embryos (A) or in sagittal sections through 10.5 dpc embryos. Note staining in the mandibular component of the 1st branchial arch (arrow) and in the developing heart (Hrt).

Fig. 19. The *mef2c*-F1 enhancer activity is dependent upon endothelin signaling. *Mef2c*-F1-*lacZ* embryos were cultured in media alone (A) or in media containing Bosentan, an inhibitor of endothelin receptors (B). Note that staining of untreated embryos is much more robust than in treated embryos, particularly in the first branchial arch (arrow). Embryos containing the *smooth muscle alpha actin* -*lacZ* transgene (*smaa-lacZ*) were also cultured in media alone (C) or in media containing Bosentan (D). Note that unlike in *Mef2c*-F1-*lacZ* transgenic embryos, *smaa-lacZ* embryos showed no changes in expression in response to Bosentan.

59

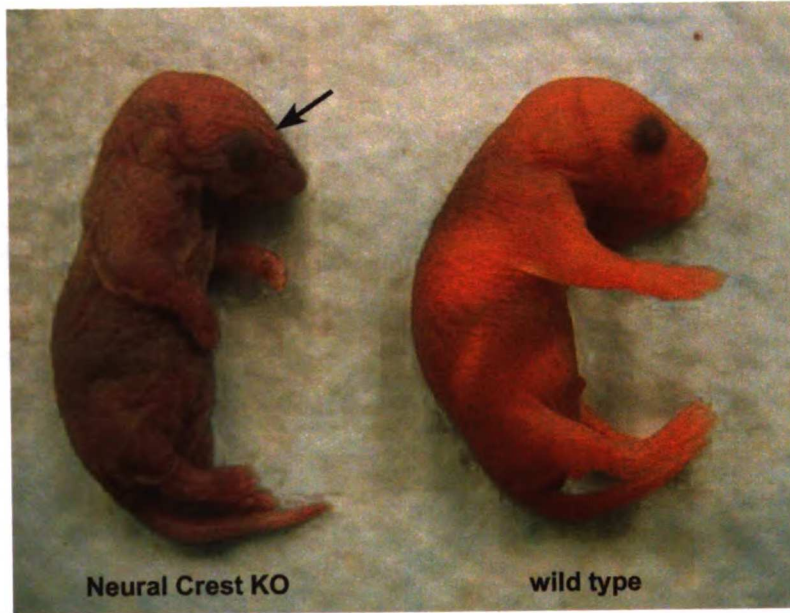


Figure 13

WEST LIBRARY

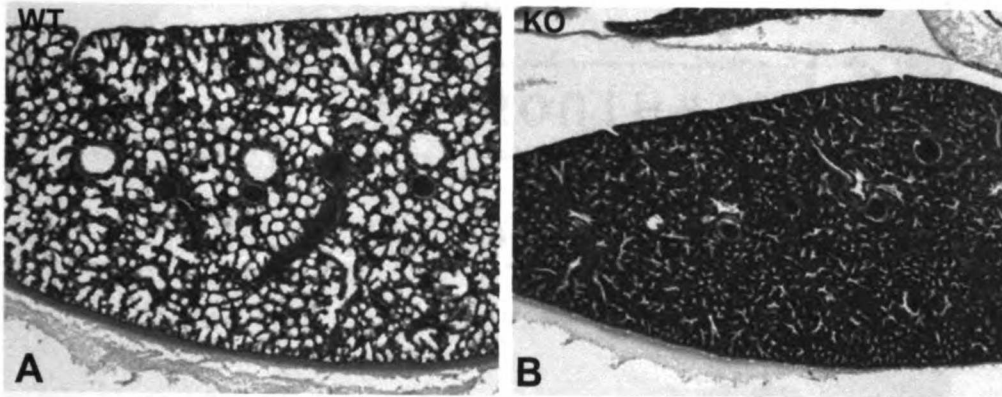


Figure 14

WT 100nm

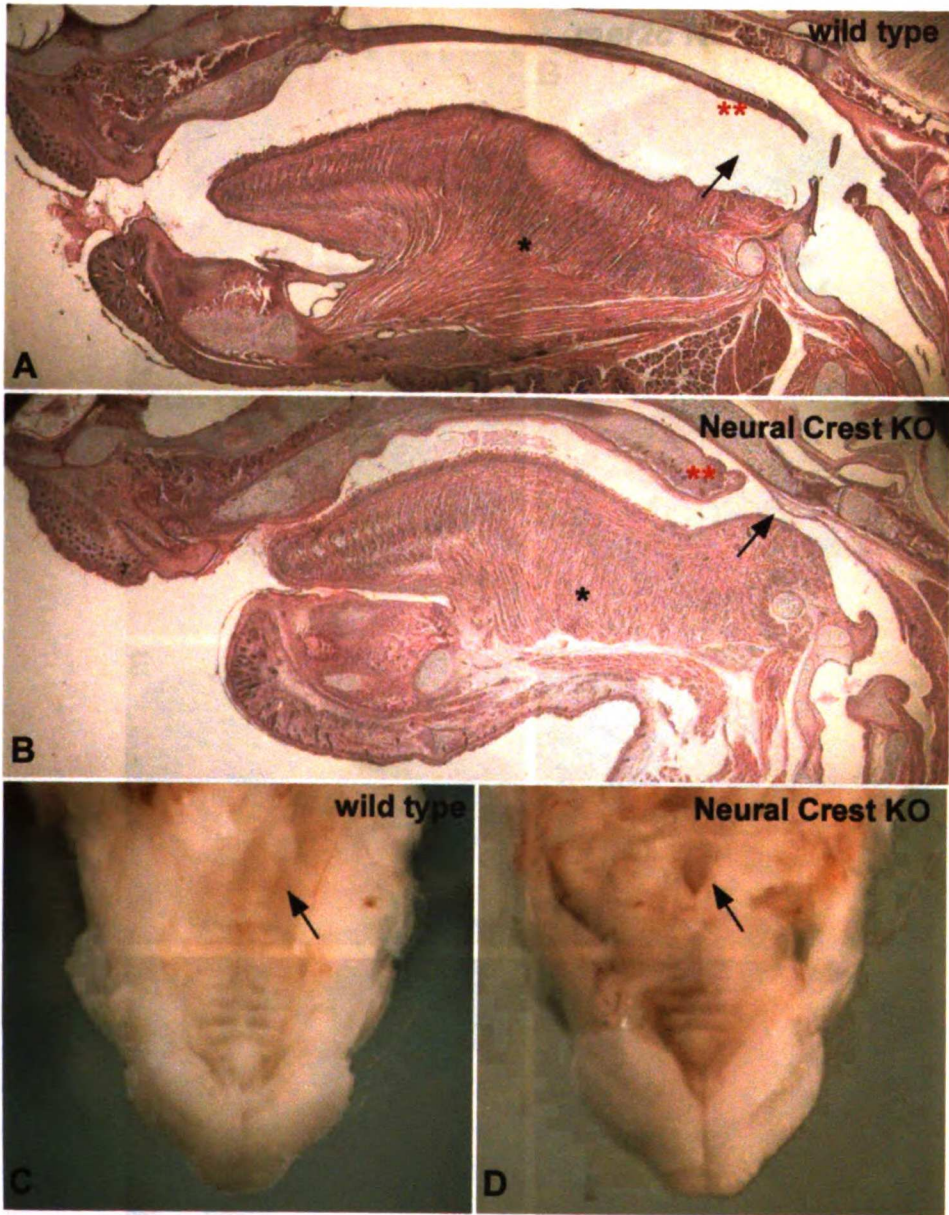


Figure 15

WRIGHT 1200

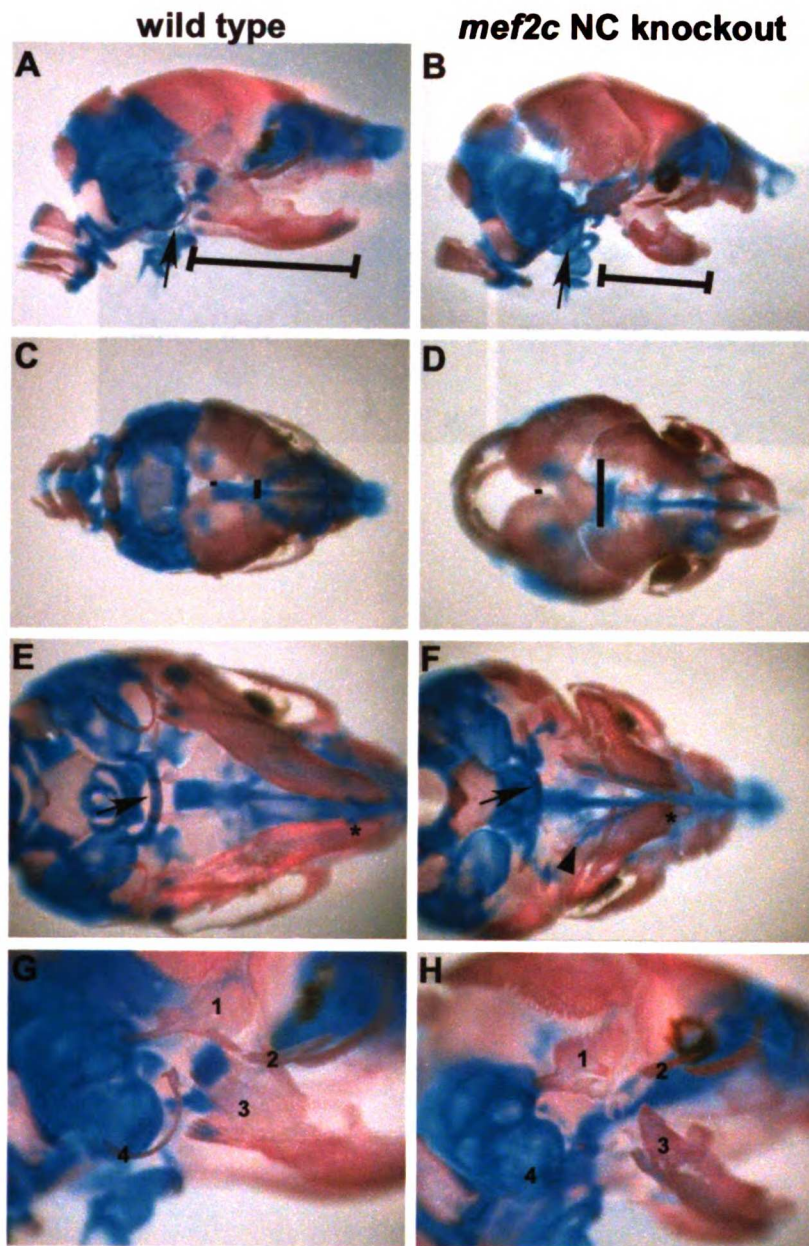


Figure 16

WEST LIBRARY

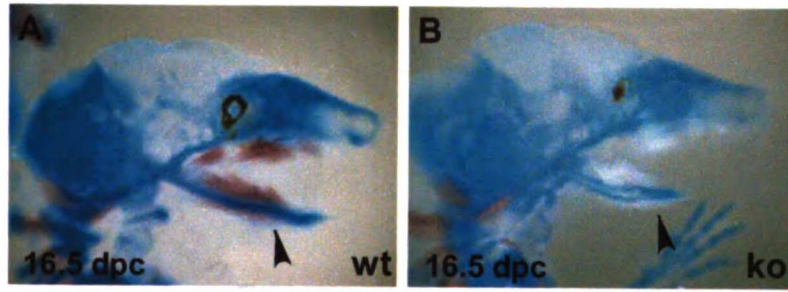


Figure 17

WEST LIBRARY

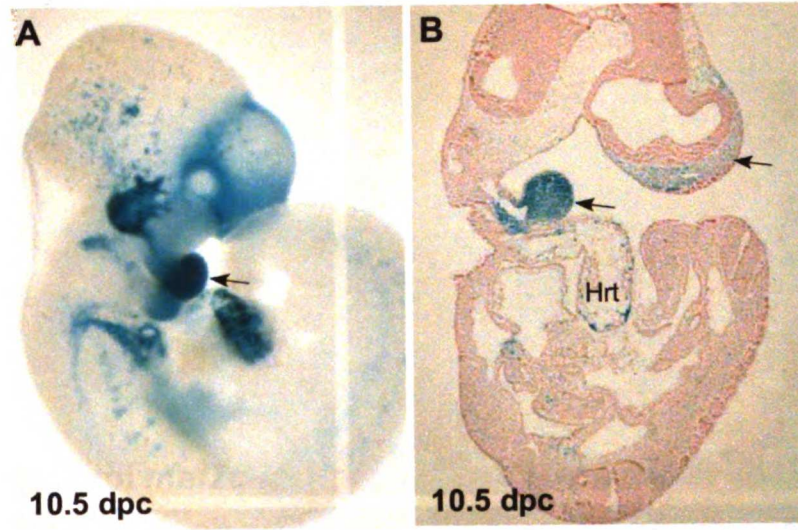


Figure 18

WST LDHFI
12071 200

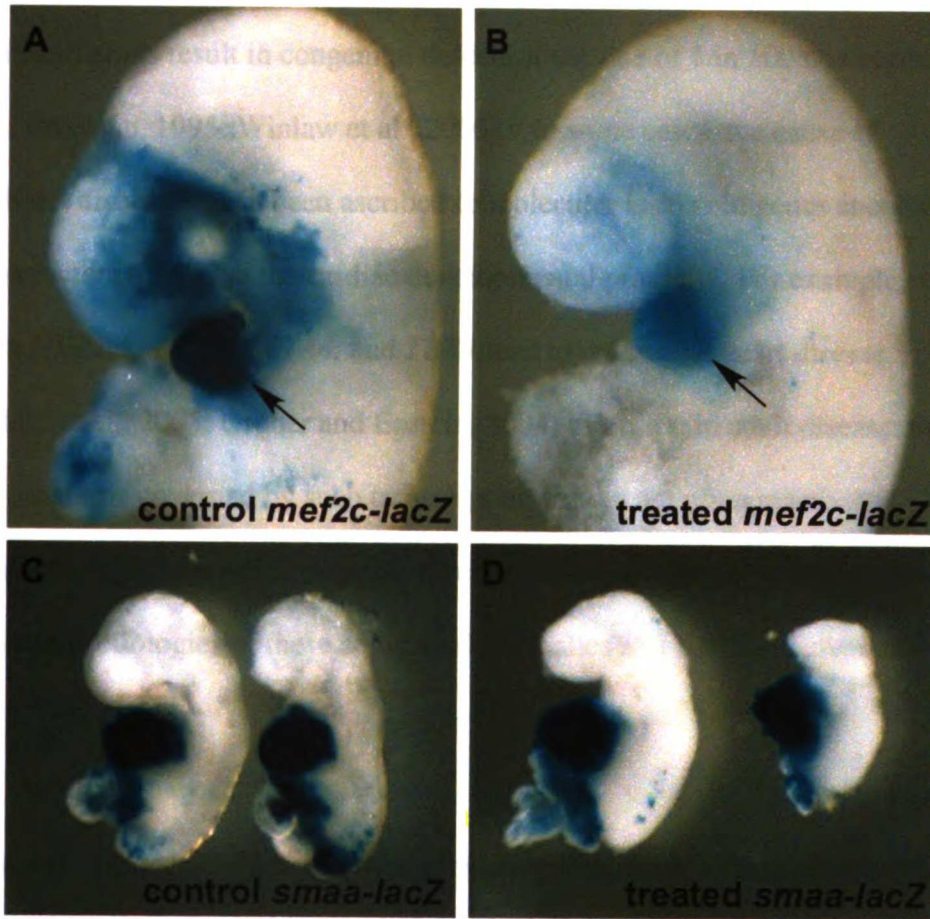


Figure 19

UJST LIBRARY

Chapter 3: Transcriptional regulation of *mef2c* in the heart

III. Introduction

The heart is the first organ to form in the developing embryo and severe complications during cardiac organogenesis are thought to be a major cause of embryonic lethality. Cardiac malformations result in congenital defects at the rate of 1 in 100 newborns (Clark et al., 2005; Hoffman, 1995; Winlaw et al., 2005). In some cases, the cause of congenital heart disorders have been ascribed to molecular lesions in genes encoding the transcription factors that drive the cardiac developmental program. For example, mutations in *NKX2.5*, *TBX5*, *GATA4*, and *TBX1* lead to congenital heart disease in humans (Clark et al., 2005; Gruber and Epstein, 2004). Further, in adult disease, the embryonic programs governed by such transcription factors are often reactivated. Thus, understanding the transcriptional programs directing heart development is critical to understanding the etiologies of these congenital anomalies and adult cardiovascular disease.

While a number of the transcription factors regulating cardiac development have been identified, the relationship between these factors, and how they cooperate to govern heart formation is incompletely understood (Cripps and Olson, 2002). Transcription Enhancer Factor 1 (TEF-1) is one transcription factor known to be essential for normal cardiac development. TEF-1 belongs to a class of transcription factors containing a TEA domain DNA-binding motif (also referred to as Tead proteins) (Kaneko, et al., 1998). A number of cardiac and skeletal muscle genes contain the TEF family member DNA binding site

W
H
I
T
E
M
A
N

known as the MCAT element (5'-CATTCT-3') and are responsive to TEF-mediated transcriptional activation (Mar and Ordahl, 1990; Larkin et al., 1996). When TEF-1 function was disrupted by a retroviral gene trap, mouse embryos failed to develop past 12 dpc. Developing hearts in *Tef-1* mutant embryos exhibited dilated cardiac chambers with reduced trabeculation, pericardial effusion, and thin ventricular walls (Chen et al., 1994). TEF family members are also believed to function in cardiac hypertrophy by mediating part of the alpha 1-adrenergic stimulated reactivation of fetal cardiac genes such as *skeletal muscle alpha-actin* and *beta myosin heavy chain* (Kariya et al., 1993; Kariya et al., 1994; Karns et al., 1995; Chen et al., 1994; Stewart et al., 1998). While it is well demonstrated that TEF family members activate transcription of muscle structural genes, it remains unclear how TEF proteins fit into the regulatory networks of transcription factors that govern cardiac development.

As discussed earlier in this thesis, MEF2C is also critical for proper cardiovascular development. *Mef2c* knockout mice fail to develop a heart past the linear tube stage and die at midgestation (Lin et al., 1997). *Mef2c* is expressed throughout the heart very early in development and its expression continues throughout cardiogenesis (Edmondson et al., 1994). Like TEF proteins, MEF2 factors have been implicated in mediating cardiac hypertrophy (Kolodziejczyk et al., 1999; Lu et al., 2000; Passier et al., 2000). While it is clear that *mef2c* is critical for normal heart development, what directs *mef2c* expression in the developing heart, and how *mef2c* fits into the transcriptional regulatory networks driving cardiogenesis has not been defined previously.

UNIVERSITY OF TORONTO

Until recently, models for cardiac development involved a single population of cells constituting a crescent shaped field of lateral mesoderm. Recent work has demonstrated that in birds and mammals this primary heart field is joined by a second cardiogenic population of cells, referred to as the secondary or anterior heart field (Kelly et al., 2001; Mjaatvedt et al., 2001; Waldo et al., 2001). The anterior heart field is located dorsal and medial to the primary heart field, in the splanchnic mesoderm at cardiac crescent stage. Following ventral morphogenesis, these anterior heart field cells are located in the pharyngeal mesoderm. Multiple fate mapping approaches suggest that the secondary heart field gives rise to the right ventricle, ventricular septum, and outflow tract (Mjaatvedt et al., 2001; Cai et al., 2003; Laugwitz et al., 2005 and see chapter 4). A better understanding of how these two cardiogenic fields come together and the transcriptional networks that govern cardiac development within each developmental field will further our understanding of heart formation and potentially uncover causes of heart disease.

Mef2c is expressed throughout the developing heart, yet its expression in cardiac lineages is controlled via multiple distinct enhancers. Using transgenic analyses, we have identified an upstream enhancer and promoter that directs expression specifically to the anterior heart field and its derivatives in the right ventricle and outflow tract (Dodou et al., 2004). The activity of this anterior heart field enhancer of *mef2c* was shown to be dependent upon GATA and Isl1 binding sites in the enhancer (Dodou et al., 2004). By defining the transcriptional network responsible for directing *mef2c* expression in the anterior heart field, this work provided the first insight into the regulatory pathway

69

governing *mef2c* expression in the heart, and identified the first direct Isl-1 target in the secondary heart field.

Here, we describe an additional *mef2c* enhancer that directs expression to the developing ventricular myocardium in a pattern distinct from the anterior heart field enhancer that we have described previously (Dodou et al., 2004). This enhancer, named *mef2c*-F1, also functions in developing neural crest. The regulation of this enhancer in the neural crest is described in this thesis in chapters 1 and 2. In this chapter, we show that activity of this enhancer in the heart is under the control of multiple, evolutionary conserved, *cis*-regulatory elements. These elements can function as MCAT and MEF2 DNA binding sites by binding to TEF and MEF2 proteins, respectively. Further, using *in vivo* transgenic analyses of enhancer function, we show that the cardiac activity of the *mef2c*-F1 enhancer is dependent upon these *cis*-regulatory sequences. We found that TEF transcription factors are required for early activation of the enhancer and that MEF2 binding is then required to maintain the enhancer's activity. Thus, for the first time, we have placed TEF in the network of transcription factors directing cardiac development. This work describes *mef2c* regulation in the developing primary heart field, and coupled with our previous work describing *mef2c* regulation in the anterior heart field, identifies distinct transcriptional regulatory networks involving *mef2c* function in two developing cardiac progenitor lineages.

MEF2

III. RESULTS

Identification of two distinct mef2c transcriptional enhancers that direct expression to the developing heart

To determine how *mef2c* transcription is regulated in the developing heart, we sought to identify regions of non-coding DNA within the *mef2c* locus that function as cardiac specific transcriptional enhancers. Evolutionary conserved segments of the locus were systematically tested for enhancer activity by fusing the putative enhancer to a heterologous promoter upstream of the *lacZ* gene and assaying for β -gal expression in transgenic embryos. This approach yielded two distinct enhancers capable of directing *lacZ* expression in the developing heart: the first enhancer directs expression in the anterior heart field, and the second enhancer is active in the developing ventricular myocardium. The anterior heart field enhancer has been characterized in detail elsewhere (Dodou et al., 2004). The second enhancer, which lies approximately 7 kb upstream of the first coding exon of *mef2c*, has been described earlier in this work and was shown to direct expression to a number of developing lineages, including glial cells of the peripheral and enteric nervous system, osteoblasts, the developing craniofacial mesenchyme, and the developing ventricular myocardium (Fig. 1). In chapters 1 and 2 of this thesis I focused upon *mef2c* enhancer activity in the developing neural crest lineages. In this chapter, I will describe how this enhancer module from *mef2c* is regulated in the developing heart.

10/10/04

The mef2c-F1 enhancer directs expression to the developing ventricular myocardium

The *mef2c*-F1 enhancer is active very early in embryonic development, beginning at 7.5 dpc within the lateral mesoderm cardiac precursor cells (Fig. 20A). Expression in the cardiogenic mesoderm persists in the cardiac crescent and then in the linear heart tube at 8.5 dpc (Fig. 20B). A more detailed examination of enhancer activity by transverse section showed that β -gal expression was present in the myocardial compartment of the linear heart tube (Fig. 20C). By 10.5 dpc, cardiac expression of the transgene was observed in both developing ventricles, though staining was consistently more intense in the left ventricle (Fig. 20D). Sections through hearts at 10.5 dpc showed that staining was restricted to the ventricular myocardium with staining in both the compact and trabecular layers (Fig. 20E). This pattern was also observed in whole mount preparations of dissected hearts (Fig. 20F). Note that no staining was observed in the atria at this or other stages and that the *mef2c*-F1 enhancer activity appears to be restricted to the developing ventricles and some cells within the outflow tract (Fig. 20D-I). In the 13.5 dpc heart, the ventricular pattern of expression directed by the *mef2c* enhancer continues with clusters of cells staining in both ventricles and with larger numbers of cells expressing β -gal in the left ventricle (Fig. 20G-H). In the neonatal heart, β -gal was still detected predominantly in the left ventricle with especially strong staining at the apex of the heart (Fig. 20I). As at earlier stages, staining was restricted to the ventricles and not detected in the atria.

WOLF LAMM

To identify the specific cells expressing *mef2c-F1-lacZ* transgene we compared the expression of β -galactosidase with the expression of known markers of endothelial cells and cardiomyocytes by immunohistochemistry (Fig. 21). At 10.5 dpc, β -gal was detected in the developing ventricular myocardium (Fig. 21A). In contrast, PECAM, a marker of endothelial cells, was detected throughout the endocardium (Fig. 21B). There was no overlap of these two markers, indicating that cardiac activity of the *mef2c-F1* enhancer was restricted to cells of the ventricular myocardium and not active in the endocardium (Fig. 21C). To confirm that β -gal was expressed in the myocardium, we compared the expression driven by the *mef2c-F1* transgene with that of Smooth Muscle Alpha-Actin, a marker of embryonic muscle. β -gal expression was detected in the ventricular myocardium (Fig. 21D). Similarly, Smooth Muscle Alpha-Actin was also detected in the myocardium (Fig. 21E). The overlapping expression of β -gal and smooth muscle alpha actin confirmed that the *mef2c-F1* enhancer directs expression specifically within the myocardial component of the embryonic ventricles (Fig. 21F).

The cardiac activity of the mef2c-F1 enhancer requires functional MCAT and MEF2 elements

The cardiac enhancer activity of the *mef2c-F1-lacZ* transgene resides within an evolutionary conserved 300 bp element that also exhibited neural crest activity (discussed in chapter 1, see Fig. 4). This 300 bp region is required for enhancer activity in the context of a 7 kb enhancer fragment, and the 300 bp element is also sufficient to direct expression in the developing cardiac and neural crest lineages (Fig. 4). To identify

UW-MADISON

transcription factors responsible for directing *mef2c*-F1-*lacZ* transgene expression to the developing ventricular myocardium, we first sought to identify the *cis*-regulatory elements responsible for enhancer activity in the heart. Figure 5 shows the 300 bp enhancer element with regions containing consensus DNA-binding sequences of known cardiac transcription factors indicated. These include GATA binding sites (5'-WGATAR-3'), which bind members of the GATA family of zinc finger transcription factors (Molkentin, 2000), an MCAT element (5'-CATTCCT-3'), which binds TEA domain containing transcription factors (Mar and Ordahl, 1990), and a MEF2 element (5'-YTAWWWWTAR-3') (Black et al., 1998). Note that while the MCAT element is well conserved across all four species in the sequence alignment (Fig. 5), neither GATA element is well conserved in the chick. The MEF2 element is not conserved to the chick, but a perfect MEF2 element is found in the chick sequence downstream of the original, and could potentially be the functional equivalent of the MEF2 element in mammals.

We next sought to test whether these putative *cis*-regulatory elements interact with their cognate transcription factors by EMSA. As discussed above, TEF-1 is essential for proper cardiac development. TEF-1 null mice exhibit dilated chambers and thin ventricular walls (Chen et al., 1994). The ability of TEF family members to bind to the *mef2c* MCAT element was compared with the ability of TEF family members to bind to a control probe containing an MCAT element from the *cTnT* promoter. In this assay, RTEF protein (also known as TEF-3 or Tead1) was used, though it should be noted that all TEF family members have been shown to have the same DNA binding specificity and relative affinity (Kaneko and DePamphilis, 1998). TEF protein bound to the *cTnT* probe,

WJL
10/11/00

causing a mobility shift (Fig. 22A, lane 2). This binding was dependent upon the consensus MCAT sequence as an excess of unlabeled probe competed for MCAT binding, while a mutant version of the unlabeled probe did not (Fig. 22A lanes 3-4). To determine if the *mef2c* MCAT element also interacted with TEF proteins, we used unlabeled *mef2c* MCAT probe to compete for TEF binding to the control probe. Excess *mef2c* MCAT probe competed for TEF binding to the *cTnT* probe, while a mutant version of the *mef2c* MCAT probe did not (Fig. 22A, lanes 5-6). We next assayed the ability of TEF to bind directly to a labeled *mef2c* MCAT element (Fig. 22A, lanes 7-12). An interaction between TEF and the *mef2c* MCAT element was detected by a mobility shift (Fig. 22A, lane 8), and this interaction was specific since it was competed by an excess of unlabeled *cTnT* MCAT probe, but not unlabeled mutant probe (Fig. 22A, lanes 9 and 10). Similarly, the interaction between TEF and the *mef2c* MCAT site was inhibited by excess unlabeled *mef2c* MCAT probe, but not by the mutant *mef2c* MCAT site (Fig. 22A, lane 11 and 12). Because the *mef2c* enhancer had functional TEF binding sites, we tested whether TEF-1 expression overlapped the *mef2c* enhancer activity by immunohistochemistry. Indeed, *mef2c*-F1-*lacZ* embryos expressed β -gal in cells also containing TEF-1 protein (Fig. 21 G-I).

In a similar experiment, the two putative GATA elements within the 300 bp *mef2c*-F1 enhancer (Fig. 5) were tested for interaction with the GATA4 transcription factor (Fig. 22B). GATA4 is essential for proper cardiac development (Molkentin, et al., 1997) and is essential for activation of the *mef2c* anterior heart field enhancer (Dodou et al., 2004). The interaction between GATA4 and the two putative *mef2c* GATA elements in the

mef2c-F1 enhancer was compared with the interaction between GATA4 and the *bona fide* GATA element from *Nkx2.5* (Lien et al., 1999). GATA4 robustly bound to the radiolabeled *Nkx2.5* GATA site (Fig. 22B, lane 2). This interaction between GATA4 and the control GATA probe was competed by an excess of unlabeled oligonucleotides containing either GATA element from the *mef2c*-F1 enhancer, but not by mutant versions of these oligonucleotides, indicating that the *mef2c*-F1 GATA elements bind GATA4 (Fig. 22B, lanes 5-8). A direct interaction between GATA4 and labeled *mef2c* GATA probes was also detected (Fig. 22B, lanes 10 and 15). Once again, this interaction was specific as it was competed by a functional GATA binding sequence, but not by unlabeled mutant probes (Fig. 22B, lanes 11, 12, 17, and 18). The interaction between *mef2c* GATA(b) and GATA4 appeared stronger than the interaction between *mef2c* GATA(a) and GATA4 either when competing with the control GATA element or when binding directly to GATA4 (compare lanes 4 versus 7 and lanes 10 versus 15).

The results of our EMSA experiments established that the putative GATA, MCAT, and MEF2 elements all formed functional interactions with their respective transcription factors *in vitro* (Figs. 7 and 22). Therefore, we tested the functional relevance of these *cis*-regulatory elements within the context of the *mef2c*-F1 enhancer *in vivo*. To do this, we made specific mutations to these elements in the context of the original 7 kilobase enhancer/reporter transgene, and assayed the consequences of mutating these elements on enhancer function *in vivo*. The wild type transgene directed expression in both the developing heart as well as neural crest derived tissues in the craniofacial mesenchyme, the peripheral nervous system, and melanocytes (Fig. 23 A, E). Disruption of the MCAT

element resulted in a complete loss of both cardiac expression and expression in the developing peripheral nervous system, suggesting that TEF proteins are required for activation of the *mef2c*-F1 enhancer in the heart and PNS (Fig. 23 B, F). Note however that expression in neural crest-derived craniofacial mesenchyme is not disrupted in the MCAT mutants, suggesting other elements are sufficient to direct expression in this neural crest-derived tissue (Fig. 23B). The MEF2 element was also required for proper function of the *mef2c*-F1 enhancer. When the MEF2 element was mutated in 9.5 dpc embryos, there was less enhancer activity than in embryos with the wild type *mef2c*-F1-*lacZ* transgene (compare Fig. 23A and C). At later time points, mutation of the MEF2 element resulted in the loss of all enhancer activity (Fig. 23G), consistent with MEF2C functioning in an autoregulatory fashion and maintaining *mef2c*-F1 activity. While the MCAT and MEF2 elements are required for normal enhancer function *in vivo*, it appeared that the GATA elements were largely dispensable for *mef2c* enhancer function. Mutation of both GATA elements resulted in no obvious change in enhancer activity (Fig. 23D, H). In some mutant GATA transgenic embryos there appeared to be a reduction of enhancer activity in the developing heart, but this reduction seemed to be within the normal range of variation observed in the wild type transgenic embryos.

Taken together, the results of the EMSA experiments and transgenic mutational analyses allow us to suggest new components of the transcriptional networks governing cardiac development. TEF proteins are required to activate *mef2c* in the developing ventricles and MEF2 is then required to maintain its expression in this lineage. Surprisingly, while

GATA factors are required for *mef2c* expression in the anterior heart field, (Dodou et al., 2004), they do not appear required for direct activation of the *mef2*-F1 enhancer.

III. Discussion

MEF2 and TEF transcription factors have been known to function critically during cardiac development based on knockout studies (Chen, et al. 1994; Lin, et al. 1997) and have been shown to directly activate the transcription of muscle structural genes (Kariya et al., 1993; Kariya et al., 1994; Karns et al., 1995; Chen et al., 1994; Stewart et al., 1998; Maeda et al., 2002b). Yet, how MEF2 and TEF fit into the transcriptional regulatory networks that direct cardiac expression has remained unclear. Here, we show that *mef2c* is a direct transcriptional target of TEF protein in the developing ventricular myocardium by characterizing a cardiac enhancer in the *mef2c* locus. We show that the enhancer is active in the developing myocardium very early during cardiogenesis, and that its activity continues past birth. We identify MEF2 and MCAT *cis*-regulatory elements that reside within this enhancer and show that they both bind to their corresponding transcription factors and are required for proper enhancer function *in vivo*.

An emerging relationship between TEF and MEF2 in the transcriptional control of cardiac function

A number of commonalities exist between MEF2 and TEF in the developing heart. Both are required for proper cardiac development and function as transcriptional activators of cardiac specific genes (Chen et al., 1994; Lin et al., 1997). Additionally, both MEF2 and

TEF have been implicated in the reactivation of the fetal gene program in models of cardiac hypertrophy (Kolodziejczyk et al., 1999; Lu et al., 2000; Passier et al., 2000). In fact, it has been demonstrated that some muscle genes, such as *beta-myosin heavy chain* and *MLC2v* are acted upon by both MEF2 and TEF factors (Maeda et al., 2002b). Further, both MEF2 and TEF factors have been shown to interact with common transcriptional co-regulators, as both MEF2 and TEF have been shown to interact with vestigial-like 2 (Maeda et al., 2002a). In addition to sharing interaction partners and functions, MEF2 and TEF factors have been shown to form a direct interaction, suggesting that these factors can function as transcriptional partners (Maeda et al., 2002b; Azakie et al., 2005), and have even been reported to share *cis*-acting elements (Karasseva, et al., 2003). Identification of *mef2c* as a direct transcriptional target of TEF proteins suggests an important hierarchical relationship between these transcription factors in cardiac development

In a number of developing lineages, *mef2c* has been shown to be a direct transcriptional target of an essential, tissue specific transcriptional regulator. Once MEF2C is expressed, it then functions as a direct transcriptional partner of its upstream regulator. This is true of a MEF2C-MyoD interaction in the skeletal muscle lineage (Black et al., 1998; Dodou et al., 2003), a MEF2C-GATA4 interaction in the second heart lineage (Dodou et al., 2004; Morin et al., 2000), and of a SOX10-MEF2C interaction in developing neural crest lineages (chapter 1). This paradigm of MEF2 function in development now appears to extend to a MEF2-TEF interaction in the developing ventricular myocardium. It will be interesting to see whether MEF2C functions in a similar fashion in the other developing

UNIVERSITY OF MICHIGAN

lineages in which it is expressed, including the developing vascular endothelium, craniofacial mesenchyme, and the immune system (De Val et al., 2004; Swanson et al., 1998, and chapter 2).

Conservation of sequence indicates conservation of function

In the field of bioinformatics, the use of evolutionary conservation is an invaluable tool for locating functional regions of the genome. In this work, the study of evolutionary conserved sequences facilitated the identification of a functional enhancer in the *mef2c* locus, and evolutionary conservation was again utilized to pinpoint exact *cis*-regulatory elements required for enhancer function. Within the 300 bp minimal enhancer region, a number of candidate elements were identified based upon known consensus DNA binding motifs, known functionality in the cardiac lineage, and evolutionary conservation across multiple species (Fig. 5). When these elements were systematically tested for function *in vivo*, only the elements most deeply conserved proved necessary for normal enhancer function. The MCAT and MEF2 elements are both conserved between birds and mammals. This deep conservation was indicative of their essential function in cardiac enhancer activity. Conversely, the GATA elements, which were not required for enhancer activity, have been conserved over less evolutionary time. Study of this enhancer provides further evidence to the value of applying sequence conservation to the identification of functional transcriptional regulatory elements using bioinformatic analyses.

UNIVERSITY OF MICHIGAN

TEF proteins are required to activate mef2c expression in multiple developmental lineages through a single enhancer

The *mef2c* enhancer described in this work not only directs expression to the developing ventricular myocardium, but also to developing neural crest lineages (chapter 1). This observation raises the question of how one enhancer can direct expression within two distinct lineages. However, our work in this chapter, combined with work on this enhancer in previous chapters, suggests that one enhancer may govern multiple different patterns of expression due to shared regulatory elements (Fig. 5). While we have shown that SOX elements are required for expression in multiple neural crest lineages, these elements are dispensable for cardiac enhancer activity (Chapter 1). The MCAT element appears necessary for enhancer function in both cardiac and a subset of neural crest-derived lineages. Recently, the TEF family member Tead2 (TEF-4) was shown to be an important early regulator of Pax3 expression in the developing neural crest, and it appears that neural crest expression of *mef2c* may be under similar TEF-mediated transcription control (Milewski et al., 2004). Thus it appears that the *mef2c*-F1 enhancer is responsive to different combinations of transcription factors in each of the developing lineages where it is active (Figs. 8, 23). It is likely that the common feature in each *mef2c*-F1 enhancer activity is the MEF2 element functioning in an autoregulatory role. As alluded to earlier, the *mef2c* enhancer is also active in the craniofacial mesenchyme, and, later in development, becomes active in developing osteoblast cells. Enhancer activity in these lineages is independent of either the SOX elements or the MCAT element, yet the MEF2 element is still required for maintenance of enhancer activity in the osteoblasts and

craniofacial mesenchyme. MEF2 has recently been shown to function as a positive autoregulator in somatic muscle development in *Drosophila* (Cripps et al., 2004), and it will be interesting to see if autoregulation is a common theme by which *mef2c* expression is regulated in other developing lineages.

11
12
13
14
15
16
17
18
19
20
21
22
23
24
25
26
27
28
29
30
31
32
33
34
35
36
37
38
39
40
41
42
43
44
45
46
47
48
49
50
51
52
53
54
55
56
57
58
59
60
61
62
63
64
65
66
67
68
69
70
71
72
73
74
75
76
77
78
79
80
81
82
83
84
85
86
87
88
89
90
91
92
93
94
95
96
97
98
99
100

Chapter 3 Figure legends

Fig. 20. The *mef2c*-F1 enhancer is active in the developing ventricular myocardium. Expression of the *mef2c*-F1-*lacZ* transgene is detected as early as 7.5 dpc in the cardiac crescent (A). *Mef2c*-F1-*lacZ* expression continues in the linear heart tube at 8.0 dpc (arrow in B). This is better visualized on transverse sections through the 8.5 dpc heart (arrow in C). By 10.5 dpc, *mef2c*-F1-*lacZ* expression is detected robustly in both the right and left ventricles (arrow), but not within the atria of the heart (D). β -gal activity is more extensive in the left ventricle rather than the right, as revealed by transverse sections through the 10.5 dpc heart (E), and in whole mount preparations of a 10.5 dpc heart (F). A similar pattern of expression is observed in the 13.5 dpc heart as well (G). Again, β -gal expression directed by *mef2c*-F1-*lacZ*, is more extensive in the left ventricle than in the right (H). In the perinatal heart, expression is still observed in groups of cells within the left and right ventricles, and is generally not observed in the atria (I). LV, left ventricle.

Fig. 21. The *mef2c*-F1 enhancer is active in the developing ventricular myocardium. Immunofluorescence was used to determine the specific cells in which the *mef2c*-F1-*lacZ* transgene was active. Cryosections of 10.5 dpc *mef2c*-F1-*lacZ* transgenic embryos were co-stained for β -gal (green, panel A) and the endothelial cell marker PECAM (red, panel B). No overlap in staining between these two cell populations was observed (C). To determine if β -gal was expressed in myocardial cells, co-staining with anti- β -gal (green, panel D) and anti-smooth muscle alpha actin (red, panel E) was performed. Expression of these two markers showed significant overlap (F), indicating that the *mef2c*-F1-*lacZ*

transgene is active in the ventricular myocardium. Note that the atria are not marked with β -gal expression. Staining was also performed to see if β -gal expression overlaps with TEF-1. When sections were co-stained with anti-Bgal (green, panel G) and anti-TEF-1 (red, panel H). Overlap of these markers was observed (I).

Fig.22. TEAD and GATA family members both bind to the *mef2c*-F1 enhancer. (A) Radiolabeled oligos containing the MCAT element from the *cTnT* promoter were used to assay for TEAD-binding by EMSA. Lysate programmed to express TEF-3 was able to induce a mobility shift of the labeled oligos (lane 2), while unprogrammed lysate was not (lane 1). This shift could be competed with an excess of cold oligo containing the *cTnT* MCAT element (lane 3), but not by a mutant version of this oligo (lane 4). Cold oligos containing the putative *mef2c* MCAT element could also compete for binding (lane 5), whereas mutant versions of these oligos could not (lane 6). Similarly, radiolabeled oligos containing the MCAT element from the *mef2c* enhancer exhibited a mobility shift in the presence of TEF-3-programmed lysate (lane 8). This shift could be competed with an excess of unlabeled *cTnT* MCAT oligos (lane 9) or wild-type *mef2c* enhancer MCAT-containing oligos (lane 11), but not by mutant versions of these oligos (lanes 10 and 12). (B) In a similar experiment, oligos containing a control GATA element from the *Nkx2.5* enhancer were radiolabeled and assayed for electrophoretic mobility shift. While unprogrammed lysate did not induce a mobility shift (lane 1), lysate programmed to express GATA4 did not induce a mobility shift (lane 2). This shift could be competed by an excess of unlabeled oligos containing the *Nkx2.5* GATA element (lane 3), but not by a mutant version of these oligos (lane 4). Unlabeled oligos containing the GATA elements

EMSA

found in the *mef2c* enhancer could also compete for binding (lanes 5 and 7), whereas mutant versions of these oligos could not (lanes 6 and 8). Similarly, oligos containing the GATA elements from the *mef2c* enhancer were labeled and assayed for a mobility shift in the presence of GATA4-programmed lysate (lanes 10 and 16). These mobility shifts were disrupted by addition of unlabeled oligos containing control or *mef2c* GATA elements, but not by mutant versions of these oligos.

Fig. 23. The *mef2c*-F1 enhancer is dependent upon TEF proteins for activation and MEF2 proteins to maintain this activity. Embryos containing the *mef2c*-F1-*lacZ* transgene exhibit β -gal activity in the developing hearts and craniofacial mesenchyme at 9.5 dpc (A) and in the hearts, melanoblasts, and PNS tissues at 11.5 dpc (E). When the MCAT element is mutated in the *mef2c*-F1-*lacZ* transgene, cardiac enhancer activity is lost in 9.5 dpc embryos, whereas expression in the craniofacial mesenchyme is uninterrupted (B). In 11.5 dpc mutant MCAT *mef2c*-F1-*lacZ* transgenic embryos, no expression is observed in either cardiac or neural crest tissues (F). Embryos containing mutant MEF2 *mef2c*-F1-*lacZ* exhibit weaker staining in the cardiac and neural crest tissues at 9.5 dpc (C), and by 11.5 dpc, no expression is observed in mutant MEF2 *mef2c*-F1-*lacZ* embryos (G). In contrast, embryos containing a *mef2c*-F1-*lacZ* transgene with the GATA elements mutated exhibit a wild-type pattern of expression (D). The wild-type expression pattern continues in the mutant GATA *mef2c*-F1-*lacZ* transgenic embryos at 11.5 dpc (H).

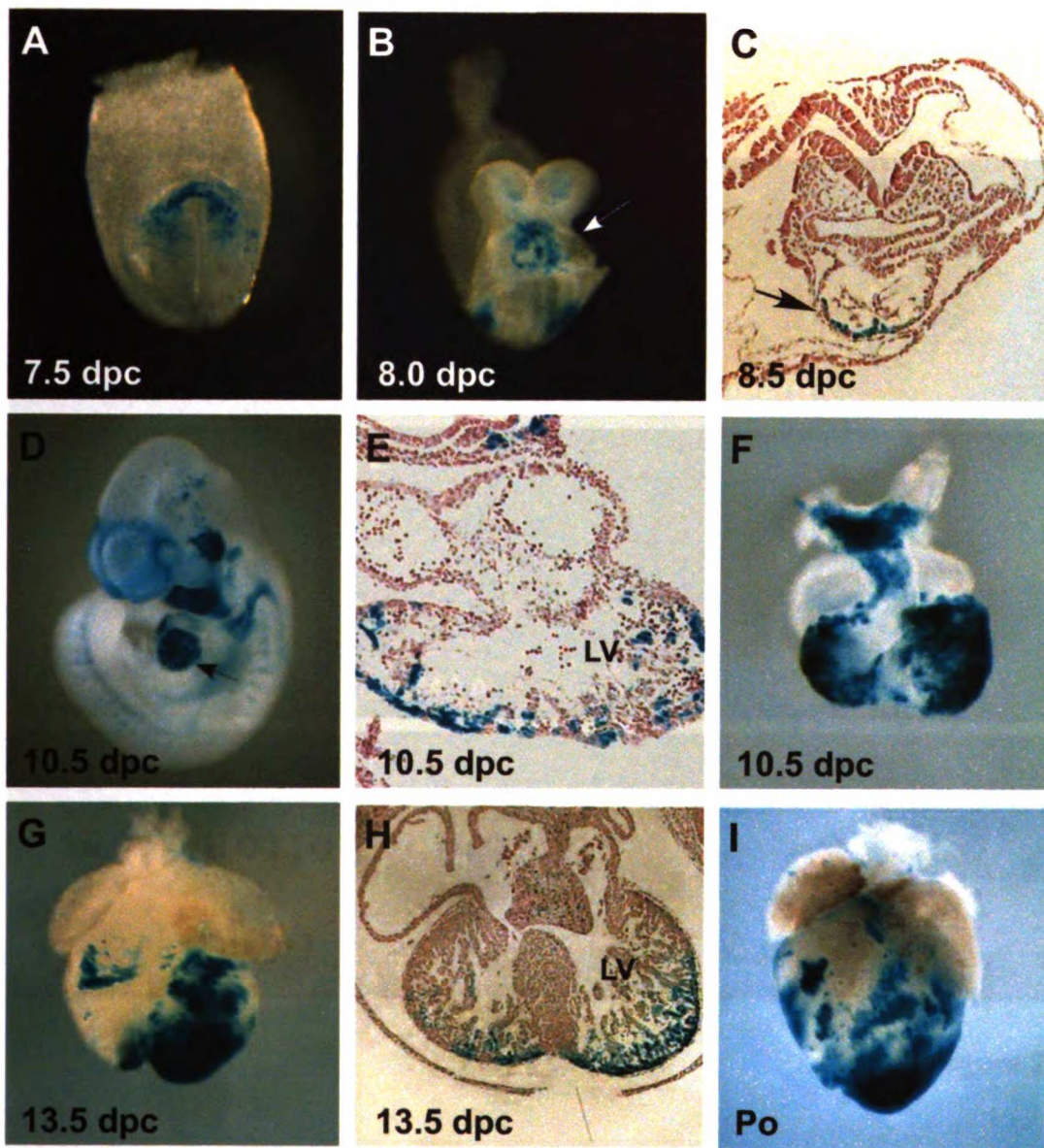


Figure 20

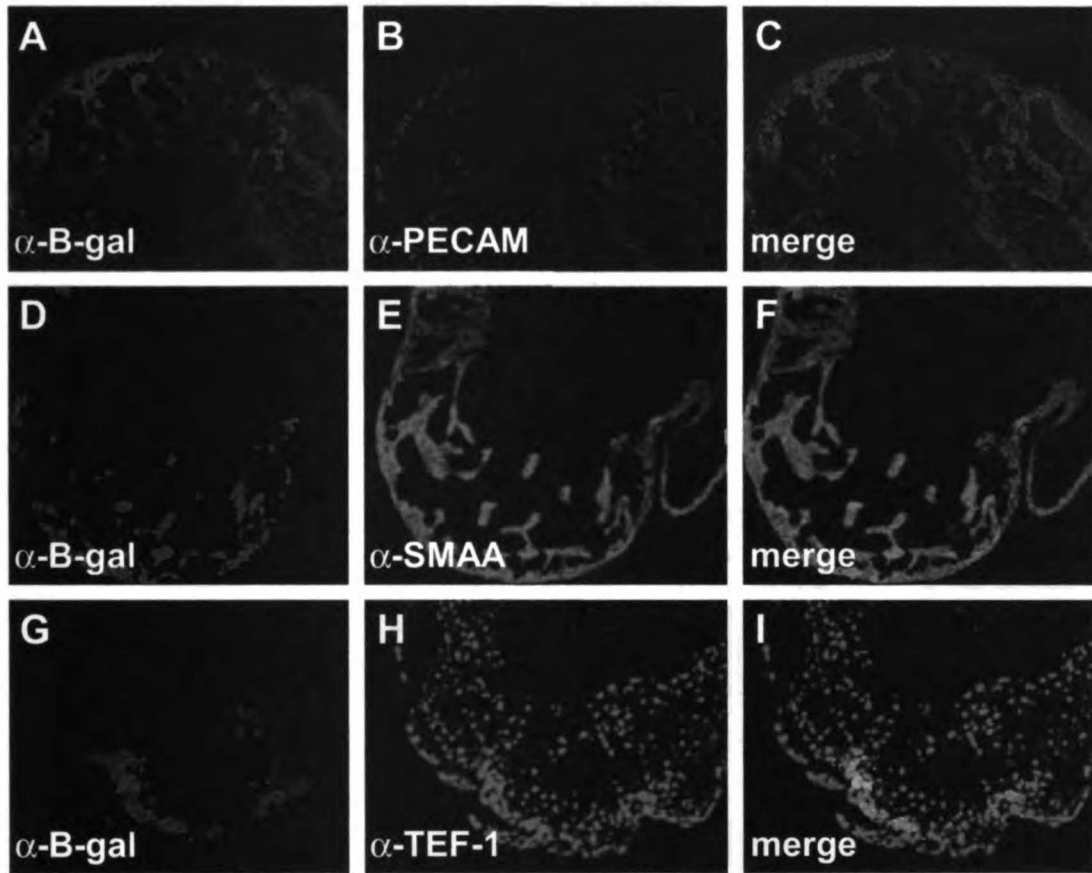
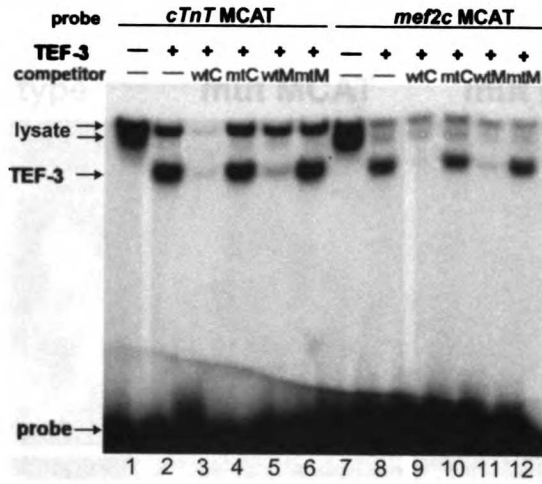


Figure 21

A



B

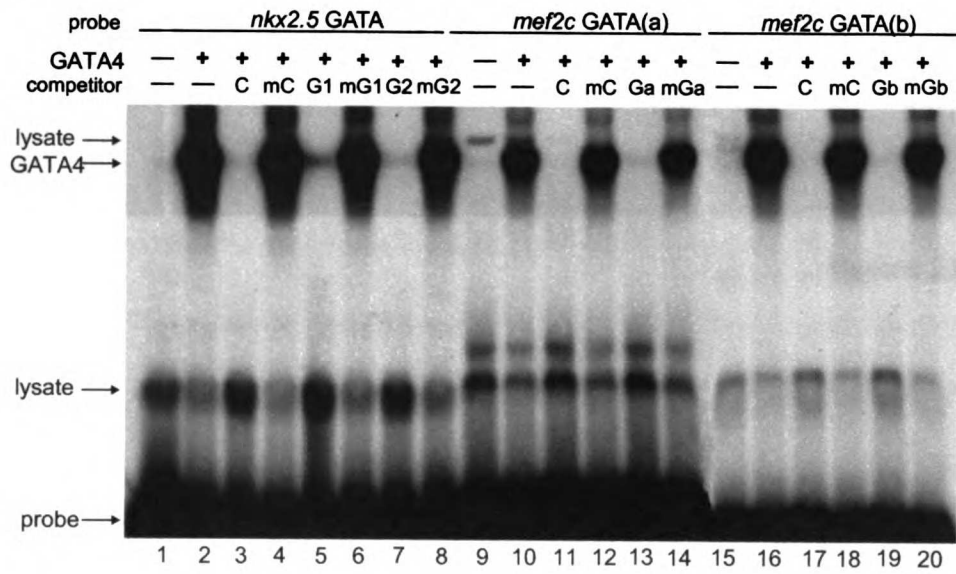


Figure 22

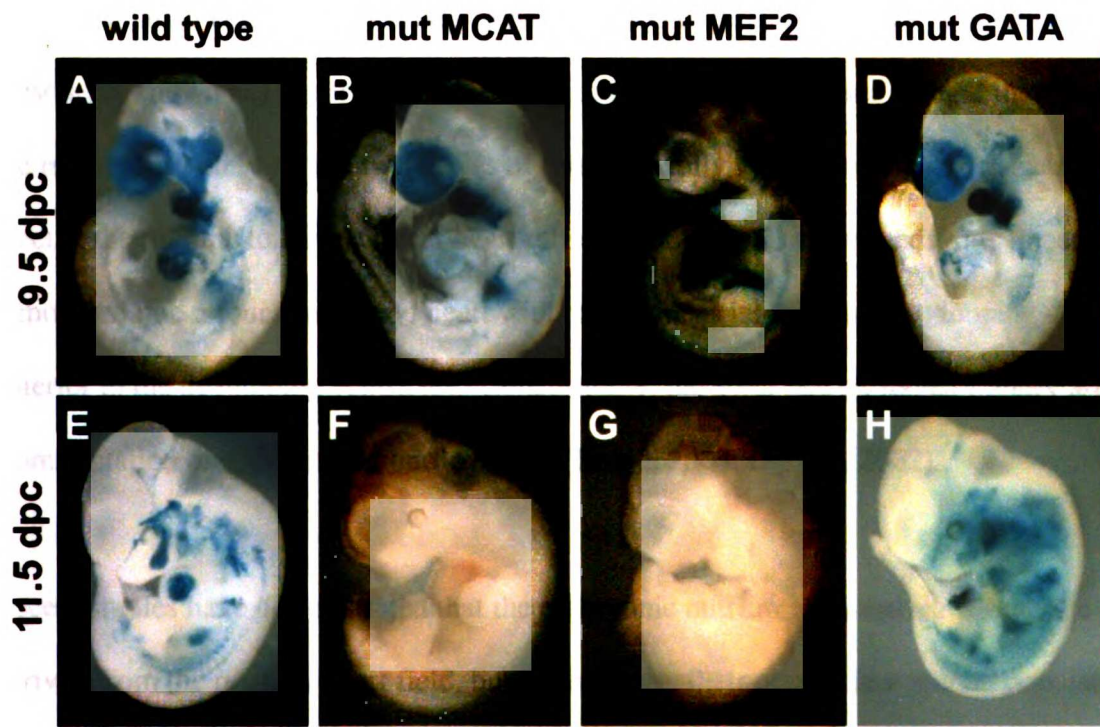


Figure 23

Chapter 4: The right ventricle, outflow tract, and ventricular septum are derived from the anterior heart field

IV. Introduction

The mammalian heart initially arises from the fusion of bilateral regions of anterior mesoderm known as the cardiac crescent. During ventral folding and foregut invagination of the mammalian embryo, the two halves of this bilaterally symmetrical primary heart field meet at the midline to form a linear heart tube. As development proceeds, this linear tube is remodeled into a four chambered heart with the future atrial myocardium looping dorsal and anterior to the developing ventricles. Concurrently, the aorta and pulmonary artery arise from septation of the common outflow tract (Brand, 2003; Harvey, 2002).

Recent studies have demonstrated that the embryonic outflow tract and right ventricle are not derived from the primary heart field, but instead have their origins in a second population of cells known as the secondary or anterior heart field (Abu-Issa et al., 2004; Kelly and Buckingham, 2002; Yutzey and Kirby, 2002). The cells that comprise the anterior heart field reside in the splanchnic and pharyngeal mesoderm and appear to be progressively added to the arterial pole of the developing heart at the time of cardiac looping (Kelly et al., 2001; Mjaatvedt et al., 2001; Waldo et al., 2001). The identification of a second population of cardiogenic mesoderm that gives rise to the right ventricle and outflow tract provides a potential explanation for the observation that numerous genes and transgenes exhibit expression that is restricted to the outflow tract and right ventricle (Kelly and Buckingham, 2002; Schwartz and Olson, 1999). In addition, mutations in several key cardiac transcription

factors, including *mef2c*, *Isl1*, *Nkx2.5*, *Hand2*, and *Foxh1*, appear to selectively affect the development of the right ventricle and outflow tract (Cai et al., 2003; Lin et al., 1997; Lyons et al., 1995; Srivastava et al., 1997; von Both et al., 2004). In each case, these mice have a single ventricular chamber, and the heart fails to undergo normal looping morphogenesis. However, it remains unclear whether addition of the anterior heart field occurs normally in these mice, and whether the observed cardiac phenotypes result from a defect in anterior heart field development.

While it is clear that the myocardium is derived from at least two mesodermal progenitor populations, the precise boundaries of the secondary/anterior heart field, the lineages derived from this population, and its contributions to the postnatal heart remain unclear. In the chick, fate mapping studies have revealed that the splanchnic mesoderm proximal to the developing outflow tract constitutes a secondary heart field that will contribute to the elongating outflow tract myocardium (Mjaatvedt et al., 2001; Waldo et al., 2001). Similarly, a population of cells in transgenic mice expressing *lacZ* under the control of *Fgf10* regulatory elements resides in the splanchnic and pharyngeal mesoderm before contributing to the myocardium at the arterial pole (Kelly et al., 2001). Other studies have suggested that the anterior heart field gives rise to the embryonic right ventricle as well as the outflow tract (Zaffran et al., 2004), or that the secondary/anterior heart field may have an even broader developmental potential (Cai et al., 2003; Laugwitz et al., 2005; Meilhac et al., 2004a). We have recently identified a promoter and enhancer from the mouse *mef2c* gene that is sufficient to direct expression exclusively to the anterior heart field during embryonic development (Dodou et al., 2004). This *cis*-acting regulatory module from *mef2c* directs expression to the anterior heart field

beginning at cardiac crescent stage at 7.5 dpc, to the pharyngeal mesoderm and the arterial pole at the linear heart tube stage, and to the outflow tract and right ventricle during subsequent embryonic development. The enhancer is not active in the left ventricle or atria and is silent during adulthood (Dodou et al., 2004). The expression domain directed by the *mef2c* anterior heart field enhancer is likely a subfield of that described elsewhere as the second heart lineage (Meilhac et al., 2004b) or a more spatially restricted component of the *Isl1* expression domain (Cai et al., 2003).

In the present study, we examined the expression of *mef2c*-AHF-*lacZ*, which expresses *lacZ* under the control of the *mef2c* anterior heart field promoter and enhancer, in *mef2c* knockout mice. We show that the common ventricular chamber in *mef2c* knockout mice expresses *mef2c*-AHF-*lacZ*, suggesting that this chamber is composed of derivatives from both the primary and secondary heart fields. Interestingly, the *mef2c*-AHF-*lacZ* transgene is only expressed on the dorsal side of the common ventricular chamber, suggesting that these mice are not defective in the addition of the anterior heart field to the common ventricle, but rather in the patterning or looping of the ventricular chamber. We have also generated transgenic mice that express Cre exclusively within the anterior heart field and its derivatives in the right ventricle and outflow tract using this regulatory element from *mef2c*. We used these anterior heart field specific Cre transgenic mice, termed *mef2c*-AHF-Cre, to generate a fate map of the embryonic, fetal, and postnatal heart. By crossing *mef2c*-AHF-Cre mice to ROSA26R Cre-dependent *lacZ* reporter mice (Soriano, 1999), we show that the outflow tract, right ventricle, and the ventricular septum are marked by the activity of the *mef2c*-AHF-Cre transgene.

In addition, the studies presented here demonstrate that cells marked by the *mef2c*-AHF-Cre transgene contribute to the endocardium of the right ventricle. We also show that within the outflow tract, the myocardium and endothelium are marked by the *mef2c*-AHF-Cre transgene, whereas the smooth muscle layer of the outflow tract is largely derived from neural crest with some anterior heart field contribution near the pulmonary trunk. These studies also demonstrate that the epicardium and coronary vessels have an embryonic origin distinct from the anterior heart field population marked by *mef2c*-AHF-Cre. Thus, these studies provide a fate map of a highly restricted subdivision within the secondary/anterior heart field in mice and describe the first transgenic mouse line with Cre activity restricted exclusively to the anterior heart field and its derivatives. These mice will be a crucial tool for examining the genetic pathways that control cardiac development by conditional gene inactivation exclusively in the anterior heart field and its derivatives in the outflow tract and right ventricle.

IV. Results

An anterior heart field-specific transgene is expressed in the common ventricular chamber in mef2c null mice

Coincident with ventral turning of an E8.5 mouse embryo is the rightward looping of the embryonic heart. Previous studies have identified a number of genes necessary for cardiac looping morphogenesis, including *Isl1*, *foxh1*, *Hand2*, *Nkx2.5*, and *mef2c* (Cai et al., 2003; Lin et al., 1997; Lyons et al., 1995; Srivastava et al., 1997; von Both et al., 2004). Mice

lacking these genes share a common phenotype: a generally hypoplastic heart with a single, linear ventricular chamber and death at midgestation. Interestingly, these genes also share a common expression pattern in the anterior heart field or in tissues derived from that progenitor population (Edmondson et al., 1994; Lints et al., 1993; Srivastava et al., 1995; Srivastava et al., 1997; Cai et al., 2003; von Both et al., 2004). It has been suggested that the migration of cells from the anterior heart field into the linear heart tube may direct looping morphogenesis, and that a lack of anterior heart field contribution to the common ventricular chamber may be the cause of the looping defect in these mutant mice (Yelbuz et al., 2002). It has also been suggested that the common ventricular chamber in these knockout mice lacks right ventricle identity, expressing primarily left ventricular markers (McFadden et al., 2000; Thomas et al., 1998).

To test whether markers of the anterior heart field are expressed in the single common ventricular chamber in *mef2c* mutant mice, we examined the expression of an anterior heart field specific *lacZ* transgene, *mef2c*-AHF-*lacZ*, in *mef2c* knockout embryos (Fig. 24). Previous work has shown that this transgene is expressed exclusively in the anterior heart field and its descendants in the right ventricle and outflow tract during development (Dodou et al., 2004). *LacZ* expression in wild type and *mef2c* null animals appeared identical from 7.75 dpc until 8.25 dpc (Fig. 24, compare panels A, B to E, F). However, by 9.0 dpc, *mef2c* null animals began to show abnormal cardiac morphology (Fig. 24G, H). At this stage, anterior heart field marked cells were observed in the right ventricle and outflow tract of wild type mice (Fig. 24C, D). Interestingly, *mef2c*-AHF-*lacZ* expression was also detected in the common ventricular chamber of *mef2c* null embryos (Fig. 24G, H). These results indicate

that the *mef2c*-AHF-*lacZ* anterior heart field marker is expressed in the common ventricular chamber in *mef2c* mutants. In the unlooped heart of these mutant mice, the anterior heart field marked cells comprise the dorsal anterior region of the common ventricular chamber (Fig. 24G, H). This result suggests that the unlooped ventricle in *mef2c* mutants has progenitor cells from the anterior heart field, which should normally give rise to the right ventricle, even though this common ventricle lacks markers of right ventricular identity (McFadden et al., 2000). The expression of this anterior heart field marker in the hearts of *mef2c* mutant embryos strongly suggests that cells from the anterior heart field are added to the ventricle in *mef2c* null mice and possibly other looping mutants.

An anterior heart field-specific Cre transgene under the control of regulatory elements from mef2c

Anterior heart field marker expression in the hearts of *mef2c* mutant mice was unexpected and suggests that we do not have a full appreciation for the contribution or role of the anterior heart field in the developing mouse heart. Indeed, there are several discrepancies regarding contribution of the secondary/anterior heart field to the developing heart (Cai et al., 2003; Kelly and Buckingham, 2002; Yutzey and Kirby, 2002), and many questions remain regarding the boundaries of anterior heart field-derived cell populations. In addition, the contribution of the secondary/anterior heart field to the postnatal heart has yet to be determined in detail. To address these issues, we used an anterior heart field-specific promoter and enhancer from *mef2c* to direct expression of Cre recombinase in transgenic mice (Fig. 25A). We crossed these mice, termed *mef2c*-AHF-Cre, to ROSA26R *lacZ*

11/11/11 11:11

reporter mice (Soriano, 1999) to determine the contribution of this population of cells to the developing mouse heart. As shown here and in previous work (Dodou et al., 2004), the *mef2c* anterior heart field enhancer is specific to the population of cells that make up the anterior heart field and its derivatives in the outflow tract and right ventricle. Expression directed by the enhancer is tightly restricted to these tissues and is not observed in the left ventricle or atria (Dodou et al., 2004).

Mef2c-AHF-Cre positive transgenic founder mice were screened by crossing to ROSA26R *lacZ* reporter mice, which activate *lacZ* expression in a Cre-dependent manner (Soriano, 1999). We screened six *mef2c*-AHF-Cre founder lines that were positive for the transgene by Southern blot. Among these, four had a pattern of β -galactosidase activity consistent with the anterior heart field and its derivatives, whereas the other two lines had no detectable X-gal staining (not shown). In the *lacZ*-expressing lines, β -galactosidase activity was detected in the right ventricle, outflow tract, and pharyngeal mesoderm at 10.0 dpc, consistent with an anterior heart field origin (Fig. 25). Three *mef2c*-AHF-Cre transgenic lines were characterized in detail for Cre expression (Fig. 25B-D), and one of these lines, 200A, was chosen for further analysis.

The mef2c-AHF-Cre transgene is active at early cardiac crescent stage and its expression overlaps with markers of the secondary/anterior heart field

To verify that Cre activity in *mef2c*-AHF-Cre mice was specifically marking the anterior heart field, we compared β -galactosidase expression in *mef2c*-AHF-Cre Tg/0; ROSA26R

lacZ⁺ embryos with the expression of *Isl1* and *Fgf10*, which are early markers of the secondary/anterior heart field in mice. *Fgf10* was the first anterior heart field marker described (Kelly et al., 2001), while *Isl1* is an essential gene required for secondary heart field development (Cai et al., 2003) and has been shown to directly activate *mef2c* transcription in the anterior heart field (Dodou et al., 2004). β -galactosidase activity was first observed in *mef2c*-AHF-Cre Tg/0; ROSA26R *lacZ*⁺ embryos in the cardiac crescent at 7.5 dpc (Fig. 26A). By 8.0 dpc, Cre activity was strongly apparent in the cardiac crescent as ventral folding was occurring to bring the two lateral fields of splanchnic mesoderm cells together in the dorsal anterior domain characteristic of the anterior heart field (Fig. 26B). This pattern of expression overlapped the expression of *Fgf10* and *Isl1*, which are expressed in the early anterior heart field but are also expressed broadly outside this domain (Fig. 26E, F). These results demonstrate that *mef2c*-AHF-Cre specifically marks cells only within the anterior heart field and is robustly active even at early stages in cardiac development. Expression of β -galactosidase at 9.5 dpc strongly marked cells within the anterior heart field and its derivatives, including the pharyngeal mesoderm, outflow tract, and right ventricular myocardium (Fig. 26C, D). Similar histological sections of E9.5 embryos showed overlapping expression between *mef2c*-AHF-Cre marked cells and *Isl1* mRNA in the pharyngeal mesoderm and in the dorsal wall of the pericardium (Fig. 26D, H). Taken together, these results show that expression of Cre in *mef2c*-AHF-Cre transgenic mice marks the anterior heart field.

Mef2c-AHF-Cre expressing cells and their descendants contribute to the right ventricle, outflow tract, and ventricular septum

While previous work has suggested that anterior heart field derived cells give rise to a number of cardiac tissues in the embryo, none have examined the contribution to the fetal or postnatal heart in detail, and some discrepancies exist regarding the boundaries of secondary/anterior heart field contribution to the mature heart (Cai et al., 2003; Meilhac et al., 2004a; Meilhac et al., 2004b; Waldo et al., 2001; Zaffran et al., 2004). To define the contribution of the *mef2c*-AHF-Cre anterior heart field marked population to the developing and postnatal heart, we crossed these mice to ROSA26R Cre-dependent *lacZ* reporter mice to generate a fate map (Fig. 27). We compared the Cre-dependent *lacZ* expression in these crosses to the expression of *lacZ* directly under the control of the *mef2c* anterior heart field enhancer using *mef2c*-AHF-*lacZ* transgenic mice (Dodou et al., 2004). The goals of these comparisons were to identify regions of the heart that were marked by the Cre-derived fate map but that never showed direct *lacZ* expression in *mef2c*-AHF-*lacZ* transgenic hearts, which would indicate regions of the heart that had embryological origins derived from the *mef2c*-AHF-Cre defined anterior heart field and its descendants. In addition, we sought to identify regions of the heart that were not marked by the *mef2c*-AHF-Cre fate map, which would indicate regions of the heart that were not derived from the *mef2c*-AHF-cre expressing population.

At 9.5 dpc, the *mef2c* anterior heart field enhancer was clearly active in the future right ventricle and outflow tract, as well as in the pharyngeal mesoderm (Fig. 27A, I). However,

no activity was observed in the future left ventricle in *mef2c*-AHF-*lacZ* transgenic embryos (Fig. 27A, I). The Cre-derived fate map also marked the right ventricle, outflow tract, and pharyngeal mesoderm at 9.5 dpc (Fig. 27E, M). β -galactosidase activity in *mef2c*-AHF-Cre embryos was also observed in the future left ventricle at this stage (Fig. 27E, M), indicating that cells marked at an earlier time by the *mef2c* enhancer contribute to the future left ventricle since the enhancer itself is never active in the left ventricle (Fig. 27A, I). The *mef2c* anterior heart field enhancer continued to be active in the outflow tract and right ventricle at 12.0 dpc (Fig. 27B, J). Again, the Cre-derived fate map also marked these regions and also marked the developing ventricular septum and proximal regions of the left ventricle at this stage (Fig. 27F, N). By comparison, the activity of the *mef2c* anterior heart field enhancer itself, as indicated in *mef2c*-AHF-*lacZ* transgenic animals, was restricted to the right ventricle and outflow tract and did not cross the ventricular septum at this or any other stage of development (Fig. 27B, J).

By 14.5 dpc, the once common outflow vessel has been distinctly divided into the pulmonary artery and aorta, and by this stage, the activity of the *mef2c* anterior heart field enhancer itself was largely restricted to a region of the right ventricle near the pulmonary trunk (Fig. 27C). There was also some weak, residual β -galactosidase activity in right ventricular myocardium near the ventricular chamber in *mef2c*-AHF-*lacZ* transgenic hearts (Fig. 27C, K). By contrast, β -galactosidase expression in *mef2c*-AHF-Cre; ROSA26R embryos was observed throughout the right ventricle, ventricular septum, the left ventricle proximal to the septum, and in both outflow vessels at this stage (Fig. 27G, O). In *mef2c*-AHF-*lacZ* neonatal hearts, β -galactosidase activity continued to be observed weakly in the right ventricular wall

especially near the pulmonary trunk (Fig. 27D, L). In *mef2c*-AHF-Cre; ROSA26R transgenic mice, β -galactosidase activity was observed throughout the right ventricle, proximal aorta and pulmonary artery, and throughout the ventricular septum, while essentially no expression was observed in the atria or most of the left ventricle (Fig. 27H, P). It is notable that no *mef2c*-AHF-Cre marked cells were detected in the majority of the left ventricle or in the atria at this or any other developmental stage (Fig. 27E-H, M-P).

Taken together, the data presented in Fig. 27 demonstrate that the outflow tract and right ventricle are marked by the activity of the *mef2c*-AHF-Cre transgene, and that the ventricular septum and proximal portions of the left ventricle are derived from *mef2c*-AHF-Cre expressing cells in the anterior heart field and their descendants. These data also demonstrate that the majority of the left ventricle and the atria are not derived from *mef2c*-AHF-Cre expressing cells in the anterior heart field and pharyngeal mesoderm, suggesting that this represents a subpopulation of the larger secondary heart field in the mouse, which is marked by the *Isl1*-Cre fate map (Cai et al., 2003).

Right ventricular and outflow tract endothelial cells are marked by the mef2c-AHF-Cre transgene

The endocardium is the endothelial cell lining of the heart and plays an important role in heart function and in reciprocal signaling with the myocardium (Brutsaert, 2003). Despite the importance of the endocardium, its developmental origins remain to be defined in detail. Previous studies have indicated that some endocardial cells are derived from the secondary

heart field, although the extent of this contribution remains unclear (Cai et al., 2003). In crosses of *mef2c*-AHF-Cre transgenic mice with ROSA26R Cre-dependent reporter mice, we observed that the endothelial cells of outflow tract and right ventricle were positively marked by X-gal staining (Fig. 27M). To examine *mef2c*-AHF-Cre directed *lacZ* expression in the endothelium in greater detail, we also assayed β -galactosidase expression directly by immunohistochemistry using an anti- β -galactosidase antibody (Fig. 28A). We compared β -galactosidase expression to the expression of the endothelial cell marker PECAM (Fig. 28B), and observed that β -galactosidase protein was co-expressed with PECAM in the right ventricle and outflow tract at 10.5 dpc (Fig. 28C). Taken together, the results from Figs. 27 and 28 demonstrate that the endothelial cells of the proximal outflow tract and right ventricle are marked by the *mef2c*-AHF-Cre transgene.

Epicardium, coronary vessels, and the majority of outflow tract smooth muscle are not derived from mef2c-AHF-Cre expressing cells in the anterior heart field

Our work presented here, as well as the work of others (Cai et al., 2003; Kelly et al., 2001; Mjaatvedt et al., 2001; Waldo et al., 2001), demonstrates that anterior heart field derived cells contribute to the myocardial component of the outflow vessels of the heart (Fig. 27). Interestingly, previous studies have shown that the cardiac neural crest also contributes to the outflow vessels, giving rise to the smooth muscle of the tunica media (Epstein et al., 2000; Jiang et al., 2000; Waldo et al., 1999). Very recently, a study performed in chick showed that the smooth muscle of the most proximal outflow tract is derived from secondary heart field rather than cardiac neural crest (Waldo et al., 2005b). To address which cells of the

outflow vessels are derived from each specific developmental field in the mouse, we compared ROSA26R directed β -galactosidase expression in the outflow tract from transgenic mice expressing *mef2c*-AHF-Cre and *Wnt1*-Cre (Danielian et al., 1998). *Wnt1*-Cre marks all neural crest cells and their descendants, including the cardiac neural crest and its derivatives in the outflow tract (Danielian et al., 1998; Jiang et al., 2000). *Mef2c*-AHF-Cre derived cells comprised the endothelial lining and outer myocardial component of the aorta and pulmonary artery, but did not appear to contribute to the smooth muscle cells in the more distal regions of the outflow tract (Fig. 28D). Instead, neural crest derived cells comprised the smooth muscle layer within the more distal outflow tract (Fig. 28E). Neural crest descendants were not observed within the endothelial lining the outflow tract or in the muscular myocardial portion of the outflow vessels (Fig. 28E). Near the base of the heart, both *Wnt1*-Cre and *mef2c*-AHF-Cre derived cells contributed to the smooth muscle cells of the pulmonary trunk and to the cells of the pulmonary valve leaflets (Fig. 28F, G). Thus, it appears that the cardiac neural crest and the anterior heart field each give rise to smooth muscle cells of the outflow tract near the base of the heart but have largely non-overlapping contributions to the more distal regions of the outflow vessels (Fig. 28D-G).

Previous studies have suggested that the coronary vessels and epicardium have a common developmental origin in the proepicardial organ (septum transversum) (Olivey et al., 2004). We examined whether these tissues might also be derived in part from the anterior heart field, particularly for the epicardium and vessels overlying the right ventricle (Fig. 29). Our results clearly show that the epicardium lying directly adjacent to the positively marked right ventricular myocardium was negative for β -galactosidase activity, indicating that the

epicardium is not derived from *mef2c*-AHF-Cre expressing cells (Fig. 29A). Similar to the epicardium, whole mount staining of neonatal hearts, or sections through coronary vessels showed little or no investment of cells marked by the *mef2c*-AHF-Cre transgene (Fig. 29B, C). Occasionally, *mef2c*-AHF-Cre marked cells were observed within coronary vessels (Fig. 29C) suggesting the possibility that some smooth muscle, or possibly endothelial, cells of anterior heart field origin might contribute or be added to the coronary vessels. Overall, however, we conclude that the coronary vessels and the epicardium have developmental origins that are largely distinct from the anterior heart field population marked by *mef2c*-AHF-Cre, which is consistent with a common developmental origin for these structures and the addition of these cells after the addition of the anterior heart field to the heart (Olivey et al., 2004).

IV. Discussion

It has only recently become clear that the arterial portion of the developing heart arises from a discrete population of cells called the secondary or anterior heart field (Kelly et al., 2001; Mjaatvedt et al., 2001; Waldo et al., 2001). Understanding the developmental potential of this novel population of cells is required for future studies focused on the role of the anterior heart field in cardiac development and its involvement in congenital heart disease. In the present study, we have described a Cre transgenic mouse line, *mef2c*-AHF-Cre, which exhibits activity that is tightly restricted spatially to a subset of cells within the secondary/anterior heart field and its descendants. We used these mice to follow the contribution of this population of cells within the anterior heart field to the embryonic and postnatal heart. These studies demonstrate that the myocardium of the outflow tract and right

ventricle is marked by *mef2c*-AHF-Cre expression and that the ventricular septum and proximal portions of the left ventricle are derived from *mef2c* expressing cells within the anterior heart field. This work also shows that the endocardium of the right ventricle and proximal outflow vessels are marked by the *mef2c*-AHF-Cre transgene, while the epicardium and coronary vessels do not share a common origin with this population of anterior heart field derived cells. Importantly, we also show that this population of cells within the anterior heart field does not contribute to the majority of the left ventricle or the atria.

Previous studies have come to differing conclusions when defining the boundaries of secondary/anterior heart field contribution to the heart. Using retrospective fate mapping, a clonal boundary was observed between the left and right ventricles, with the ventricular septum arising from both right and left ventricular myocyte clones, suggesting a dual origin for the septum (Meilhac et al., 2004a). The *mef2c*-AHF-Cre generated fate map described here spans this clonal boundary, suggesting that the entire ventricular septum is derived from this anterior heart field population of cells (Fig. 27). Indeed, more recent retrospective clonal analyses suggest that myocyte clones can span the septal boundary and further suggested that the outflow tract is derived exclusively from secondary heart field, while the right ventricle and atria are derived from progenitors from both the primary and secondary heart fields (Meilhac et al., 2004b). Other recent work defines the secondary heart field as *Isl1* expressing progenitors that give rise to the outflow tract and right ventricle, as well as the majority of the cells in the left ventricle and developing atrium (Cai et al., 2003). By contrast, the fate map generated by *mef2c*-AHF-Cre described here has more restricted spatial boundaries and does not include the atria or the majority of the left ventricle. One

possible explanation for this discrepancy is that *Isl1* is expressed in the precardiac mesoderm prior to the partitioning of the primary and secondary heart fields, and therefore *Isl1* may mark descendants of both heart fields (Abu-Issa et al., 2004; Meilhac et al., 2004b). *Mef2c*-AHF-Cre may be activated in the precardiac mesoderm after the secondary heart field has a distinct identity from the primary heart field (Fig. 26) and, therefore, marks only the secondary/anterior heart field. This notion is consistent with fate mapping studies done in chick embryos where the secondary heart field appears to contribute only to the arterial pole of the developing heart (Mjaatvedt et al., 2001; Waldo et al., 2001). Alternatively, the *mef2c*-AHF-Cre derived fate map may represent a restricted subdomain of the secondary heart field with the *mef2c* enhancer marking only a portion of the larger *Isl1* expression domain, which is a notion that is also consistent with previous studies (Cai et al., 2003; Meilhac et al., 2004b).

Genetic fate mapping has several advantages over other fate mapping approaches, which rely on embryological manipulations and *ex vivo* culture systems. A Cre-based, genetic fate mapping approach, such as the one utilized here, provides nearly exact spatial resolution and does not require any perturbations to the developing embryo, thus allowing an embryonic fate map to be extended into adulthood. The disadvantage of the fate map presented here is that it does not provide a strict temporal boundary from which to map the fate of cells. By comparing the activity of the *mef2c* enhancer driving *lacZ* expression directly to the enhancer generated fate map, we were able to identify regions of the heart that did not exhibit enhancer activity at any time during development yet were marked by the fate map. This allowed us to use *mef2c*-AHF-Cre to identify the contribution of this population of cells within the anterior

heart field to the postnatal heart, and importantly, to identify regions of the heart that lacked contribution from anterior heart field cells marked by the *mef2c*-AHF-Cre transgene. The use of multiple fate mapping methods, including genetic and other approaches, is essential for a detailed understanding of the developmental potential of the secondary/anterior heart field, including the subpopulations and expression domain gradients within this progenitor pool.

Anterior heart field contribution in mutant mice with defective heart looping

Knockout studies in mice have shown that several cardiac transcription factors are required for cardiac development. Mice with mutations in *mef2c*, *Hand2*, *Nkx2.5*, *Isl1*, and *Foxh1* exhibit defects in looping morphogenesis, each has only a single hypoplastic common ventricular chamber, and each is strongly expressed in the anterior heart field (Cai et al., 2003; Lin et al., 1997; Lyons et al., 1995; Srivastava et al., 1997; von Both et al., 2004). It has been proposed that the common ventricular chamber in mice with mutations in these genes may lack right ventricular identity, which is consistent with a failure of the anterior heart field to be added to the developing heart (McFadden et al., 2000; Srivastava et al., 1997). We examined the expression of a transgenic marker of the anterior heart field, *mef2c*-AHF-*lacZ*, in *mef2c* knockout embryos. Our results show that this marker of the anterior heart field is expressed in the common ventricular chamber of *mef2c* null embryos, suggesting that the looping defects seen in *mef2c*, and possibly other mutant mice, are not due to failure of anterior heart field migration into the ventricular chamber. Interestingly, however, the *mef2c*-AHF-*lacZ* anterior heart field marker is misexpressed in *mef2c* knockout

embryos in a dorsal rather than a right-sided pattern. These observations suggest that the failure in looping morphogenesis in *mef2c* knockout animals may be due to a failure of anterior heart field derived cells to properly differentiate, migrate in an appropriate pattern, or communicate with adjacent tissues. A failure of anterior heart field cells to differentiate properly is consistent with previous observations of the *Hand2* cardiac enhancer in *mef2c* null mice, which suggested that the common ventricular chamber lacked cells with right ventricular identity (McFadden et al., 2000). Future studies will explore the role of the anterior heart field in cardiac morphogenesis.

Interaction of the anterior heart field with the cardiac neural crest and other tissues

The studies presented here have focused primarily on the expression of a transgenic marker of the anterior heart field and the embryological contributions of that population of cells to the heart, however, it is clear that anterior heart field derived components of the heart do not function autonomously and must integrate with several other lineages. We have described that the epicardium and coronary vessels come from a developmental origin distinct from the anterior heart field, consistent with addition to the heart from the proepicardial organ after addition of the anterior heart field (Kirby, 2002). It will be interesting to determine how anterior heart field derived cardiomyocytes create a permissive environment for subsequent addition of these tissues to the heart. The data presented here demonstrate that the majority of the left ventricle and the atria are not derived from the regions of anterior heart field marked by the activity of the *mef2c*-AHF-Cre transgene. It remains to be determined how the primary and secondary heart fields are merged and whether reciprocal interactions

between these two cardiogenic populations control boundary formation between the ventricles.

The cardiac neural crest is required for proper outflow tract development (Hutson and Kirby, 2003), and it has been shown to contribute to the smooth muscle of the outflow vessels (Epstein et al., 2000; Jiang et al., 2000; Waldo et al., 1999). Before septation, the outflow tract is primarily a myocardial tissue of secondary heart field origin. As the outflow tract shortens, the myocardial component is reduced, potentially by programmed cell death (Sugishita et al., 2004; Watanabe et al., 1998) or by transdifferentiation of myocardium to smooth muscle cells (Ya et al., 1998). Concurrent with outflow tract shortening, cardiac neural crest cells migrate into the outflow tract and contribute to the developing aorticopulmonary septum as well as to the tunica media of the developing great vessels (Jiang et al., 2000).

The smooth muscle cells of the outflow tract are positioned between the anterior heart field derived myocardial and endocardial components of these vessels, and anterior heart field progenitors in the pharyngeal mesoderm are juxtaposed with neural crest derived mesenchyme in the branchial arches. The close proximity of these two lineages and their eventual co-contribution to the outflow tract suggests the possibility of an intricate reciprocal signaling relationship between the secondary/anterior heart field and the cardiac neural crest. Indeed, in animals lacking cardiac neural crest cells, secondary heart field myocardium fails to be added properly to the arterial pole of the embryonic heart (Waldo et al., 2005a; Yelbuz et al., 2002). It will be interesting to determine if the neural crest also requires signaling

from the anterior heart field for proper addition to the outflow tract and valves. The *mef2c*-AHF-Cre transgenic mouse line will allow the ability to ablate genes specifically in the anterior heart field and its derivatives, which will permit a more detailed study of reciprocal signaling interactions in the outflow tract.

Implications of an anterior heart field specific Cre transgenic mouse line

Several common congenital anomalies result from outflow tract defects, including tetralogy of Fallot, double outlet right ventricle, persistent truncus arteriosus, and transposition of the great arteries (Srivastava, 2003; Winlaw et al., 2005). Because the outflow tract is derived from at least two distinct embryological origins, the anterior heart field and the neural crest, it will be important to define the role of each of these lineages in congenital malformations.

Conditional gene inactivation is an integral approach to understanding developmental processes such as cardiac development. In order to understand the function of genes specifically within the anterior heart field, lineage restricted Cre mice must be developed. Currently, the only existing Cre line described for this lineage is *Isl1*-Cre, which is expressed broadly in the embryo, including the secondary heart field (Srinivas et al., 2001). *Isl1*-Cre has the advantage of being expressed earlier than the *mef2c*-AHF-Cre transgene described here (Cai et al., 2003). Indeed, ISL1 binding is required for *mef2c* anterior heart field enhancer activation (Dodou et al., 2004). In addition, an inducible *Isl1*-Cre transgenic mouse has been developed and has the advantage of temporal control of Cre activity (Laugwitz et al., 2005). Furthermore, *Isl1* is not expressed in many of the

anterior heart field derived cells that comprise the developing myocardium and outflow tract (Cai et al., 2003). However, *Isl1* is expressed in many developing tissues and lineages outside of cardiac progenitor populations, including motor neurons, oral epithelium, cranial sensory ganglia, inner ear, thalamus, pituitary, pancreatic endothelium and mesenchyme, and distal tubular cells of the kidney (Ahlgren et al., 1997; Dong et al., 1991; Mitsiadis et al., 2003; Nakagawa and O'Leary, 2001; Pfaff et al., 1996; Radde-Gallwitz et al., 2004). Consistent with the broad expression of *Isl1*, the *Isl1*-Cre transgene is also broadly expressed during development and is clearly expressed outside cardiac progenitor populations. Indeed, the *Isl1*-Cre transgenic mouse line was first utilized to mark cells of motor neurons and dorsal root ganglia (Srinivas et al., 2001). In contrast, expression of the *mef2c*-AHF-Cre transgene described in the present study is highly restricted to the anterior heart field and its derivatives in the developing heart, and this novel reagent will allow for conditional inactivation of genes exclusively in the anterior heart field and its derivatives. This will be particularly relevant since many genes expressed in the anterior heart field are also expressed in the primary heart field or in the neural crest, and conditional inactivation approaches will be necessary to determine specific functions of these genes in the anterior heart field, right ventricle, and outflow tract independent of other lineages. These types of studies and the use of multiple distinct Cre lines will provide important insights into the mechanisms underlying the congenital anomalies that appear to impact the secondary/anterior heart field and its derivatives in the outflow tract.

Chapter 4 fig legends

Fig. 24. The anterior heart field contributes to the common ventricular chamber in *mef2c* null embryos. Whole mount and sectioned embryos from wild-type (A-D) and *mef2c* knockout (E-H) embryos containing the *mef2c*-AHF-*lacZ* transgene were assayed for β -galactosidase activity. (A, E) Frontal view of presomite embryos collected at 7.5 dpc with β -galactosidase activity detected in the medial portion of the cardiac crescent, consistent with the anterior heart field expression. (B, F) Frontal view of 6 somite embryos collected at 8.25 dpc and stained with X-gal. (C, G) Lateral view (right side) of 16 somite embryos collected at 9.0 dpc and stained with X-gal. Notice that in the mutant (G), the unlooped heart is stained in the dorsal portion of the common ventricular chamber, whereas staining in the wild-type embryo is restricted to the right side of the ventricle (bulbus cordis). (D, H) Transverse sections through 16 somite embryos. Staining in the knockout is observed in the outflow and dorsal portion of the common ventricle (H). Arrowheads mark the dorsal anterior portion of the common ventricular chamber in *mef2c* mutant mice. LV, left ventricle; NT, neural tube; OFT, outflow tract; PM, pharyngeal mesoderm; RV, right ventricle; VC, common ventricular chamber. Bar is equal to 100 μ m.

Fig. 25. Generation of an anterior heart field specific-Cre transgenic mouse line. (A) Schematic representation of the *mef2c*-AHF-Cre transgene. The *mef2c* anterior heart field promoter and enhancer was subcloned upstream of the cDNA encoding Cre recombinase and the SV40 splice and polyadenylation signal sequence. The resulting construct was used to generate transgenic mice. (B-D) Three different *mef2c*-AHF-Cre

transgenic founders were crossed to ROSA26R Cre-dependent *lacZ* reporter mice, and embryos were collected at 10.0 dpc. Cre activity was readily apparent in the pharyngeal mesoderm (arrowheads), outflow tract (OFT) and future right ventricle (RV). No expression was observed in the atria. RA, right atrium.

Fig. 26. The *mef2c*-AHF-Cre fate map overlaps with the expression of anterior heart field markers during early cardiac development. (A-D) Embryos from *mef2c*-AHF-Cre transgenic mice crossed to ROSA26R Cre-dependent *lacZ* reporter mice exhibit β -galactosidase activity exclusively in the anterior heart field and its derivatives. Cre activity directed by the *mef2c*-AHF-Cre transgene is first detectable in the dorsomedial region of the cardiac crescent at 7.5 dpc (A). By 8.0 dpc (B), *mef2c*-AHF-Cre robustly expresses Cre in the migrating cells of the anterior heart field (arrowhead). Expression of Cre at 8.0 dpc overlaps with the expression of the anterior heart field markers *Fgf10* (E) and *Isl1* (F) as shown by *in situ* hybridization. Expression of *Fgf10* and *Isl1* is considerably more broad than the anterior heart field; arrowheads point to the anterior heart field stained cells in panels E and F. By 9.5 dpc (C), Cre activity directed by the Cre transgene is detectable throughout the right ventricle (RV) and outflow tract (OFT), as well as in the pharyngeal mesoderm (PM) component of the branchial arches (BA) and in the outlet region of the future left ventricle (LV). Cre expression overlaps the expression of *Isl1* in the pharyngeal mesoderm (G). Transverse sections of embryos collected at 9.5 dpc show similar expression patterns between *mef2c*-AHF-Cre marked cells (D) and *Isl1* expressing cells (H) in the pharyngeal mesoderm (PM). al, allantois; DA, dorsal aorta; NT, neural tube.

Fig. 27. The right ventricle, outflow tract, and ventricular septum are derived from the anterior heart field. Hearts collected from *mef2c*-AHF-Cre Tg/0, ROSA26R *lacZ*⁺ mice and stained for β -galactosidase activity with X-gal (A-D). In panels E and F, whole embryos were stained with X-gal and then cut in transverse sections. In panels G and H, dissected hearts were cut in transverse sections and X-gal stained. At 9.5 dpc (A, E), β -galactosidase expression was detected in the right ventricle (RV), outflow tract (OFT), the dorsal aorta (DA), the pharyngeal mesoderm (PM) of the branchial arches (BA) and in the right-most portion of the left ventricle (LV). X-gal staining was also detected in the endocardium (en) at this stage, no expression was observed in the common atrial chamber (At) at this stage. Fate mapped cells in the hearts collected at 12.0 dpc (B, F) were present in the same domains as in the 9.5 dpc heart, and in the developing ventricular septum (asterisk). Note the lack of staining in the right and left atria (RA and LA, respectively). At 14.5 dpc (C, G), *mef2c*-AHF-Cre fate mapped cells were evident in the pulmonary artery (PA) and aorta (Ao) as well as the right ventricle and the portion of the left ventricle proximal to the septum. No staining was observed in the atria. Note the absence of staining in the epicardium (arrow in panel G). In the postnatal heart (D, H), Cre positive cells were detected in the right ventricle, outflow vessels, and the ventricular septum (asterisk). The atria, the majority of the left ventricle, the coronary vessels, and the epicardium were not marked by the *mef2c*-AHF-Cre. NT, neural tube. Bar equals 100 μ m.

Fig. 28. The right ventricular endocardium and the endothelium and myocardium of the outflow tract are derived from the anterior heart field while the smooth muscle of the outflow tract is neural crest derived. (A) Immunohistochemical detection of β -galactosidase (β -gal) protein in a transverse section through the right ventricle (RV) and outflow tract (OFT) of a representative *mef2c*-AHF-Cre Tg/0; ROSA26R *lacZ*/+ transgenic heart collected at 10.5 dpc. (B) PECAM staining to detect endothelial cells in the same section shown in panel A. (C) Merged image of (A) and (B) showing overlap of β -galactosidase and PECAM in the endocardium (EC), but not in the myocardium (Myo), which was only marked by β -galactosidase. (D) A representative transverse section through the pulmonary artery of a *mef2c*-AHF-Cre Tg/0; ROSA26R *lacZ*/+ transgenic embryo at 14.5 dpc. Cre activity was evident in the myocardial (myo) and endothelial cell (EC) layers of the outflow tract, while no activity was observed in the smooth muscle cell (SMC) layer. (E) Section through the pulmonary artery of *Wnt1*-Cre Tg/0; ROSA26R *lacZ*/+ embryo at 14.5 dpc. Cre activity was evident in the smooth muscle layer, but not in endothelial cells or the myocardial layer of the outflow tract. (F) Representative parafrontal section through the pulmonary artery (pulm. trunk) at the junction with the right ventricle from a *Wnt1*-Cre Tg/0; ROSA26R *lacZ*/+ embryo at 14.5 dpc. Cre activity was detected in the smooth muscle cell layer of the pulmonary artery and aorta (Ao), the leaflets of the pulmonary valves (asterisks), and in the conotruncal (CT) septum. Bar is equal to 100 μ m.

Fig. 29. The epicardium and coronary vessels are not derivatives of the anterior heart field. (A) Representative section from a *mef2c*-AHF-Cre Tg/0; ROSA26R *lacZ*/+ heart

collected at 14.5 dpc shows strong β -galactosidase activity in the myocardium (Myo), and negative staining in the adjacent epicardium (Epi). The coronary vessels of the neonatal heart were negative for β -galactosidase activity as seen in whole mount (B), or transverse sections (C). Notice also that the epicardium of the neonatal heart is negative for β -galactosidase staining. EC, endothelial cells; LA, left atrium; PA, pulmonary artery; RA, right atrium; RV, right ventricle. Bar is equal to 100 μ m.

115

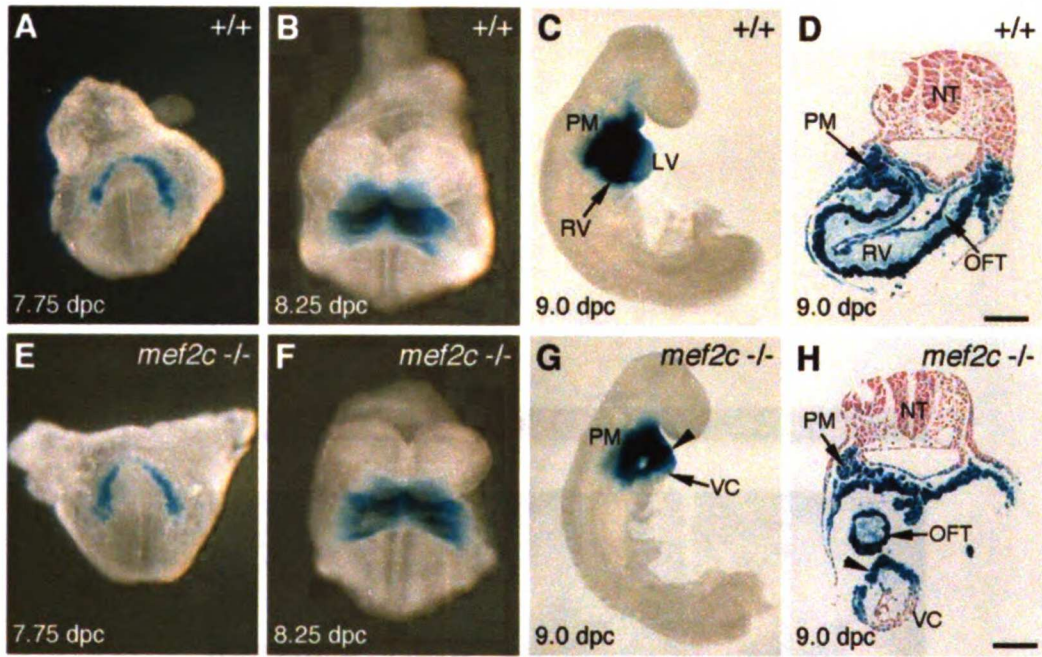


Figure 24

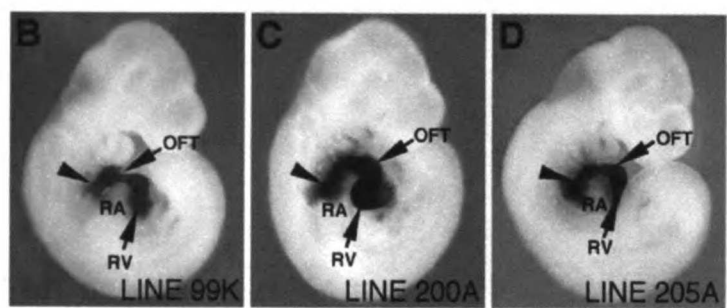
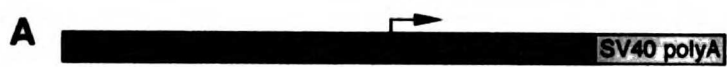


Figure 25

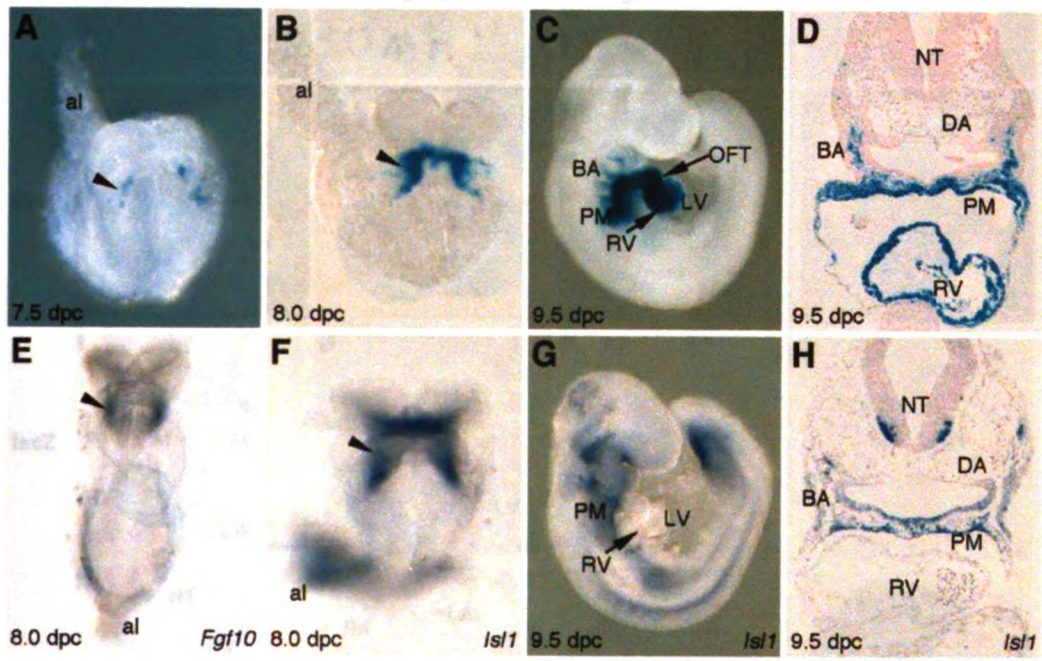


Figure 26

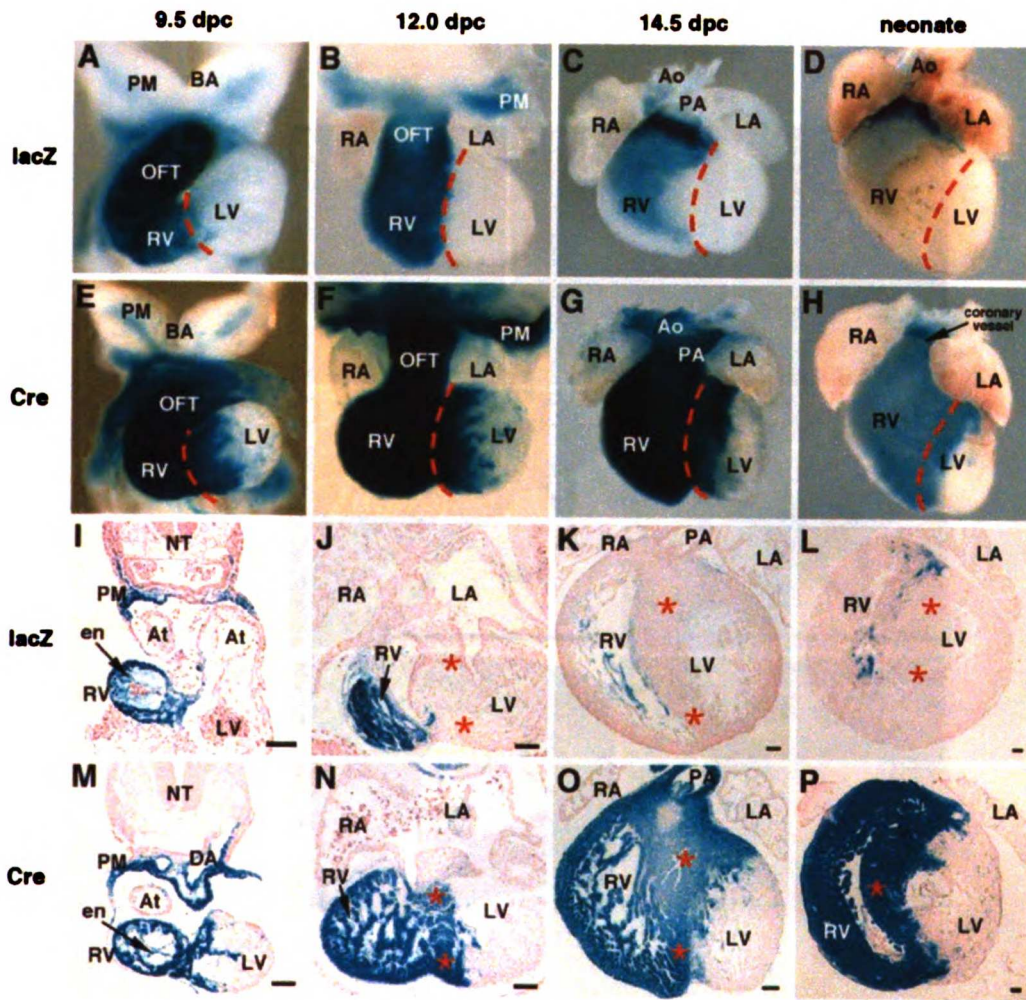


Figure 27

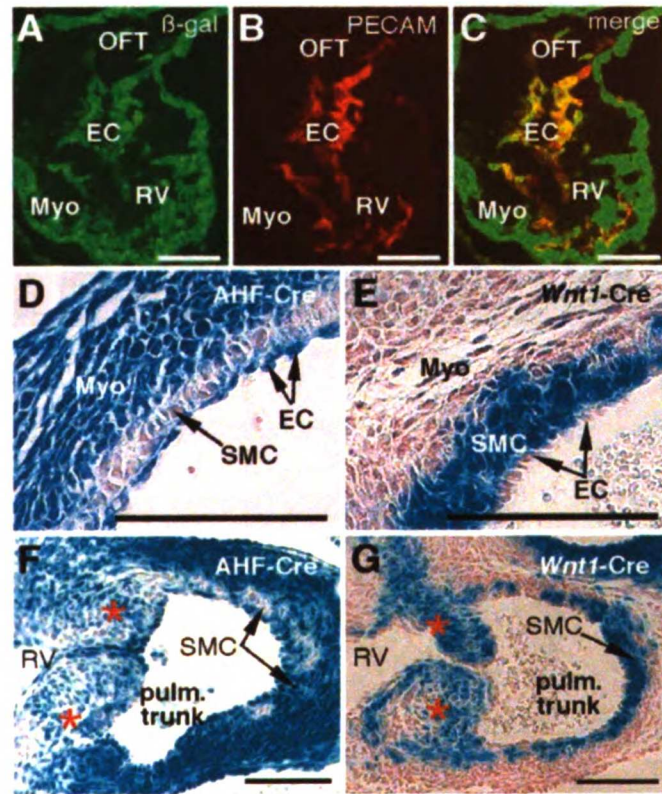


Figure 28

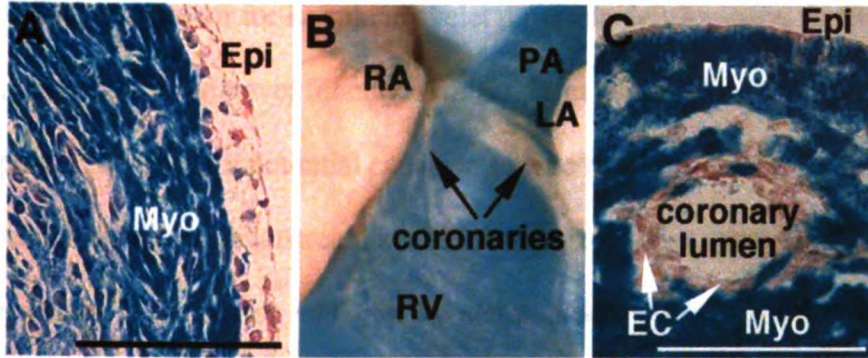


Figure 29

FINAL CONCLUSIONS

***Mef2c* in disorders of the neural crest**

MEF2C is best known for its role in skeletal muscle development. In the work described here, we demonstrate novel functions for *mef2c* in the developing neural crest lineages and propose *mef2c* as a potential cause or genetic modifier of neural crest disorders. We show that *mef2c* lies downstream of the Waardenburg/Hirschsprung disease gene *Sox10*. Additionally, mice lacking *mef2c* in the neural crest exhibit pigmentation defects similar to those observed in mice deficient in *Sox10*. Our work has also demonstrated an essential function for *mef2c* in craniofacial development. In *mef2c* neural crest knockout mice, several craniofacial structures appear hypoplastic or missing, ultimately leading to upper airway blockage and neonatal lethality. While the mechanism underlying these craniofacial defects remains under investigation, we have observed that the craniofacial phenotype of the *mef2c* knockout animals closely resembles knockouts deficient in components of endothelin signaling. Further, we have observed that an enhancer of *mef2c* active in the craniofacial primordia is sensitive to perturbations of endothelin signaling and therefore propose that *mef2c* may function as a downstream effector of endothelin signaling during craniofacial development. Based upon its function in mice, it will be interesting to investigate whether *mef2c* mutations in humans are potential causes for congenital birth defects associated with complications in neural crest development.

Multiple, distinct transcriptional enhancers control *Mef2c* expression in the heart

The heart is a complex organ, with multiple tissue types and moving components all built upon an initial linear tube. As may be expected, the different components and functions of the heart are guided by different transcriptional programs. Our work has revealed that expression of *mef2c* is under the control of at least three transcriptional enhancers: an enhancer directing expression to the anterior heart field, an enhancer directing expression to subsets of the ventricular myocardium, and an enhancer active throughout the adult heart (see chapters 3-4, and (Dodou et al., 2004a; Verzi et al., 2005). Identification of distinct enhancer modules not only allows us to gain insight into the transcriptional regulatory networks governing *mef2c* expression, but the pattern of expression directed by these modules is likely to teach us about the expressing tissue. Work on the *mef2c* anterior heart field enhancer helped draw attention to a molecularly distinct progenitor population once thought to be indistinct from the previously identified cardiac progenitor population (Dodou et al., 2004a; Verzi et al., 2005). Similarly, the cells active for the *mef2c* ventricular myocardial enhancer are likely to have a distinct function from neighboring cells lacking enhancer activity (see chapter 3). Further identification and investigation of modular transcriptional enhancers should broaden our understanding of transcriptional regulatory pathways and unappreciated functional cell populations in the future.

A paradigm for MEF2C function in cellular differentiation

Mef2c is expressed in a large number of developing tissues during the time of cellular differentiation. In our work and in previous studies, a pattern for *MEF2C* function has emerged. Transcriptional regulation of *mef2c* in developing tissues appears to be under the direct control of specifying transcription factors. Once active, MEF2C then functions as a transcriptional partner of its activator, and together, these factors direct expression of genes required for differentiation. MEF2C function in this capacity has now been documented in tissues as diverse as melanocytes, skeletal muscles, Schwann cells, and cardiac muscle. Based upon these examples, we hypothesize that *mef2c* is downstream of transcriptional partners in the other *mef2c*-expressing lineages, including the osteoblast, smooth muscle cell, craniofacial mesenchyme, and B and T lymphocyte lineages. It will be interesting to see whether future studies identify upstream transcriptional regulators that also function as MEF2C partners in these tissues.

METHODS

Generation of anterior heart field-specific Cre transgene and mice

The *mef2c*-AHF-Cre transgene was generated by excising the 3970 bp *mef2c* anterior heart field enhancer and promoter as an XhoI fragment from plasmid *Mef2c*-F6/Frag3, which has been described previously (Dodou et al., 2004a). This enhancer and promoter fragment was then cloned into a Cre expression plasmid containing the Cre cDNA and the SV40 splice and polyA signal sequence to create plasmid *mef2c*-AHF-Cre. The approximately 5.5 kb *mef2c*-AHF-Cre transgene fragment was then purified as a NotI fragment and injected into the male pronuclei of fertilized oocytes as described previously (Dodou et al., 2003). Cre positive founder mice were identified by Southern blot using a Cre-specific radiolabeled probe on genomic DNA isolated from tail biopsies. Male *Mef2c*-AHF-Cre transgenic mice were crossed to female ROSA26R Cre-dependent *lacZ* reporter mice (Soriano, 1999) to screen for Cre recombinase activity. *Wnt1*-Cre mice have been described (Danielian et al., 1998) and were used to fate map neural crest descendants in the outflow tract (Jiang et al., 2000). *Mef2c* knockout and *Mef2c* conditional knockout mice were kindly provided by John Schwarz (Albany), and have been described (Lin et al., 1997; Vong, et al, 2005). *Mef2c*-AHF-*lacZ* mice, containing the *mef2c* anterior heart field enhancer directing expression of *lacZ* have also been described previously as *mef2c* F6/Frag2-*lacZ* (Dodou et al., 2004).

Immunohistochemistry and in situ hybridization

Immunohistochemical detection of β -galactosidase and PECAM-1 was performed as described previously with minor modifications (Cripps et al., 2004). Briefly, embryos were

collected at the appropriate developmental stage and fixed overnight in 4% paraformaldehyde in PBS, transferred into increasingly concentrated sucrose solutions from 0 to 30 % in PBS, embedded in OCT on dry ice, and cryosectioned at a thickness of 14 μ m. In some cases, embryos were immediately transferred into sucrose solution and then into OCT. Sections were then analyzed for immunohistochemical detection as follows: Sections analyzed for β -galactosidase expression by immunohistochemistry using rabbit anti- β -galactosidase (ICN) as primary antibody diluted 1 in 1000 in 3% normal goat serum. Primary antibody binding was detected using Alexa Fluor 488 goat anti-rabbit secondary antibody (Molecular Probes) diluted 1 in 300 in 3% normal goat serum. The endothelial cell marker PECAM-1 was detected using a rat anti-mouse PECAM-1 antibody (Pharminogen) diluted 1:300 in 3% normal goat serum, and the secondary antibody was Cy3-conjugated goat anti-rat (Jackson ImmunoResearch) diluted 1 in 300 in 3% normal goat serum. Similarly Mouse anti-TEF-1 (BD Biosciences) was diluted 1:150, and a Cy3-conjugated mouse anti-alpha-smooth muscle actin (Sigma) was diluted 1:300. Prior to antibody treatment, slides were fixed briefly in either cold 4% paraformaldehyde or in cold Acetone, rinsed in PBS, and blocked with PBS containing 3% normal goat serum.

Whole mount *in situ* hybridization was performed as described previously (Wilkinson and Nieto, 1993). Briefly, embryos were fixed overnight in 4% paraformaldehyde and then washed twice with phosphate buffered saline (PBS) and dehydrated through a series of PBT (1X PBS + 0.1% Tween20)-methanol washes. Embryos were then rehydrated through a reciprocal series of PBT-methanol washes and were treated at room temperature with 10 μ g/ml proteinase K for varied times depending on age as described (Wilkinson and Nieto,

1993). After proteinase K treatment, embryos were rinsed with 2 mg/ml glycine in PBT followed by two successive washes in PBT at room temperature. Embryos were fixed in 4% paraformaldehyde and 0.2% glutaraldehyde for 20 minutes at room temperature, rinsed three times in PBT, and incubated in hybridization solution (50% formamide, 1% SDS, 5X SSC, 50 µg/ml yeast tRNA, 50 µg/ml heparin) for 16 hours at 70°C.

For *in situ* hybridization on sections, embryos were fixed, embedded in paraffin, sectioned, and dewaxed as described previously (De Val et al., 2004). Sections were then digested for 8.5 minutes in 40 µg/ml proteinase K, fixed in 4% paraformaldehyde for 20 minutes, dehydrated through a series of ethanol washes and allowed to dry. 50 µl of hybridization solution was added to each slide, and slides were incubated at 70°C for 16 hours. *In situ* hybridization was carried out with digoxigenin-labeled antisense or sense RNA probes at 100 ng/ml (whole mount) or 1 µg/ml (sections) in hybridization buffer. Following hybridization, embryos or slides were rinsed through a series of formamide and SSC washes and treated with RNaseA as described previously (Verzi et al., 2002). Signal was detected using an alkaline phosphatase-conjugated anti-digoxigenin antibody and BM Purple alkaline phosphatase substrate (Roche Pharmaceuticals). Following staining, slides were counterstained with Neutral Fast Red for visualization of embryonic structures. The *Isl1 in situ* probe plasmid was generously provided by S. Evans (UCSD) and has been described (Cai et al., 2003). The *Fgf10* antisense probe was kindly provided by P. T. Chuang (UCSF) and has been described previously (Chuang et al., 2003). The *Sox10* antisense probe was generated from pBS-Sox10 as described in the plasmids section of the Methods.

Mouse Embryo Culture

Embryo culture experiments were performed similarly to that described in Rojas, et al. (2005). Briefly, embryos from a stable transgenic line, either *mef2c* neural crest enhancer-*lacZ* or *SMAa-lacZ*, were harvested at the appropriate developmental stages after timed mating into cold and sterile PBS. The portion of the embryo caudal to the heart was removed to reduce strain on the culture system. The remaining rostral embryo was then immediately cultured in 1 ml of Dulbecco's modified Eagle's medium supplemented with 1% fetal bovine serum, penicillin (100U/ml), streptomycin (100U/ml) and 2mM L-glutamine at 37 degrees and 5% CO₂. The process was repeated until all embryos had been processed and placed into culture media, and then each embryo was moved into a new 1 ml containing either media alone, or media containing 0.5 - 1 mg/ml Bosentan for 24-36 hours. After incubation, the embryos were pre-fixed, washed, and stained for β-galactosidase activity as described (below). Bosentan was a generous gift from Actelion Pharmaceuticals, Switzerland.

GST Pulldowns

GST pull down assays were performed similarly that described by Chen, et al. 2000. Briefly, *E. coli* (BL21) codon+ bacteria were transformed with either pGEX2T-MEF2C-Flag or pGEX2T alone, cultured, and induced to express the GST-MEF2C-Flag fusion protein or GST alone, respectively. Glutathione Sepharose 4B beads were prepared according to manufacturer's instructions, preincubated with bacterial lysates for 30 minutes at room temperature, and washed extensively in PBS. Beads bound with the

fusion proteins were then aliquoted and co-incubated with either radiolabeled Sox10, or Sox10 N-terminal and DBD domain proteins (described and name the plasmids and constructs somewhere) in HEMG buffer (100mM KCl, 40mM HEPES (pH 7.4), 0.2mM EDTA, 0.1% NP-40, 1.5 mM DTT, 10% glycerol, and freshly supplemented 5% glycine and 1% BSA) at 4 degrees for 2 hours with rocking. The beads were then washed 3 times in HEMG buffer with BSA and glycine, and 2 times in HEMG buffer without BSA or glycine. Samples were then resolved by 10% SDS-PAGE and an autoradiogram was generated. The TNT-coupled transcription translation system (Promega) was used to generate the S³⁵-methionine labeled proteins according to the manufacturer's protocol.

Transactivation Assays

Transactivation assays were performed as described previously (Verzi, et al. 2002). C3H10T1/2 cells were maintained in Dulbecco's Modified Eagle Medium (DMEM) supplemented with 10% fetal calf serum. Transfections were performed with either Superfect (Qiagen) or Fugene 6 (Roche) according to manufacturer's instructions. In each transfection, generally a total of 1 µg of reporter plasmid and 1 µg of expression plasmid(s) were used for a total of 2 µg DNA. The quantity of DNA was held constant at 2 µg in each sample. Cells were typically cultured for 48 hours after transfection and then washed twice in 1 ml of PBS, harvested by scraping with a rubber policeman, and collected by centrifugation. Cellular extracts were then prepared by 3 freeze thaw cycles in lysis buffer (91.5 mM K₂HP0₄, 8.5 mM KH₂PO₄, 1 mM DTT), centrifugation, and collection of the supernatant. Extracts were normalized for total protein content by

Bradford assay (Biorad) and assayed using either luminescent β -gal (clontech) or luciferase (Promega) detection systems.

Electrophoretic Mobility Shift Assay

Electrophoretic Mobility Shift Assays (EMSA) were performed as described previously (Verzi et al., 2002). Briefly, proteins were co-transcribed and translated using the TNT coupled transcription translation system according to manufacturers protocols (Promega). DNA-binding reactions were performed as described previously (Gossett et al., 1989). 1 μ g of annealed oligos were end-labeled with Klenow and gel or column purified. 20,000 cpm of radiolabeled probe was incubated with programmed lysate, 1 μ g dI:dC-dI:dC (or in Sox10 EMSAs, 1 μ g dG:dC-dG:dC), and in some cases cold annealed oligonucleotide competitors at concentrations up to 25 ng / μ l, all in 1X binding buffer (40 mM KCl, 15 mM HEPES, pH 7.9, 1mM EDTA, 0.5 mM DTT, 5% glycerol) to a total of 20 μ l. Oligos used in these experiments were as follows:

For the TEF1-MCAT EMSA, control oligos containing MCAT element were based upon those published previously (Farrance et al., 1992; Stewart et al., 1994). The control MCAT oligo sequence used was 5'-gccgtgttgattcctctctgga annealed with 5'-gtccagagaggaatgcaacacgg and the control mutant MCAT oligos used were 5'-gcggtgttggtacctctctgct annealed with 5'-gagcagagaggtaccaacaccg. The wild type and mutant *mef2c* enhancer MCAT oligos used were 5'-gcagttgggagaggaatgcactgacta annealed with 5'-gtagtcagtgattcctctcccaactg and 5'-gcagttgggagaggtaccactgacta annealed with 5'-gtagtcagtggtacctctcccaactg, respectively.

For the Sox10 EMSA, positive control oligos were based upon those in the protein zero promoter published previously (Peirano and Wegner, 2000). The sequence of these control and mutant control oligos are:

sox10+ca - gatcctacacaaagccctccgcgtaga
sox10+cb - gggctaccgcgagggtttgtgtag
mutSox10a - gatcctaccggtcctccgcgtaga
mutSox10b - gggctaccgcgaggaccgcgtag

Sequences from the *mef2c* enhancer containing the wild-type and mutant SOX elements:

Sox10F1-1a - gaatgcactgactacaaagtgcacacctgaag
Sox10F1-1b - gcttcaggatgcacttgcagtcagtgcatt
mutSox10F1-1a - gaatgcactgacccgcggttgcacacctgaag
mutSox10F1-1b - gcttcaggatgcaaccgcggtcagtcatt
sox10F1-2a - gaatagctctatacaaaagtaactacagagt
sox10F1-2b - gactctgtagttactttgttatagagctatt
mutsox10F1-2a - gaatagctctatccgccgtaactacagagt
mutsox10F1-2b - gactctgtagttaacggcgatagagctatt
sox10F1-3a - ggccatttagctcacaatgaaggctctgtgtt
sox10F1-3b - gaacacagaccttcattgtgagctaaatggc
mutsox10F1-3a - ggccatttagctcgaggtaaggctctgtgtt
mutsox10f1-3b - gaacacagaccttacctcgagctaaatggc

Control oligos for the GATA shifts were described previously (Lien et al., 1999). Sequences from the *mef2c* enhancer containing the wild-type and mutant GATA elements are:

F1gata1a - gagtcttgcacagataaaggaaggatacagt
F1gata1b - gactgtatccttcctttatctgtgcaagact
F1mutgata-1a - gagtcttgcacgtgcaaaggaaggatacagt
F1mutgata-1b - gactgtatccttcctttgcacgtgcaagact
F1gata2a - gtagtagccattatcagtttaaccata
F1gata2b - gtatggttaaactgataatggctacta
F1mutgata-2a - gtagtagccatctgcagtttaaccata
F1mutgata-2b - gtatggttaaactgcagatggctacta

Control oligos for the MEF2 EMSA were from the myogenin enhancer were described previously (Dodou et al., 2003). Sequences from the *mef2c* enhancer containing the wild-type and mutant MEF2 element are:

F1mef2a - gggctccaactattatagaactgagta
F1mef2b - gtactcagttctataaatagttggagcc
F1mutmefa - gggctccaactatctgtagaactgagta
F1mutmefb - gtactcagttctgcagatagttggagcc

β-galactosidase staining and General Histology

β-galactosidase expression was detected as described in (Rojas et al., 2005). Embryos from timed matings were collected at the appropriate developmental stages and dissected in cold phosphate buffered saline (PBS). The yolk sac was saved for genotyping when needed.

Embryos were fixed in 2% paraformaldehyde, 0.2% glutaraldehyde for 15 minutes to 2 hours depending on size, then washed for 30 minutes in PBS and stained with 5-bromo-4-chloro-3-indolyl β-D-galactopyranoside (X-Gal) to detect β-galactosidase activity. After an appropriate time in stain solution, usually overnight at room temperature, embryos were

again washed in PBS for 30 minutes and then fixed in 4% paraformaldehyde for 24 hours. For sections from embryos younger than 14.5 dpc, representative X-gal stained embryos were prepared for paraffin sections as described previously (Anderson et al., 2004) and counterstained with Neutral Fast Red for better visualization of histology.

Cryosectioning followed by β -galactosidase staining

Embryos older than 14.5 dpc and neonatal hearts were fixed briefly in 2% paraformaldehyde, 0.2% glutaraldehyde and embedded in OCT (Tissue Tek #4583) on dry ice. Frozen samples were then sectioned on a cryostat (Leica) at a thickness of 10 μ m and allowed to dry overnight. Sections were fixed in 4% paraformaldehyde, rinsed in phosphate-buffered saline, pH 7.4 (PBS), and stained in X-gal solution. After adequate staining (6-16 hours), sections were rinsed in PBS and counterstained in Neutral Fast Red.

Skeleton and Cartilage Preparations

Skeleton and cartilage preparations have been performed according to standard procedure. Briefly, embryos or perinatal mice were cleaned, skinned, and eviscerated when appropriate, and then fixed in 95% ethanol for 3 days at room temperature. To detect cartilage, samples were then stained in Alcian Blue (15mg in 20% acetic acid, 80% 95% ethanol) for approximately 36 hours. Samples were then cleared in 1% KOH until clear, generally 2-6 hours, followed by counterstaining in Alizarin Red (50 mg per liter of 2% KOH) for 1-3 hours. Samples were cleared again in 2% KOH and then transferred slowly into glycerol over several days with decreasing concentrations of KOH until samples were in 100% glycerol, in which they could be stored indefinitely.

Mouse Lines Utilized and Constructed

***Mef2c* TM1** – these mice contain a null allele and were generated as described (Lin et al., 1997) and kindly provided by John Schwarz (Albany).

***Mef2c*^{flox/flox}** - A conditional allele of *mef2c* generated and kindly provided by John Schwarz (Albany) (Vong et al., 2005).

R26R (ROSA *lacZ* indicator mice) – were generated elsewhere (Soriano, 1999) and kindly provided by Shaun Coughlin (UCSF).

***Sox10*^{dom}** – These mice were identified based upon a spontaneously occurring mutation and purchased from the Jackson Laboratories (Lane and Liu, 1984).

F6s6-*lacZ* – Were generated by Evie Dodou and have been published (Dodou et al., 2004).

F6s6-*alkphos* – these mice were generated with David McCulley and have been published. Also known as *mef2c-AHF-hPlap* (Stennard et al., 2005).

Wnt1-cre – were provided by Lou Reichardt (UCSF) and were generated previously (Danielian et al., 1998).

F6-*cre* L200A – mice were created and have been described in chapter 4, and are also known as *Mef2c-AHF-Cre* (Verzi et al., 2005).

mMEF F1 – *Hsp68-lacZ*, 3xmutSOX F1– *Hsp68-lacZ*, and F1s3-3.3 – *Hsp68-lacZ* – these lines were created using the corresponding constructs explained under the heading entitled “plasmid construction” later in this Methods section. Transgenics were then generated as described above for F6-*cre*.

Genotyping

Mouse and embryo genotyping was performed by Southern blot using standard methods and probes specific for each allele unless otherwise indicated.

Genotyping the *Dom* allele:

PCR was performed on genomic DNA obtained from tail biopsy. Using the following primers, SoxgenoF2 5'-aggtgggcactctttagtg and SoxgenoR3 5'-tccggatgcagcacaaaaagg (75ng of each primer were used in a 50 ul PCR reaction), using Promega Taq, the genomic region containing the *Dom* frameshift mutation was amplified using the following conditions: 95° 3 minutes, then 35 cycles of 95° 30 seconds, 49° 1 minute, 72° 1 minute, then 72° 5 minutes. The resulting PCR product was then digested with MwoI. Since the *Dom* allele contains an additional MwoI site, PCR product amplified from the mutant allele will have smaller restriction fragments than the product from the wild-type allele (127 bp for wild-type versus 98 bp and 29 bp for the mutant).

Genotyping other mice used in these studies:

Mice containing Cre transgenes were identified by southern blot using a radiolabeled Cre probe. Genotyping at the *mef2c* locus was performed as described by Dustin Khiem. Mice containing *lacZ* were identified by southern blot using a radiolabeled *lacZ* probe.

Plasmid Construction

Plasmid constructs used to generate transgenic mice:

F1 – *Hsp68 lacZ*:

Cloned by Evie Dodou, this is a 7 kb intronic region of the *mef2c* locus approximately 7 kb upstream of the first translated exon and was cloned by PCR using engineered XmaI sites in the primers FR1-F 5'-agtgggaagcataaggcccgggaactctgat-3' and FR1-R 5'-atgtaccgtgtatggtggtcccgggaatgt-3'. The PCR product was digested and cloned into XmaI linear *Hsp68-lacZ*

Fragment1 1.7 – 5.7

This plasmid was cloned using the primers FR1-1746F 5'-cagcaccgggaggcagagacaggcggatttc-3' and FR1-5705R 5'-taaaactcccggtaacctcgtcagtaaataaccag-3', which generated XmaI restriction sites. These were cloned into the XmaI linear *Hsp68-lacZ* vector.

Fragment1 4.3-5.7

This injection construct was generated from fragment 1.7 to 5.7 digesting at an endogenous PstI site at 4.3 and at a NotI site in the polylinker of the vector of *Hsp68-lacZ*.

Fragment 1 3-4.3

This plasmid was cloned using engineered XmaI sites in the primers FR1-2994F 5'-cagcccGggcatgtttgcagtgtggagagtct-3' and FR1-4329R 5'-tactactgatgtttgaccgggcactgaag-3'

F1s3-3.7 Hsp68-lacZ (aka X101125-1)

This plasmid was made by Josh Anderson and cloned as an XmaI fragment into XmaI linear Hsp68-lacZ vector. The 5' XmaI site in this construct was PCR generated using the oligo FR1-2994F 5'-cagcccGggcatgttttcagtggtggagagtct-3' The 3' XmaI site in X101125-1 was PCR generated using 3770R 5'-ctcagtaaagcaaagcagaccccg-3'

F1s3-3.3 Hsp68-lacZ (aka X101123-2)

This plasmid was made by Josh Anderson and cloned as a 300bp XmaI – H3 subfragment from Fragment1 3-4.3 and cloned into XmaI –H3 linear Hsp68-lacZ vector

Fragment 1 3.3- 4.3

This injection construct was generated by digesting the Fragment 1 3-4.3 Hsp68 lacZ construct with the H3 site in the *mef2c* locus at 3.3 and the NotI site in the polylinker of Hsp68 lacZ.

Mutations of *cis*-regulatory elements were generated using the “gene SOEing” method (Horton, 1997). The outside primers used for generating the SOEing “arms” were:

On the 5' side of the mutation: 5pmMef2 tgggtcatctctgtgtcaca

On the 3' side of the mutation: mMefB2 ggcctttctacctcatc

These primers were paired with the mutagenic primers as follows, and then used again in the SOEing reaction of the resulting two PCR product “arms”. The resulting SOE product was then digested with the NsiI sites endogenous to *mef2c* and subcloned into Fragment 1-*Hsp68-lacZ*.

Fragment 1 del 3-3.3 was generated by PCR mutagenesis as described above using the primers:

F1deltaA aaagaaatctcagcccgggctgtgtagcacacag

F1deltaB acacagcccgggctgagatttcttttaaatgcatag

Fragment 1 triple Sox mutant was generated by PCR mutagenesis as described above with the following primers:

mutSox1a gggagaggaatgcactgacccgcggtgcatcc

mutSox1b ggccttcaggatgcaaaccggggtcagtgc

mutSox2a gtgtttaaaatagctctatccgccgtaactacag

mutSox2b gccagcactctgtagttaacggcggtatagagc
--

mutSox3a cctgaaggccatttagctcgagggttaaggtctgtg

mutSox3b ctattttaaaacacagacctaccctcgagctaaatggcc
--

Fragment 1 double mutant GATA-*Hsp68-lacZ* was generated by PCR mutagenesis as described above with the following primers:

F1mgata1SOEa: ctggttgctcctggagtcttgacgtgcaaaggaagg
--

F1mgata1SOEb: ctccaactgtatccttctttgcacgtgcaagac

F1mgata2SOEa: gggaaaaaaaaatcatagtagccatctgcagttaacc

F1mgata2SOEb: cccaagcttccgtatggtaaactgcagatggctac

Fragment 1 mutant MCAT-*Hsp68-lacZ* was generated by PCR mutagenesis as described above with the following primers:

mMCATa: ggatacagttgggagaggtaccactgactacaaagtgcaccc
mMCATb: ggccttcaggatgcactttgtagtcagtggtacctctccc

Fragment 1 mutant MEF-*Hsp68-lacZ* was generated by PCR mutagenesis as described above with the following primers:

mMEFA: cacgccttactcagttctgcagatagttgg
mMEFB: ggcaagggctccaactatctgcagaactgag

F6sub6-ERT2-cre

ERT2-cre (Chambon lab) was digested with Sall, blunted, and digested with ClaI, and the 1.3 kb fragment was purified and ligated into F6.6-Cre (Dodou) that had been digested with NotI blunted, and then digested with ClaI.

Plasmids used for in situ hybridization, protein expression constructs, tissue culture reporter constructs, and as cloning vectors:

pBS Sox10 for *in situ* probe:

An 802 bp PstI fragment from the 3' UTR of Sox10 was excised from pZL1Sox10 (a gift from the Ingraham lab containing the full length rat SOX10 cDNA 3022 bp, with the ORF from 583-1981, and the PstI 3'UTR fragment from 2093-2895) and cloned into pBluescript II SK. This plasmid was then linearized with NotI and used as an RNA template with the T7 promoter for a sense probe or linearized with XhoI and used as an RNA template with the T3 promoter for an anti-sense probe.

pRK5-Mef2C-FLAG

Mef2c was amplified from pCDNA1-Mef2c using the primers Mef2NotIF 5'-gagaagaaacgcggccgctatgg and Mef2NcoIR 5'-gtaataatgtgcatggtgcccattcc to create restriction sites at the 5' end upstream of the start codon (NotI) and to make an NcoI site to replace the stop codon. The PCR product was cloned into pCR2.1 by TA cloning and mini#14 was selected to subclone into pECE-FLAG as a NotI-NcoI which put the FLAG tag at the C-terminal end. To clone into pRK5 (a better expression vector), the mef2c-FLAG was subcloned into pRK5 as a NotI blunt – XbaI fragment into pRK5 SmaI-XbaI vector prep.

pCITE-Sox10-DBD:

pZL1Sox10 (see above) was cut with NcoI and blunt, then digested with EagI and ligated into pCITE2b that has been linearized with XbaI, blunted, and then digested with EagI. The resulting construct contains the N-terminal 235 amino acids including the DNA-binding domain.

pRK5-Sox10

This plasmid was cloned by linearizing pRK5 with EcoRI and subcloning in the entire Sox10 cDNA as an EcoRI fragment from the pZL1 Sox10 plasmid (see above). Sox10 was also cloned into pEMSV and pCDNA1 with the same cloning strategy.

pCITE-Sox10-CDS

The following primers, Sox10Ndef 5'-Gccgggagccatattggccgaggagca and Sox10RIrev 5'-cgtgggcacgaattctgacagggcc were used to amplify the Sox10 coding sequence from pZL1 Sox10 (see above). The resulting PCR product was digested with NdeI and EcoRI and cloned into pCITE2a that had also been digested with EcoRI and NdeI.

Sox10-DBD-VP16

pCITE2B-Sox10-DBD was digested with H3, blunted with Klenow, and then cut with EagI. The released fragment was then subcloned into pECE-FLAG that had been digested with SmaI and NotI. The resulting plasmid was then linearized by EcoRI digestion and an EcoRI insert containing VP16 was cloned in-frame at the C-terminus of the Sox10-DBD construct.

TK-AUG- β -gal

The TK promoter had been generated by digesting TKpGL3 with H3, blunting with Klenow, then digesting with BglII. This was then cloned into the pAUG- β -gal vector that had been digested with BamHI and SmaI.

TK-p β -gal basic

p β -gal basic was digested with H3 and BglII and the TK promoter from TK-pGL3 was subcloned in as an H3-BglII fragment.

pRK5-HA-Sox10

The following primers, Sox10Rif 5'-gccgggagcgaattcgccgaggagcaag, and Sox10Rrev, 5'-cgtgggcacgaattctgacagggcc were used to amplify the Sox10 coding region from pZL1Sox10 (see above). PCR product was digested with EcoRI and cloned into the vector in-frame.

F1 3-3.3 TK pBgal basic

The primers 2994F and 4329R were used to amplify a 1.3 kb region of the *mef2c* intronic enhancer region (see above for primer sequence) from F1-Hsp68-lacZ. The resulting product was digested with HindIII, blunted with Klenow, and then digested with XmaI. The 300 bp fragment was then cloned into TK-p β -gal basic (see above) that had been digested with NheI, blunted with Klenow, and then digested with XmaI.

F1 3xmutSox-TK-p β -gal basic

F1 2xmutSox-TK-pBgal basic

F1 mMEF-TK-p β -gal basic

These plasmids were cloned as described for F1 3-3.3 TK pBgal basic except the PCR template was the relevant mutant version of F1 Hsp68-lacZ

mE2-pSV1RecA:

to make the shuttle vector construct for mE2-L8, the plasmid from BB called 100801-17 containing the mutant E2 E-box was digested with H3 and the subfragment was ligated *into* a pBluescript II SK construct containing a PCR product from the *mef2c* locus

generated with the forward 73K and reverse 73K primers as an HI-XbaI fragment. The resulting construct, called 121402-17, was released as a SalI fragment and cloned into the SalI site in the pSVRecA shuttle vector.

F7delB-B-pSV1.RecA

F7DeltaB-B (Sarah de Val) was digested with EcoRV and SmaI and cloned into pSV1.RecA that had been digested with SalI and blunted with Klenow.

F10delta44-pSV1.RecA

Delta44F10pLD53Sca-mini#2 was digested with EcoRI and AflIII to release a 1.4 kb fragment containing the F10 region with the 44 bp deletion. This was blunted with Klenow and cloned into the pSV1.RecA vector that had been linearized with SalI and blunted.

pGEX2T-Sox10

pZL1-Sox10 (above) was digested with XmaI and EcoRI and cloned into pGEX2T as an XmaI-EcoRI to create an in-frame GST fusion that had an additional 14 aa on the 5' end of the full length protein.

pGEX2T-HA-Sox10

The primers pRK5-HA_{bam}F 5'-cgccgccaccaggatcctaccatag and SoxMfeR 5'-cacgtgggcaccaattgtgacagggcc were used to amplify HA-Sox10 from the pRK5-HA-Sox10 plasmid (see above). The product was digested with MfeI and BamHI and cloned

into pGEX2T that had been digested with BamHI and EcoRI to generate the in frame GST-HA-Sox10 construct.

pGEX2T-Mef2c-FLAG (GST-Mef2c-FLAG)

The primers MefBamHF 5'-tcggttctatggatccaattccccggccgctatg and mefmfeR 5'-tctagagctccaattgcccggggta were used to amplify mef2c-FLAG from pRK5-mef2c-flag (see above). The resulting product was digested with MfeI and BamHI and cloned into pGEX2T that had been digested with BamHI and EcoRI to generate the in frame GST-Mef2c-FLAG construct.

pRK5-VP16 vector

A vp16 fragment from Sox10-DBD-VP16 was generated by EcoRI-BamHI digest and cloned into pRK5 that had been digested with BamHI and EcoRI.

All experiments using animals complied with the federal and institutional guidelines, and each experiment was reviewed and approved by the UCSF Institutional Animal Care and Use Committee.

REFERENCES

- Abu-Issa, R., Waldo, K. and Kirby, M. L.** (2004). Heart fields: one, two or more? *Dev Biol* **272**, 281-5.
- Ahlgren, U., Pfaff, S. L., Jessell, T. M., Edlund, T. and Edlund, H.** (1997). Independent requirement for ISL1 in formation of pancreatic mesenchyme and islet cells. *Nature* **385**, 257-60.
- Anderson, J. P., Dodou, E., Heidt, A. B., De Val, S. J., Jaehnig, E. J., Greene, S. B., Olson, E. N. and Black, B. L.** (2004). HRC is a direct transcriptional target of MEF2 during cardiac, skeletal, and arterial smooth muscle development in vivo. *Mol Cell Biol* **24**, 3757-3768.
- Andres, V., Cervera, M. and Mahdavi, V.** (1995). Determination of the consensus binding site for MEF2 expressed in muscle and brain reveals tissue-specific sequence constraints. *J Biol Chem* **270**, 23246-9.
- Arai, H., Hori, S., Aramori, I., Ohkubo, H. and Nakanishi, S.** (1990). Cloning and expression of a cDNA encoding an endothelin receptor. *Nature* **348**, 730-2.
- Auerbach R.** Analysis of the developmental effects of a lethal mutation in the house mouse. *J Exp Zool* 1954;**127**: 305–329
- Azaki, A., Lamont, L., Fineman, J. R. and He, Y.** (2005). Divergent transcriptional enhancer factor-1 regulates the cardiac troponin T promoter. *Am J Physiol Cell Physiol* **289**, C1522-34.
- Baker, C. V. and Bronner-Fraser, M.** (1997). The origins of the neural crest. Part I: embryonic induction. *Mech Dev* **69**, 3-11.

Baxter, L. L., Hou, L., Loftus, S. K. and Pavan, W. J. (2004). Spotlight on spotted mice: a review of white spotting mouse mutants and associated human pigmentation disorders. *Pigment Cell Res* **17**, 215-24.

Baynash, A. G., Hosoda, K., Giaid, A., Richardson, J. A., Emoto, N., Hammer, R. E. and Yanagisawa, M. (1994). Interaction of endothelin-3 with endothelin-B receptor is essential for development of epidermal melanocytes and enteric neurons. *Cell* **79**, 1277-85.

Bi, W., Drake, C. J. and Schwarz, J. J. (1999). The transcription factor MEF2C-null mouse exhibits complex vascular malformations and reduced cardiac expression of angiopoietin 1 and VEGF. *Dev Biol* **211**, 255-67.

Black, B. L. (2006). A single mutation causes a spectrum of cardiovascular defects: the potential role of genetic modifiers, epigenetic influences, and stochastic events in phenotypic variability. *J Mol Cell Cardiol.* **40**(2):201-4.

Black, B. L., Molkentin, J. D. and Olson, E. N. (1998). Multiple roles for the MyoD basic region in transmission of transcriptional activation signals and interaction with MEF2. *Mol Cell Biol* **18**, 69-77.

Black, B. L. and Olson, E. N. (1998). Transcriptional control of muscle development by myocyte enhancer factor-2 (MEF2) proteins. *Annu Rev Cell Dev Biol* **14**, 167-96.

Bondurand, N., Girard, M., Pingault, V., Lemort, N., Dubourg, O. and Goossens, M. (2001). Human Connexin 32, a gap junction protein altered in the X-linked form of Charcot-Marie-Tooth disease, is directly regulated by the transcription factor SOX10. *Hum Mol Genet* **10**, 2783-95.

- Bondurand, N., Pingault, V., Goerich, D. E., Lemort, N., Sock, E., Caignec, C. L., Wegner, M. and Goossens, M.** (2000). Interaction among SOX10, PAX3 and MITF, three genes altered in Waardenburg syndrome. *Hum Mol Genet* **9**, 1907-17.
- Brand, T.** (2003). Heart development: molecular insights into cardiac specification and early morphogenesis. *Dev Biol* **258**, 1-19.
- Britsch, S., Goerich, D. E., Riethmacher, D., Peirano, R. I., Rossner, M., Nave, K. A., Birchmeier, C. and Wegner, M.** (2001). The transcription factor Sox10 is a key regulator of peripheral glial development. *Genes Dev* **15**, 66-78.
- Brutsaert, D. L.** (2003). Cardiac endothelial-myocardial signaling: its role in cardiac growth, contractile performance, and rhythmicity. *Physiol Rev* **83**, 59-115.
- Cai, C. L., Liang, X., Shi, Y., Chu, P. H., Pfaff, S. L., Chen, J. and Evans, S.** (2003). Isl1 identifies a cardiac progenitor population that proliferates prior to differentiation and contributes a majority of cells to the heart. *Dev Cell* **5**, 877-89.
- Cantrell, V. A., Owens, S. E., Chandler, R. L., Airey, D. C., Bradley, K. M., Smith, J. R. and Southard-Smith, E. M.** (2004). Interactions between Sox10 and EdnrB modulate penetrance and severity of aganglionosis in the Sox10^{Dom} mouse model of Hirschsprung disease. *Hum Mol Genet* **13**, 2289-301.
- Charite, J., McFadden, D. G., Merlo, G., Levi, G., Clouthier, D. E., Yanagisawa, M., Richardson, J. A. and Olson, E. N.** (2001). Role of Dlx6 in regulation of an endothelin-1-dependent, dHAND branchial arch enhancer. *Genes Dev* **15**, 3039-49.
- Chen, Z., Friedrich, G. A. and Soriano, P.** (1994). Transcriptional enhancer factor 1 disruption by a retroviral gene trap leads to heart defects and embryonic lethality in mice. *Genes Dev* **8**, 2293-301.

- Chuang, P. T., Kawcak, T. and McMahon, A. P.** (2003). Feedback control of mammalian Hedgehog signaling by the Hedgehog-binding protein, Hip1, modulates Fgf signaling during branching morphogenesis of the lung. *Genes Dev* **17**, 342-7.
- Clark, K. L., Yutzey, K. E. and Benson, D. W.** (2005). Transcription Factors and Congenital Heart Defects. *Annu Rev Physiol*.
- Clouthier, D. E., Hosoda, K., Richardson, J. A., Williams, S. C., Yanagisawa, H., Kuwaki, T., Kumada, M., Hammer, R. E. and Yanagisawa, M.** (1998). Cranial and cardiac neural crest defects in endothelin-A receptor-deficient mice. *Development* **125**, 813-24.
- Clouthier, D. E. and Schilling, T. F.** (2004). Understanding endothelin-1 function during craniofacial development in the mouse and zebrafish. *Birth Defects Res C Embryo Today* **72**, 190-9.
- Clouthier, D. E., Williams, S. C., Yanagisawa, H., Wieduwilt, M., Richardson, J. A. and Yanagisawa, M.** (2000). Signaling pathways crucial for craniofacial development revealed by endothelin-A receptor-deficient mice. *Dev Biol* **217**, 10-24.
- Cripps, R. M., Lovato, T. L. and Olson, E. N.** (2004). Positive autoregulation of the Myocyte enhancer factor-2 myogenic control gene during somatic muscle development in *Drosophila*. *Dev Biol* **267**, 536-47.
- Cripps, R. M. and Olson, E. N.** (2002). Control of cardiac development by an evolutionarily conserved transcriptional network. *Dev Biol* **246**, 14-28.
- Danielian, P. S., Muccino, D., Rowitch, D. H., Michael, S. K. and McMahon, A. P.** (1998). Modification of gene activity in mouse embryos in utero by a tamoxifen-inducible form of Cre recombinase. *Curr Biol* **8**, 1323-6.

De Val, S., Anderson, J. P., Heidt, A. B., Khiem, D., Xu, S. M. and Black, B. L.

(2004). Mef2c is activated directly by Ets transcription factors through an evolutionarily conserved endothelial cell-specific enhancer. *Dev Biol* **275**, 424-34.

Dinwiddie, R. (2004). Congenital upper airway obstruction. *Paediatr Respir Rev* **5**, 17-24.

Dodou, E., Verzi, M. P., Anderson, J. P., Xu, S. M. and Black, B. L. (2004b). *Mef2c* is a direct transcriptional target of ISL1 and GATA factors in the anterior heart field during mouse embryonic development. *Development* **131**, 3931-3942.

Dodou, E., Xu, S. M. and Black, B. L. (2003). *mef2c* is activated directly by myogenic basic helix-loop-helix proteins during skeletal muscle development in vivo. *Mech Dev* **120**, 1021-32.

Dong, J., Asa, S. L. and Drucker, D. J. (1991). Islet cell and extrapancreatic expression of the LIM domain homeobox gene *isl-1*. *Mol Endocrinol* **5**, 1633-41.

Edmondson, D. G., Lyons, G. E., Martin, J. F. and Olson, E. N. (1994). *Mef2* gene expression marks the cardiac and skeletal muscle lineages during mouse embryogenesis. *Development* **120**, 1251-63.

Emoto, N. and Yanagisawa, M. (1995). Endothelin-converting enzyme-2 is a membrane-bound, phosphoramidon-sensitive metalloprotease with acidic pH optimum. *J Biol Chem* **270**, 15262-8.

Epstein, D. J., Vogan, K. J., Trasler, D. G. and Gros, P. (1993). A mutation within intron 3 of the *Pax-3* gene produces aberrantly spliced mRNA transcripts in the *splotch* (Sp) mouse mutant. *Proc Natl Acad Sci U S A* **90**, 532-6.

- Epstein, J. A., Li, J., Lang, D., Chen, F., Brown, C. B., Jin, F., Lu, M. M., Thomas, M., Liu, E., Wessels, A. et al.** (2000). Migration of cardiac neural crest cells in Splotch embryos. *Development* **127**, 1869-78.
- Farrance, I. K., Mar, J. H. and Ordahl, C. P.** (1992). M-CAT binding factor is related to the SV40 enhancer binding factor, TEF-1. *J Biol Chem* **267**, 17234-40.
- Gossett, L. A., Kelvin, D. J., Sternberg, E. A. and Olson, E. N.** (1989). A new myocyte-specific enhancer-binding factor that recognizes a conserved element associated with multiple muscle-specific genes. *Mol Cell Biol* **9**, 5022-33.
- Gruber, P. J. and Epstein, J. A.** (2004). Development gone awry: congenital heart disease. *Circ Res* **94**, 273-83.
- Harvey, R. P.** (2002). Patterning the vertebrate heart. *Nat Rev Genet* **3**, 544-56.
- Herbarth, B., Pingault, V., Bondurand, N., Kuhlbrodt, K., Hermans-Borgmeyer, I., Puliti, A., Lemort, N., Goossens, M. and Wegner, M.** (1998). Mutation of the Sry-related Sox10 gene in Dominant megacolon, a mouse model for human Hirschsprung disease. *Proc Natl Acad Sci U S A* **95**, 5161-5.
- Hodgkinson, C. A., Moore, K. J., Nakayama, A., Steingrimsson, E., Copeland, N. G., Hutson, M. R. and Kirby, M. L.** (2003). Neural crest and cardiovascular development: a 20-year perspective. *Birth Defects Res C Embryo Today* **69**, 2-13.
- Horton, R.M.**, 1997. In vitro recombination and mutagenesis of DNA: SOEing together tailor-made genes. In: White, B.A., (Ed.). PCR Cloning Protocols, vol. 67. Humana Press, Totowa, NJ, pp. 141-149.
- Hoffman, J. I.** (1995). Incidence of congenital heart disease: I. Postnatal incidence. *Pediatr Cardiol* **16**, 103-13.

- Hosking, B. M., Wang, S. C., Chen, S. L., Penning, S., Koopman, P. and Muscat, G. E.** (2001). SOX18 directly interacts with MEF2C in endothelial cells. *Biochem Biophys Res Commun* **287**, 493-500.
- Hosoda, K., Hammer, R. E., Richardson, J. A., Baynash, A. G., Cheung, J. C., Giaid, A. and Yanagisawa, M.** (1994). Targeted and natural (piebald-lethal) mutations of endothelin-B receptor gene produce megacolon associated with spotted coat color in mice. *Cell* **79**, 1267-76.
- Hughes, M. J., Lingrel, J. B., Krakowsky, J. M. and Anderson, K. P.** (1993). A helix-loop-helix transcription factor-like gene is located at the mi locus. *J Biol Chem* **268**, 20687-90.
- Inoue, K., Khajavi, M., Ohyama, T., Hirabayashi, S., Wilson, J., Reggin, J. D., Mancias, P., Butler, I. J., Wilkinson, M. F., Wegner, M. et al.** (2004). Molecular mechanism for distinct neurological phenotypes conveyed by allelic truncating mutations. *Nat Genet* **36**, 361-9.
- Jenkins, N. A. and Arnheiter, H.** (1993). Mutations at the mouse microphthalmia locus are associated with defects in a gene encoding a novel basic-helix-loop-helix-zipper protein. *Cell* **74**, 395-404.
- Jiang, X., Rowitch, D. H., Soriano, P., McMahon, A. P. and Sucov, H. M.** (2000). Fate of the mammalian cardiac neural crest. *Development* **127**, 1607-16.
- Jiao, Z., Mollaaghababa, R., Pavan, W. J., Antonellis, A., Green, E. D. and Hornyak, T. J.** (2004). Direct interaction of Sox10 with the promoter of murine Dopachrome Tautomerase (Dct) and synergistic activation of Dct expression with Mitf. *Pigment Cell Res* **17**, 352-62.

- Johnston, M. C. and Bronsky, P. T.** (1995). Prenatal craniofacial development: new insights on normal and abnormal mechanisms. *Crit Rev Oral Biol Med* **6**, 368-422.
- Kaneko, K. J., and DePamphilis, M. L.** (1998). Regulation of gene expression at the beginning of mammalian development and the TEAD family of transcription factors. *Dev Genet.* **22** (1), 43-55.
- Karasseva, N., Tsika, G., Ji, J., Zhang, A., Mao, X., and Tsika R.** (2003)
Transcription enhancer factor 1 binds multiple muscle MEF2 and A/T-rich elements during fast-to-slow skeletal muscle fiber type transitions. *Mol Cell Biol* **23** (15), 5143-64.
- Kariya, K., Farrance, I. K. and Simpson, P. C.** (1993). Transcriptional enhancer factor-1 in cardiac myocytes interacts with an alpha 1-adrenergic- and beta-protein kinase C-inducible element in the rat beta-myosin heavy chain promoter. *J Biol Chem* **268**, 26658-62.
- Kariya, K., Karns, L. R. and Simpson, P. C.** (1994). An enhancer core element mediates stimulation of the rat beta-myosin heavy chain promoter by an alpha 1-adrenergic agonist and activated beta-protein kinase C in hypertrophy of cardiac myocytes. *J Biol Chem* **269**, 3775-82.
- Karns, L. R., Kariya, K. and Simpson, P. C.** (1995). M-CAT, CA₂G, and Sp1 elements are required for alpha 1-adrenergic induction of the skeletal alpha-actin promoter during cardiac myocyte hypertrophy. Transcriptional enhancer factor-1 and protein kinase C as conserved transducers of the fetal program in cardiac growth. *J Biol Chem* **270**, 410-7.
- Kelly, R. G., Brown, N. A. and Buckingham, M. E.** (2001). The arterial pole of the mouse heart forms from Fgf10-expressing cells in pharyngeal mesoderm. *Dev Cell* **1**, 435-40.

- Kelly, R. G. and Buckingham, M. E.** (2002). The anterior heart-forming field: voyage to the arterial pole of the heart. *Trends Genet* **18**, 210-6.
- Kirby, M. L.** (2002). Molecular embryogenesis of the heart. *Pediatr Dev Pathol* **5**, 516-43.
- Knecht, A. K. and Bronner-Fraser, M.** (2002). Induction of the neural crest: a multigene process. *Nat Rev Genet* **3**, 453-61.
- Kolodziejczyk, S. M., Wang, L., Balazsi, K., DeRepentigny, Y., Kothary, R. and Megeney, L. A.** (1999). MEF2 is upregulated during cardiac hypertrophy and is required for normal post-natal growth of the myocardium. *Curr Biol* **9**, 1203-6.
- Kurihara, Y., Kurihara, H., Suzuki, H., Kodama, T., Maemura, K., Nagai, R., Oda, H., Kuwaki, T., Cao, W. H., Kamada, N. et al.** (1994). Elevated blood pressure and craniofacial abnormalities in mice deficient in endothelin-1. *Nature* **368**, 703-10.
- Lane, P. W. and Liu, H. M.** (1984). Association of megacolon with a new dominant spotting gene (Dom) in the mouse. *J Hered* **75**, 435-9.
- Larkin, S. B., Farrance, I. K. and Ordahl, C. P.** (1996). Flanking sequences modulate the cell specificity of M-CAT elements. *Mol Cell Biol* **16**, 3742-55.
- Laugwitz, K. L., Moretti, A., Lam, J., Gruber, P., Chen, Y., Woodard, S., Lin, L. Z., Cai, C. L., Lu, M. M., Reth, M. et al.** (2005). Postnatal *Isl1*⁺ cardioblasts enter fully differentiated cardiomyocyte lineages. *Nature* **433**, 647-53.
- Le Douarin, N., and Kalchheim, C.,** 1999. *The Neural Crest*. Cambridge University Press, Cambridge, UK.

- Lee, M., Goodall, J., Verastegui, C., Ballotti, R. and Goding, C. R.** (2000). Direct regulation of the Microphthalmia promoter by Sox10 links Waardenburg-Shah syndrome (WS4)-associated hypopigmentation and deafness to WS2. *J Biol Chem* **275**, 37978-83.
- Leifer, D., Li, Y. L. and Wehr, K.** (1997). Myocyte-specific enhancer binding factor 2C expression in fetal mouse brain development. *J Mol Neurosci* **8**, 131-43.
- Li, J., Chen, F. and Epstein, J. A.** (2000). Neural crest expression of Cre recombinase directed by the proximal Pax3 promoter in transgenic mice. *Genesis* **26**, 162-4.
- Lien, C. L., Wu, C., Mercer, B., Webb, R., Richardson, J. A. and Olson, E. N.** (1999). Control of early cardiac-specific transcription of Nkx2-5 by a GATA-dependent enhancer. *Development* **126**, 75-84.
- Lilly, B., Zhao, B., Ranganayakulu, G., Paterson, B. M., Schulz, R. A. and Olson, E. N.** (1995). Requirement of MADS domain transcription factor D-MEF2 for muscle formation in *Drosophila*. *Science* **267**, 688-93.
- Lin, Q., Lu, J., Yanagisawa, H., Webb, R., Lyons, G. E., Richardson, J. A. and Olson, E. N.** (1998). Requirement of the MADS-box transcription factor MEF2C for vascular development. *Development* **125**, 4565-74.
- Lin, Q., Schwarz, J., Bucana, C. and Olson, E. N.** (1997). Control of mouse cardiac morphogenesis and myogenesis by transcription factor MEF2C. *Science* **276**, 1404-7.
- Lints, T. J., Parsons, L. M., Hartley, L., Lyons, I. and Harvey, R. P.** (1993). Nkx-2.5: a novel murine homeobox gene expressed in early heart progenitor cells and their myogenic descendants. *Development* **119**, 969.

- Lu, J., McKinsey, T. A., Nicol, R. L. and Olson, E. N.** (2000). Signal-dependent activation of the MEF2 transcription factor by dissociation from histone deacetylases. *Proc Natl Acad Sci U S A* **97**, 4070-5.
- Lyons, G. E., Micales, B. K., Schwarz, J., Martin, J. F. and Olson, E. N.** (1995). Expression of *mef2* genes in the mouse central nervous system suggests a role in neuronal maturation. *J Neurosci* **15**, 5727-38.
- Lyons, I., Parsons, L. M., Hartley, L., Li, R., Andrews, J. E., Robb, L. and Harvey, R. P.** (1995). Myogenic and morphogenetic defects in the heart tubes of murine embryos lacking the homeo box gene *Nkx2-5*. *Genes Dev* **9**, 1654-66.
- Maeda, T., Chapman, D. L. and Stewart, A. F.** (2002a). Mammalian vestigial-like 2, a cofactor of TEF-1 and MEF2 transcription factors that promotes skeletal muscle differentiation. *J Biol Chem* **277**, 48889-98.
- Maeda, T., Gupta, M. P. and Stewart, A. F.** (2002b). TEF-1 and MEF2 transcription factors interact to regulate muscle-specific promoters. *Biochem Biophys Res Commun* **294**, 791-7.
- Maka, M., Stolt, C. C. and Wegner, M.** (2005). Identification of *Sox8* as a modifier gene in a mouse model of Hirschsprung disease reveals underlying molecular defect. *Dev Biol* **277**, 155-69.
- Mar, J. H. and Ordahl, C. P.** (1990). M-CAT binding factor, a novel trans-acting factor governing muscle-specific transcription. *Mol Cell Biol* **10**, 4271-83.
- Martin, J. F., Bradley, A. and Olson, E. N.** (1995). The paired-like homeo box gene *MHox* is required for early events of skeletogenesis in multiple lineages. *Genes Dev* **9**, 1237-49.

- McFadden, D. G., Charite, J., Richardson, J. A., Srivastava, D., Firulli, A. B. and Olson, E. N.** (2000). A GATA-dependent right ventricular enhancer controls dHAND transcription in the developing heart. *Development* **127**, 5331-41.
- McKinsey, T. A., Zhang, C. L. and Olson, E. N.** (2001). Control of muscle development by dueling HATs and HDACs. *Curr Opin Genet Dev* **11**, 497-504.
- Meilhac, S. M., Esner, M., Kelly, R. G., Nicolas, J. F. and Buckingham, M. E.** (2004a). The clonal origin of myocardial cells in different regions of the embryonic mouse heart. *Dev Cell* **6**, 685-98.
- Meilhac, S. M., Esner, M., Kerszberg, M., Moss, J. E. and Buckingham, M. E.** (2004b). Oriented clonal cell growth in the developing mouse myocardium underlies cardiac morphogenesis. *J Cell Biol* **164**, 97-109.
- Milewski, R. C., Chi, N. C., Li, J., Brown, C., Lu, M. M. and Epstein, J. A.** (2004). Identification of minimal enhancer elements sufficient for Pax3 expression in neural crest and implication of Tead2 as a regulator of Pax3. *Development* **131**, 829-37.
- Mitsiadis, T. A., Angeli, I., James, C., Lendahl, U. and Sharpe, P. T.** (2003). Role of Islet1 in the patterning of murine dentition. *Development* **130**, 4451-60.
- Mjaatvedt, C. H., Nakaoka, T., Moreno-Rodriguez, R., Norris, R. A., Kern, M. J., Eisenberg, C. A., Turner, D. and Markwald, R. R.** (2001). The outflow tract of the heart is recruited from a novel heart-forming field. *Dev Biol* **238**, 97-109.
- Molkentin, J.D.**, The zinc finger-containing transcription factors GATA-4, -5, and -6. Ubiquitously expressed regulators of tissue-specific gene expression. *J Biol Chem.* 2000 Dec 15;275(50):38949-52.

- Molkentin, J. D., Black, B. L., Martin, J. F. and Olson, E. N.** (1995). Cooperative activation of muscle gene expression by MEF2 and myogenic bHLH proteins. *Cell* **83**, 1125-36.
- Molkentin, J. D., Lin, Q., Duncan, S. A., and Olson, E. N.,** (1997) Requirement of the transcription factor GATA4 for heart tube formation and ventral morphogenesis. *Genes Dev.* **11**, 1061-1072
- Morin, S., Charron, F., Robitaille, L. and Nemer, M.** (2000). GATA-dependent recruitment of MEF2 proteins to target promoters. *Embo J* **19**, 2046-55.
- Nakagawa, Y. and O'Leary, D. D.** (2001). Combinatorial expression patterns of LIM-homeodomain and other regulatory genes parcellate developing thalamus. *J Neurosci* **21**, 2711-25.
- Noden, D. M. and Trainor, P. A.** (2005). Relations and interactions between cranial mesoderm and neural crest populations. *J Anat* **207**, 575-601.
- Olivey, H. E., Compton, L. A. and Barnett, J. V.** (2004). Coronary vessel development: the epicardium delivers. *Trends Cardiovasc Med* **14**, 247-51.
- Parisi, M. A. and Kapur, R. P.** (2000). Genetics of Hirschsprung disease. *Curr Opin Pediatr* **12**, 610-7.
- Passier, R., Zeng, H., Frey, N., Naya, F. J., Nicol, R. L., McKinsey, T. A., Overbeek, P., Richardson, J. A., Grant, S. R. and Olson, E. N.** (2000). CaM kinase signaling induces cardiac hypertrophy and activates the MEF2 transcription factor in vivo. *J Clin Invest* **105**, 1395-406.

Peirano, R. I., Goerich, D. E., Riethmacher, D. and Wegner, M. (2000). Protein zero gene expression is regulated by the glial transcription factor Sox10. *Mol Cell Biol* **20**, 3198-209.

Peirano, R. I. and Wegner, M. (2000). The glial transcription factor Sox10 binds to DNA both as monomer and dimer with different functional consequences. *Nucleic Acids Res* **28**, 3047-55.

Perez-Losada, J., Sanchez-Martin, M., Rodriguez-Garcia, A., Sanchez, M. L., Orfao, A., Flores, T. and Sanchez-Garcia, I. (2002). Zinc-finger transcription factor Slug contributes to the function of the stem cell factor c-kit signaling pathway. *Blood* **100**, 1274-86.

Pingault, V., Bondurand, N., Kuhlbrodt, K., Goerich, D. E., Prehu, M. O., Puliti, A., Herbarth, B., Hermans-Borgmeyer, I., Legius, E., Matthijs, G. et al. (1998). SOX10 mutations in patients with Waardenburg-Hirschsprung disease. *Nat Genet* **18**, 171-3.

Pfaff, S. L., Mendelsohn, M., Stewart, C. L., Edlund, T. and Jessell, T. M. (1996). Requirement for LIM homeobox gene *Isl1* in motor neuron generation reveals a motor neuron-dependent step in interneuron differentiation. *Cell* **84**, 309-20.

Potterf, S. B., Furumura, M., Dunn, K. J., Arnheiter, H. and Pavan, W. J. (2000). Transcription factor hierarchy in Waardenburg syndrome: regulation of MITF expression by SOX10 and PAX3. *Hum Genet* **107**, 1-6.

Potterf, S. B., Mollaaghababa, R., Hou, L., Southard-Smith, E. M., Hornyak, T. J., Arnheiter, H. and Pavan, W. J. (2001). Analysis of SOX10 function in neural crest-derived melanocyte development: SOX10-dependent transcriptional control of dopachrome tautomerase. *Dev Biol* **237**, 245-57.

Radde-Gallwitz, K., Pan, L., Gan, L., Lin, X., Segil, N. and Chen, P. (2004).

Expression of Islet1 marks the sensory and neuronal lineages in the mammalian inner ear. *J Comp Neurol* **477**, 412-21.

Rivera-Perez, J. A., Mallo, M., Gendron-Maguire, M., Gridley, T. and Behringer, R.

R. (1995). Goosecoid is not an essential component of the mouse gastrula organizer but is required for craniofacial and rib development. *Development* **121**, 3005-12.

Rojas, A., De Val, S., Heidt, A. B., Xu, S. M., Bristow, J. and Black, B. L. (2005).

Gata4 expression in lateral mesoderm is downstream of BMP4 and is activated directly by Forkhead and GATA transcription factors through a distal enhancer element. *Development* **132**, 3405-17.

Sakurai, T., Yanagisawa, M., Takuwa, Y., Miyazaki, H., Kimura, S., Goto, K. and

Masaki, T. (1990). Cloning of a cDNA encoding a non-isopeptide-selective subtype of the endothelin receptor. *Nature* **348**, 732-5.

Sanchez-Martin, M., Perez-Losada, J., Rodriguez-Garcia, A., Gonzalez-Sanchez, B.,

Korf, B. R., Kuster, W., Moss, C., Spritz, R. A. and Sanchez-Garcia, I. (2003).

Deletion of the SLUG (SNAI2) gene results in human piebaldism. *Am J Med Genet A* **122**, 125-32.

Sanchez-Martin, M., Rodriguez-Garcia, A., Perez-Losada, J., Sagrera, A., Read, A.

P. and Sanchez-Garcia, I. (2002). SLUG (SNAI2) deletions in patients with Waardenburg disease. *Hum Mol Genet* **11**, 3231-6.

Schlierf, B., Ludwig, A., Klenovsek, K. and Wegner, M. (2002). Cooperative binding

of Sox10 to DNA: requirements and consequences. *Nucleic Acids Res* **30**, 5509-16.

- Schwartz, R. J. and Olson, E. N.** (1999). Building the heart piece by piece: modularity of cis-elements regulating Nkx2-5 transcription. *Development* **126**, 4187-92.
- Selleck, M. A. and Bronner-Fraser, M.** (1995). Origins of the avian neural crest: the role of neural plate-epidermal interactions. *Development* **121**, 525-38.
- Shore, P. and Sharrocks, A. D.** (1995). The MADS-box family of transcription factors. *Eur J Biochem* **229**, 1-13.
- Soriano, P.** (1999). Generalized lacZ expression with the ROSA26 Cre reporter strain. *Nat Genet* **21**, 70-1.
- Southard-Smith, E. M., Angrist, M., Ellison, J. S., Agarwala, R., Baxevanis, A. D., Chakravarti, A. and Pavan, W. J.** (1999). The Sox10(Dom) mouse: modeling the genetic variation of Waardenburg-Shah (WS4) syndrome. *Genome Res* **9**, 215-25.
- Southard-Smith, E. M., Kos, L. and Pavan, W. J.** (1998). Sox10 mutation disrupts neural crest development in Dom Hirschsprung mouse model. *Nat Genet* **18**, 60-4.
- Spritz, R. A., Chiang, P. W., Oiso, N. and Alkhateeb, A.** (2003). Human and mouse disorders of pigmentation. *Curr Opin Genet Dev* **13**, 284-9.
- Srinivas, S., Watanabe, T., Lin, C. S., William, C. M., Tanabe, Y., Jessell, T. M. and Costantini, F.** (2001). Cre reporter strains produced by targeted insertion of EYFP and ECFP into the ROSA26 locus. *BMC Dev Biol* **1**, 4.
- Srivastava, D.** (2003). Building a heart: implications for congenital heart disease. *J Nucl Cardiol* **10**, 63-70.
- Srivastava, D., Cserjesi, P. and Olson, E. N.** (1995). A subclass of bHLH proteins required for cardiac morphogenesis. *Science* **270**, 1995-9.

- Srivastava, D., Thomas, T., Lin, Q., Kirby, M. L., Brown, D. and Olson, E. N.** (1997). Regulation of cardiac mesodermal and neural crest development by the bHLH transcription factor, dHAND. *Nat Genet* **16**, 154-60.
- Stennard, F. A., Costa, M. W., Lai, D., Biben, C., Furtado, M. B., Solloway, M. J., McCulley, D. J., Leimena, C., Preis, J. I., Dunwoodie, S. L. et al.** (2005). Murine T-box transcription factor Tbx20 acts as a repressor during heart development, and is essential for adult heart integrity, function and adaptation. *Development* **132**, 2451-62.
- Stewart, A. F., Larkin, S. B., Farrance, I. K., Mar, J. H., Hall, D. E. and Ordahl, C. P.** (1994). Muscle-enriched TEF-1 isoforms bind M-CAT elements from muscle-specific promoters and differentially activate transcription. *J Biol Chem* **269**, 3147-50.
- Stewart, A. F., Suzow, J., Kubota, T., Ueyama, T. and Chen, H. H.** (1998). Transcription factor RTEF-1 mediates alpha1-adrenergic reactivation of the fetal gene program in cardiac myocytes. *Circ Res* **83**, 43-9.
- Sugishita, Y., Leifer, D. W., Agani, F., Watanabe, M. and Fisher, S. A.** (2004). Hypoxia-responsive signaling regulates the apoptosis-dependent remodeling of the embryonic avian cardiac outflow tract. *Dev Biol* **273**, 285-96.
- Suri, M.** (2005). Craniofacial syndromes. *Semin Fetal Neonatal Med* **10**, 243-57.
- Swanson, B. J., Jack, H. M. and Lyons, G. E.** (1998). Characterization of myocyte enhancer factor 2 (MEF2) expression in B and T cells: MEF2C is a B cell-restricted transcription factor in lymphocytes. *Mol Immunol* **35**, 445-58.
- Tachibana, M., Kobayashi, Y. and Matsushima, Y.** (2003). Mouse models for four types of Waardenburg syndrome. *Pigment Cell Res* **16**, 448-54.

Tassabehji, M., Hammond, P., Karmiloff-Smith, A., Thompson, P., Thorgeirsson, S. S., Durkin, M. E., Popescu, N. C., Hutton, T., Metcalfe, K., Rucka, A. et al. (2005). GTF2IRD1 in craniofacial development of humans and mice. *Science* **310**, 1184-7.

Tassabehji, M., Newton, V. E. and Read, A. P. (1994). Waardenburg syndrome type 2 caused by mutations in the human microphthalmia (MITF) gene. *Nat Genet* **8**, 251-5.

Thomas, T., Kurihara, H., Yamagishi, H., Kurihara, Y., Yazaki, Y., Olson, E. N. and Srivastava, D. (1998). A signaling cascade involving endothelin-1, dHAND and msx1 regulates development of neural-crest-derived branchial arch mesenchyme. *Development* **125**, 3005-14.

Trainor, P. A. (2005). Specification of neural crest cell formation and migration in mouse embryos. *Semin Cell Dev Biol* **16**, 683-93.

Verastegui, C., Bille, K., Ortonne, J. P. and Ballotti, R. (2000). Regulation of the microphthalmia-associated transcription factor gene by the Waardenburg syndrome type 4 gene, SOX10. *J Biol Chem* **275**, 30757-60.

Verzi, M. P., Anderson, J. P., Dodou, E., Kelly, K. K., Greene, S. B., North, B. J., Cripps, R. M. and Black, B. L. (2002). N-twist, an evolutionarily conserved bHLH protein expressed in the developing CNS, functions as a transcriptional inhibitor. *Dev Biol* **249**, 174-90.

Verzi, M. P., McCulley, D. J., De Val, S., Dodou, E. and Black, B. L. (2005). The right ventricle, outflow tract, and ventricular septum comprise a restricted expression domain within the secondary/anterior heart field. *Dev Biol*.

von Both, I., Silvestri, C., Erdemir, T., Lickert, H., Walls, J. R., Henkelman, R. M., Rossant, J., Harvey, R. P., Attisano, L. and Wrana, J. L. (2004). Foxh1 is essential for development of the anterior heart field. *Dev Cell* **7**, 331-45.

Vong, L. H., Ragusa, M. J. and Schwarz, J. J. (2005). Generation of conditional Mef2cloxP/loxP mice for temporal- and tissue-specific analyses. *Genesis* **43**, 43-8.

Waldo, K. L., Hutson, M. R., Stadt, H. A., Zdanowicz, M., Zdanowicz, J. and Kirby, M. L. (2005a). Cardiac neural crest is necessary for normal addition of the myocardium to the arterial pole from the secondary heart field. *Dev Biol* **281**, 66-77.

Waldo, K. L., Hutson, M. R., Ward, C. C., Zdanowicz, M., Stadt, H. A., Kumiski, D., Abu-Issa, R. and Kirby, M. L. (2005b). Secondary heart field contributes myocardium and smooth muscle to the arterial pole of the developing heart. *Dev Biol* **281**, 78-90.

Waldo, K. L., Kumiski, D. H., Wallis, K. T., Stadt, H. A., Hutson, M. R., Platt, D. H. and Kirby, M. L. (2001). Conotruncal myocardium arises from a secondary heart field. *Development* **128**, 3179-88.

Waldo, K. L., Lo, C. W. and Kirby, M. L. (1999). Connexin 43 expression reflects neural crest patterns during cardiovascular development. *Dev Biol* **208**, 307-23.

Wang, D. Z., Valdez, M. R., McAnally, J., Richardson, J. and Olson, E. N. (2001). The Mef2c gene is a direct transcriptional target of myogenic bHLH and MEF2 proteins during skeletal muscle development. *Development* **128**, 4623-33.

Watanabe, M., Choudhry, A., Berlan, M., Singal, A., Siwik, E., Mohr, S. and Fisher, S. A. (1998). Developmental remodeling and shortening of the cardiac outflow tract involves myocyte programmed cell death. *Development* **125**, 3809-20.

- Wilkie, A. O. and Morriss-Kay, G. M.** (2001). Genetics of craniofacial development and malformation. *Nat Rev Genet* **2**, 458-68.
- Wilkinson, D. G. and Nieto, M. A.** (1993). Detection of messenger RNA by in situ hybridization to tissue sections and whole mounts. *Methods Enzymol* **225**, 361-73.
- Winlaw, D. S., Sholler, G. F. and Harvey, R. P.** (2005). Progress and challenges in the genetics of congenital heart disease. *Med J Aust* **182**, 100-101.
- Wollnik, B., Tukel, T., Uyguner, O., Ghanbari, A., Kayserili, H., Emiroglu, M. and Yuksel-Apak, M.** (2003). Homozygous and heterozygous inheritance of PAX3 mutations causes different types of Waardenburg syndrome. *Am J Med Genet A* **122**, 42-5.
- Xu, D., Emoto, N., Giaid, A., Slaughter, C., Kaw, S., deWit, D. and Yanagisawa, M.** (1994). ECE-1: a membrane-bound metalloprotease that catalyzes the proteolytic activation of big endothelin-1. *Cell* **78**, 473-85.
- Ya, J., van den Hoff, M. J., de Boer, P. A., Tesink-Taekema, S., Franco, D., Moorman, A. F. and Lamers, W. H.** (1998). Normal development of the outflow tract in the rat. *Circ Res* **82**, 464-72.
- Yamada, G., Mansouri, A., Torres, M., Stuart, E. T., Blum, M., Schultz, M., De Robertis, E. M. and Gruss, P.** (1995). Targeted mutation of the murine goosecoid gene results in craniofacial defects and neonatal death. *Development* **121**, 2917-22.
- Yanagisawa, H., Clouthier, D. E., Richardson, J. A., Charite, J. and Olson, E. N.** (2003). Targeted deletion of a branchial arch-specific enhancer reveals a role of dHAND in craniofacial development. *Development* **130**, 1069-78.

Yanagisawa, H., Hammer, R. E., Richardson, J. A., Williams, S. C., Clouthier, D. E. and Yanagisawa, M. (1998a). Role of Endothelin-1/Endothelin-A receptor-mediated signaling pathway in the aortic arch patterning in mice. *J Clin Invest* **102**, 22-33.

Yanagisawa, H., Yanagisawa, M., Kapur, R. P., Richardson, J. A., Williams, S. C., Clouthier, D. E., de Wit, D., Emoto, N. and Hammer, R. E. (1998b). Dual genetic pathways of endothelin-mediated intercellular signaling revealed by targeted disruption of endothelin converting enzyme-1 gene. *Development* **125**, 825-36.

Yanagisawa, M., Kurihara, H., Kimura, S., Tomobe, Y., Kobayashi, M., Mitsui, Y., Yazaki, Y., Goto, K. and Masaki, T. (1988). A novel potent vasoconstrictor peptide produced by vascular endothelial cells. *Nature* **332**, 411-5.

Yelbuz, T. M., Waldo, K. L., Kumiski, D. H., Stadt, H. A., Wolfe, R. R., Leatherbury, L. and Kirby, M. L. (2002). Shortened outflow tract leads to altered cardiac looping after neural crest ablation. *Circulation* **106**, 504-10.

Yutzey, K. E. and Kirby, M. L. (2002). Wherefore heart thou? Embryonic origins of cardiogenic mesoderm. *Dev Dyn* **223**, 307-20.

Zaffran, S., Kelly, R. G., Meilhac, S. M., Buckingham, M. E. and Brown, N. A. (2004). Right ventricular myocardium derives from the anterior heart field. *Circ Res* **95**, 261-8.

Zhu, L., Lee, H. O., Jordan, C. S., Cantrell, V. A., Southard-Smith, E. M. and Shin, M. K. (2004). Spatiotemporal regulation of endothelin receptor-B by SOX10 in neural crest-derived enteric neuron precursors. *Nat Genet* **36**, 732-7.

UCSF LIBRARY

San Francisco
LIBRARY

7537619
3 1378 00753 7619



San Francisco
LIBRARY

San Francisco
LIBRARY

San Francisco
LIBRARY

San Francisco
LIBRARY

San Francisco
LIBRARY

San Francisco
LIBRARY

San Francisco
LIBRARY

San Francisco
LIBRARY

San Francisco
LIBRARY

San Francisco
LIBRARY

San Francisco
LIBRARY

San Francisco
LIBRARY

San Francisco
LIBRARY

San Francisco
LIBRARY

San Francisco
LIBRARY

San Francisco
LIBRARY

For reference

Not to be taken from the room.

